Helsinki University of Technology Control Engineering

Espoo 2010 Report 166

IDENTIFICATION AND CONTROL OF DEPOSITION PROCESSES

Alexander Mendelson

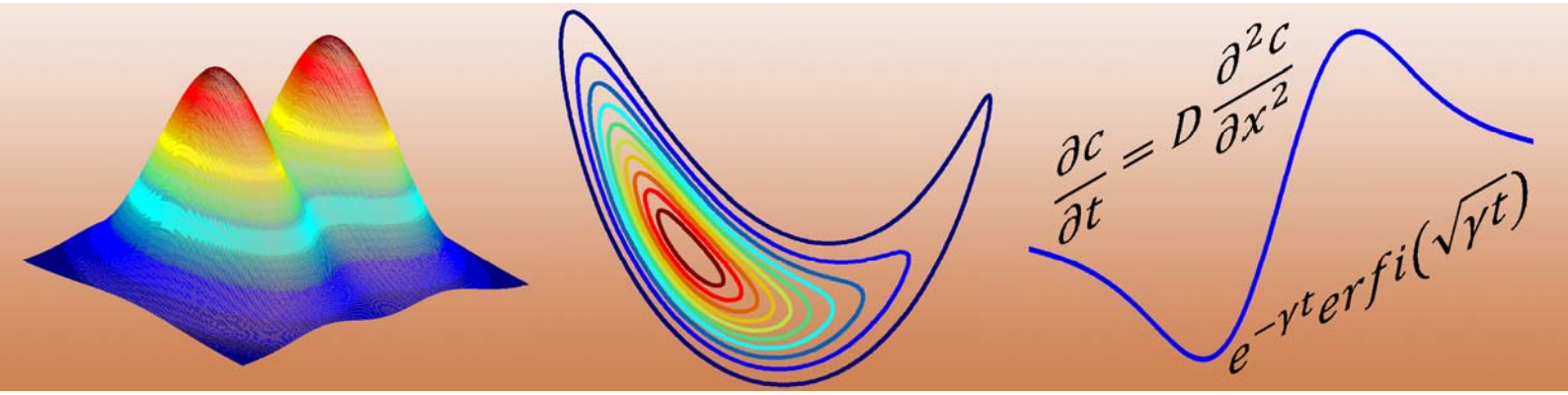

AALTO UNIVERSITY
SCHOOL OF SCIENCE AND TECHNOLOGY
DEPARTMENT OF AUTOMATION AND SYSTEMS TECHNOLOGY

Helsinki University of Technology Control Engineering

Espoo March 2010 Report 166

IDENTIFICATION AND CONTROL OF DEPOSITION PROCESSES

Alexander Mendelson

Doctoral dissertation for the degree of Doctor of Science in Techology to be presented with due permission of the Faculty of Electronics, Communications and Automation for public examination and debate in Auditorium AS1 at the Aalto University School of Science and Technology (Espoo, Finland) on the 6th of May 2010 at 12 noon.

Aalto University

School of Science and Technology

Faculty of Electronics, Communications and Automation

Department of Automation and Systems Technology

Distribution:
Aalto University
Department of Automation and Systems Technology
P.O. Box 15500
FI-00076 Aalto, Finland
Tel. +358-9-470 25201
Fax. +358-9-470 25208
E-mail: control.engineering@tkk.fi
http://autsys.tkk.fi/

ISBN 978-952-60-3126-2 (printed)
ISBN 978-952-60-3127-9 (pdf)
ISSN 0356-0872

URL: http://lib.tkk.fi/Diss/2010/isbn9789526031279

Yliopistopaino
Helsinki 2010

Aalto University

ABSTRACT OF DOCTORAL DISSERTATION	AALTO UNIVERSITY SCHOOL OF SCIENCE AND TECHNOLOGY P.O. BOX 11000, FI-00076 AALTO http://www.aalto.fi

Author Alexander Mendelson

Name of the dissertation
Identification and Control of Deposition Processes

Manuscript submitted 14.12.2009	Manuscript revised 29.03.2010
Date of the defence 06.05.2010	
☒ Monograph	☐ Article dissertation (summary + original articles)

Faculty	Faculty of Electronics, Communication and Automation
Department	Department of Automation and Systems Technology
Field of research	Control Engineering
Opponent(s)	Prof. Hannu Toivonen, Prof. Seppo Pohjolainen
Supervisor	Prof. Heikki Koivo
Instructor	Prof. Robert Tenno

Abstract

The electrochemical deposition process is defined as the production of a coating on a surface from an aqueous solution composed of several substances. Electrochemical deposition processes are characterized by strong nonlinearity, large complexity and disturbances. Therefore, improving production quality requires the identification of a reasonably accurate model which should be found from data in a reasonable amount of time and with a reasonable computational effort. This identification makes it possible to predict the behavior of unmeasured signals and design a control algorithm to meet the demands of consumers.

This thesis addresses the identification and control of the deposition processes. A model for an electrochemical cell that takes into account both electrode interfaces and the activity of ions participating in the deposition process is developed and a method for taking into account uncompensated resistance is proposed. Identifiability of two models, the conventional model and the developed model, is investigated under step and sweep form of applied voltage. It is proven that conventional electrochemical cell model can be identified uniquely using a series of step voltage experiments or in a single linear sweep voltammetry experiment on the basis of the measurements of cell current.

The Zakai filtering and pathwise filtering methods are applied to a nonlinear in the parameters electrochemical cell model to estimate the electrode kinetics and mass-transfer parameters of the copper electrodeposition process. In the case of known parameters the feedforward controllers that force the concentration at the boundary to follow the desired reference concentration are designed for the deposition processes. The adaptive boundary concentration control problem for the electrochemical cell with simultaneous parameter identification is solved using the Zakai filtering method. Using such a control, depletion in industrial applications, such as copper deposition baths, can be avoided.

An identification method for identifying kinetic parameters and a time-varying mixed potential process of the nonlinear electroless nickel plating model is proposed. The method converts the original nonlinear time-varying identification problem into a time-invariant quadratic optimization problem solvable by conventional least squares.

Keywords Identification, parameter estimation, nonlinear filtering, diffusion equation, electrode kinetics

ISBN (printed) 978-952-60-3126-2	ISSN (printed) 0356-0872
ISBN (pdf) 978-952-60-3127-9	ISSN (pdf)
Language English	Number of pages 126

Publisher Aalto University School of Science and Technology, Dpt. of Automation and Systems Technology

Print distribution Aalto University School of Science and Technology, Dpt. of Automation and Systems Technology

☒ The dissertation can be read at http://lib.tkk.fi/Diss/2010/isbn9789526031279

Preface

The research work presented in this thesis has been carried out in the Control Engineering Group (CEG) at Helsinki University of Technology (nowadays Aalto University School of Science and Technology) during the years 2005-2009.

I would like to thank my supervisor Prof. Heikki Koivo, the head of the CEG, for giving the opportunity to do my doctoral studies in his research group and for providing a relaxed and pleasant working atmosphere in the laboratory. I wish to express my sincere gratitude to my instructor Prof. Robert Tenno for his guidance, support and encouragement. His inspiration and insightful ideas have strongly influenced my dissertation. I am also indebted to D.Sc. Antti Pohjoranta for helping me with the experimental part and for proofreading several of my publications. I would like to thank Maurizio Bocca for the good company during lunch and coffee breaks. The humor, jokes and the conversations with Prof. Kai Zenger gave me a lot of positive energy and reflected in the progress of my work. I am also grateful to Mr. Pauli Sipari for his help with all the practical issues and arrangements. In addition, I wish to thank Mr. William Martin for proofreading the thesis.

I also appreciate all the financial support I have received during my doctoral studies. My research work was mainly funded by the Graduate School in Electronics, Telecommunications, and Automation (GETA). The additional funding has been given from the Centre for International Mobility (CIMO) and the Control Engineering Group. I am also grateful to the personal grants received from the Emil Aaltonen Foundation and from the Automation Foundation.

I wish to thank Prof. Seppo Pohjolainen and D.Sc. Ülle Kotta, who were the preliminary examiners of this thesis, for their constructive comments and suggestions which helped to improve the quality of this work.

Many thanks go to my friends in Finland for making every-day life enjoyable. Especially, I would like to thank Marija and Andrej Burakov and their son Gleb for being the best company during my studies in Finland. I also would like to thank Tatjana and Alexander Poutanen for Tuesday sauna evenings and amazing dinners after that. I greatly appreciate the friendship of Andrey Timofeev with whom we spent many evenings over tea discussing the problems of the world.

Finally, I warmly thank my dear parents Tatyana and Mark and my sister Elena for their continuous love, support and strong belief in me throughout all my life. Without them, it would have been impossible for me to complete this work.

Espoo, March 2010

Alexander Mendelson

Contents

Preface **i**

List of abbreviations **v**

List of symbols **vi**

1 Introduction **1**

1.1 Motivation and background 1
1.2 Outline of the thesis 4
1.3 Contribution of the thesis 5
1.4 List of related publications 6

2 Modeling of the electrode kinetics of Cu-Cu system **8**

2.1 Introduction 8
2.2 Contribution 11
2.3 Electrochemical cell model 11
2.3.1 Electrode kinetics model 12
2.3.2 Mass-transfer model 15
2.3.3 Ohmic potential drop 17
2.4 Model validation 21
2.5 Conclusions 27

3 Identifiability analysis and knowledge-based identification of electrochemical cells **28**

3.1 Introduction 28
3.2 Contribution 29
3.3 Identifiability under step form of applied voltage 29
3.3.1 Concentration boundary measurements 30
3.3.2 Current measurements 35
3.3.3 Parameter identification 37
3.4 Identifiability under sweep form of applied voltage 39
3.4.1 Identification of models linear in the concentration 40
3.4.2 Identification of models nonlinear in the concentration 42
3.5 Conclusions 47

4 Electrochemical parameters identification using Zakai equation 49
4.1 Introduction ... 49
4.2 Contribution ... 51
4.3 Estimation via Zakai equation ... 51
4.3.1 The estimation problem ... 51
4.3.2 The solution to the estimation problem ... 52
4.3.3 Application to estimation of static models ... 56
4.4 Electrochemical parameters identification ... 57
4.4.1 Identification of single parameter ... 58
4.4.2 Identification of two parameters ... 66
4.5 Experimental study ... 76
4.6 Conclusion ... 78

5 Adaptive boundary tracking control of electrochemical cells 79
5.1 Introduction ... 79
5.2 Contribution ... 80
5.3 Tracking control of electrochemical systems ... 81
5.4 Adaptive tracking control of electrochemical cells ... 87
5.4.1 Adaptive current control ... 88
5.4.2 Adaptive boundary concentration control ... 91
5.4.3 Solving the separated control problem ... 92
5.5 Simulation results ... 93
5.5.1 Adaptive current control ... 93
5.5.2 Adaptive boundary concentration control ... 94
5.6 Conclusion ... 99

6 Identification of the mixed potential processes 100
6.1 Introduction ... 100
6.2 Contribution ... 101
6.3 Process model ... 101
6.4 Parameter identification ... 104
6.4.1 Converting to a linear optimization problem ... 104
6.4.2 Solving the constrained optimization problem with genetic algorithms ... 107
6.4.3 Converting the solution to primary regression vector ... 108
6.5 Simulation results ... 112
6.6 Conclusion ... 115

Bibliography 116

List of abbreviations

AUX	Auxiliary electrode
CV	Cyclic voltammetry
DAQ	Data acquisition
EMF	Electromotive force
GA	Genetic algorithm
LMS	Least mean square
LQG	Linear-quadratic-gaussian controller
LSV	Linear sweep voltammetry
MRAC	Model reference adaptive control
ODE	Ordinary differential equation
PDE	Partial differential equation
PI	Proportional and integral controller
PID	Proportional, integral and derivative controller
PC	Personal computer
SHE	Standard hydrogen electrode
SPDE	Stochastic partial differential equation
STD	Standard deviation
WE	Working electrode

List of symbols

The symbols listed below are used in several chapters or in large segments of a chapter. Some symbols have different local meaning depending on the context of the text. Typically, scalars are presented in non-bolded symbols and all vectors and matrixes are presented in bold symbols.

Subscripts

a	Anodic	M	Metal
AUX	Auxiliary electrode	O	Oxidized species
b	Bulk	p	Peak
c	Cathodic	$p/2$	Half-peak
Cu	Copper	R	Reduced species
eq	Equilibrium	ref	Reference
m	Model	WE	Working electrode

Roman symbols

a	(a) Activity
	(b) Free term of the Taylor series expansion
a_M	Activity of a metal
$\mathbf{A}$, $\mathbf{a}$	Piecewise smooth vector functions
b	(a) $\alpha nF/(RT)\nu$, s^{-1}
	(b) Linear term of the Taylor series expansion
$\mathbf{b}$	Non-negative definite matrix
$\mathbf{B}$	Positive definite matrix
c	Concentration of species, mol/m^3
$c(t, 0)$	Concentration of species in near vicinity to the electrode surface, mol/m^3
c_0	Standard concentration, 1000 mol/m^3
c_b	Bulk solution concentration, mol/m^3
c_{ref}	Reference concentration, mol/m^3
c^i	Boundary concentration evaluated from the modeled current density, mol/m^3
c^ξ	Boundary concentration evaluated from the measured current density, mol/m^3
d	Distance between the electrodes, m
D	Diffusivity coefficient, m^2/s

e	Error signal between a plant and its model
E	Applied voltage, V
E_{eq}	Equilibrium potential, V
E_i	Initial potential, V
f	Flux, mol/m^2/s
F	Faraday's constant, 96487 C/mol
h	Arbitrary nonlinear function
i	Current density, A/m^2
i_{ref}	Reference current density, A/m^2
I	Current, A
I_{fi}	$\frac{I_0}{nFAc_O^b} e^{-\alpha \frac{nF}{RT}\left(E_i - E_{eq}\right)}$, m/s
i_0	Exchange current density, A/m^2
I_0	Exchange current, A
J	Cost function
l	Depth in the stagnation layer, m
k	Temperature voltage, V^{-1}
k_A	Areas ratio
$\mathbf{m}$	Conditional mean of estimated parameters
M	Number of sweep experiments
M_{Cu}	Molar mass of copper, 0.06355 kg/mol
n	Number of exchanged electrons
N	Number of measurements
p	Normalized probability density
q	Unnormalized probability density
R	(a) Ideal gas constant, 8.314 J/(mol·K) (b) Resistance, Ω
$R_{\Delta x}$	Resistance of a disc of thickness Δx, Ω
T	(a) Absolute temperature, K (b) Sweep period, s
t	Time, s
u	(a) Input signal (b) Equilibrium potential of a reaction, V
u_0	Linearization point of an equilibrium potential, V
U	Standard equilibrium potential of a reaction, V
U_d	Voltage drop, V
$\mathbf{V}$, $\mathbf{W}$	Independent Wiener processes
x	Spatial variable, m
x_{Cu}	Thickness of the copper deposit, m
x, y, z	Possible values (candidates) of unknown parameters i_0, α, D, respectively
$\mathbf{x}$	Vector of possible values of unknown parameters

Greek symbols

α	Apparent transfer coefficient
β	$\alpha_a \alpha_c / (\alpha_a + \alpha_c)$
$\boldsymbol{\gamma}$	Conditional covariance matrix
δ	Thickness of the stagnation layer, m
ε	Gaussian white noise
ζ	Measured current density, A/m^2
η	Surface overpotential, V
θ	Unmeasurable process
λ	Eigenvalue
μ	Control price
ν	Sweep rate, V/s
ν^E	Functional to be minimized
ξ	Surface charge density, C/m^2
ρ	Pathwise solution (transformed probability)
ρ_{Cu}	Density of copper, 8960 kg/m^3
σ	Solution conductivity, S
τ	Time, s
ϕ	Electrode potential, V
φ	Basis function
Φ	Mixed potential, V
Φ_0	Linearization point of mixed potential, V
$\chi(bt)$	Dimensionless current

Operators

$\mathbf{X}^T$	Transpose of $\mathbf{X}$
L^{-1}	Inverse Laplace transformation operator
L^*	Formal adjoint of an infinitesimal operator
∇	Vector differential operator
$\dfrac{\partial^n f(\cdot)}{\partial x^n}$	nth order partial derivative of f with respect to x

Chapter 1

Introduction

1.1 Motivation and background

Electrochemical deposition has attracted great attention in the scientific community due to a variety of applications in nanotechnology, microelectronics and biotechnology (Paunovic and Schlesinger, 1998). Low equipment cost, reliability, environmental advantages and the capability to accommodate different length scales are the clear benefits of the technology (Deligianni, 2006). The electrochemical deposition process is defined as the production of a coating on a surface from an aqueous solution composed of several substances. The deposit can be formed by passing a current through an electrochemical cell provided with an external power supply. Alternatively, it can be formed by making a complex solution where chemical reactions take place continuously without any power source due to the sufficiently high potential between the surface and a solution. The two mentioned technologies are known as *electrodeposition* and *electroless deposition*, respectively.

Electrochemical deposition processes are characterized by strong nonlinearity, large complexity and disturbances. Therefore, improving production quality requires the identification of a reasonably accurate model which should be found from data in a reasonable amount of time and with a reasonable computational effort. This identification makes it possible to predict the behavior of unmeasured signals and design a control algorithm to meet the demands of consumers. Plating processes, where the application of identification and control is desired, are numerous. Two important such processes from them related to this thesis are outlined below.

- Copper electrodeposition

  The thickness of the copper deposit on a substrate must be stabilized at the desired level through controlling the plating time and current density in the cell by adjusting the external power supply output. Concentration of copper(II) ions is unmeasured and, therefore, a model is required to design controls.

- Electroless nickel deposition

  The control objective here is to maintain the desired nickel alloy thickness and phosphorous content to meet production requirements. However, the nickel thickness and phosphorous content cannot be measured directly during the plating process. Therefore, once again, a model is required to design controls.

Choosing a suitable model structure is one of the basic steps of system identification theory (Ljung, 1999). The model usually depends on the parameters that cannot be measured directly and should be estimated by minimizing some cost function based on the measured data. This problem is commonly referred to as a parameter identification problem. This thesis mostly focuses on the development of the parameter identification methods for the deposition processes. However, questions, related to the selection of the model structure and design of the control law, are also addressed in Chapters 2 and 5 respectively.

As mentioned in Aström and Hägglund (2005), there are two general approaches that can be used for modeling dynamical systems. They are physical modeling and modeling from data. In physical modeling, basic physical laws such as mass and energy balances are used to obtain a process model. Thus, the model is based on our knowledge of the process. On the other hand, in modeling from data only input and output signals are used to build a model. Physical modeling has such an attractive feature as understanding the dependence of the model on the physical processes. This thesis deals with the physical models of the plating processes.

The three most important processes taking place in electrochemical systems are electron transfer, mass-transfer and adsorbtion (Berthier et al., 1996). The general structure of the deposition process without adsorbtion phenomena is depicted in Fig. 1.1.

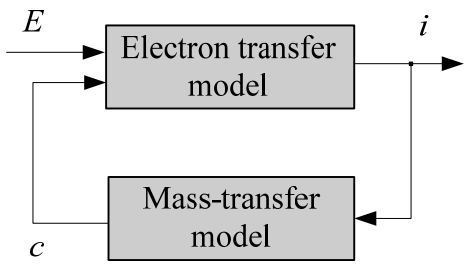

Figure 1.1: General structure of the deposition process.

The model is composed of an electron transfer block in feedback interconnection with a mass-transfer block. The electron transfer block addresses modeling dependence of current i (A) in an electrochemical cell on the applied voltage E (V) and the concentration of species c (mol/m^3) while the mass-transfer block addresses modeling evolution of the concentration in the electrochemical cell. Even in simple models the dependence of the cell current on the applied voltage is nonlinear and mass-transfer is commonly modeled by a diffusion equation that is a partial differential equation (PDE) of parabolic type. Therefore, developing identification methods for the deposition processes requires identification of the PDE with boundary conditions nonlinear in the unknown parameters. Identification of such a model has been developing in two ways. In the electrochemical community attempts have been made to build experiments in such a way that experimental conditions are chosen to observe only the primary electrochemical effects and to avoid the secondary effects (Mattsson, 1959). Based on this suggestion, the cell is presumed to be unstirred and the ratio of solution volume to the electrode is assumed large. These assumptions admit a linear semi-infinite diffusion

equation to describe the mass-transfer effects in the electrochemical cell and constant bulk solution concentration during the experiment. The resulting diffusion equation can be solved analytically and estimation methods based on the analytical solutions have been proposed. One of the first works has been done by Berzins and Delahay (1953) who derived a diagnostic feature for the reversible deposition of metals on solid electrodes. This feature makes it possible to estimate the diffusion coefficient of species based on measurements of peak current. Later Delahay (1953) extended the previous work to an irreversible reaction case and his results enabled, in addition to the diffusion coefficient, estimation of the electrode kinetic parameters. Matsuda and Ayabe (1955) gave a way to estimate both electron transfer and mass-transfer parameters for quasi-reversible reactions. The results of their work are applicable for reactions where both oxidized and reduced species are soluble in a solution. Nicholson and Shain (1964) gave a nice overview of the current-potential equations and diagnostic criteria for reactions where both species are soluble in a solution and extended the theoretical work to systems in which preceding or following chemical reactions are coupled with reversible or irreversible charge transfers. Polcyn and Shain (1966) studied multistep electron transfer and derived corresponding diagnostic features. White and Lawson (1970) investigated metal deposition processes and derived current-potential equations for special cases. Further research activity in this direction has dealt with different forms of electrode which affects the diffusion equation studied. Applications of these works are limited to dilute solutions where the reaction to occur is assumed to be a first order process. This assumption greatly simplifies the electron transfer model.

In the second way, in the control engineering community the general problem of identifying constant and spatial dependent parameters in nonlinear PDE has been studied extensively and a variety of methods have been proposed. Bhikkaji and Söderström (2001) have studied different approximations of PDE and then have estimated parameters of the initial model by direct search methods. The approximations they have considered include finite differences, the Galerkin method, the Tau-method and the collocation method. The method works well when the approximated system is linear in the unknown parameters, but may diverge for nonlinear parameters, which is the case of an electron transfer process. Finite-differences in combination with least squares to estimate parameters in a diffusion equation have also been used by Beck (1970). A similar method where PDE is reduced to set of ordinary differential equations and then the parameters are estimated using an optimization technique, such as the method of steepest descent, has been proposed by Polis et al. (1973). Coca and Billings (2000), in addition to finite-difference approximation and a least-squares method, have used smoothing the measured data and estimating the temporal derivatives using a fixed interval smoother to estimate the parameters from noisy experimental data. Seinfeld and Chen (1971) have developed the estimation methods for constant parameters in nonlinear PDE based on the method of steepest descent, quasilinearization, and collocation methods.

Several works made an attempt to use nonlinear filtering theory to estimate the parameters of PDE (Hwang et al., 1972; Seinfeld et al., 1971). Hwang et al. (1972) have converted the estimation problem into an optimal control problem. By defining a least-square criterion, using the necessary conditions for optimality and linearizing each of

the nonlinear terms they have derived the distributed nonlinear filter for PDE. Unfortunately, this method requires a lot of computational effort because several PDE have to be solved.

Demetriou and Rosen (1994) have considered adaptive estimation of parameters for a second-order linear PDE. Recently, Orlov and Bentsman (2000) have proposed an adaptive distributed parameter identification method, particularly for parabolic systems. Moreover, they have given identifiability conditions for the systems studied. However, though the method covers wide class of the systems it is not applicable for the systems where mass-transfer is described by a diffusion equation with mixed boundary conditions. Another disadvantage is that the method does not admit only boundary measurements available.

Model reference adaptive control (MRAC) of a diffusion equation with simultaneous parameter identification has also been addressed in the literature (Hong and Bentsman, 1994; Orlov and Bentsman, 1995). Again the proposed algorithms are not applicable to deal with mixed boundary conditions and distributed measurements and control are assumed. Moreover, the adaptive parameter identification schemas unknown parameters appear only in the PDE, while in a diffusion equation for modeling mass-transfer in the electrochemical process the parameters appear also in the boundary conditions.

In this thesis, an attempt has been made to extend analytical identification methods for the case of general reaction order, to study the identifiability of the model, to apply a nonlinear filtering technique developed for lumped parameter systems to distributed parameter systems and to design adaptive control of the plating process simultaneously with parameter estimation.

1.2 Outline of the thesis

This thesis is divided into 6 chapters. Chapter 1 handles introductory questions. In Chapter 2 modeling of the electrodeposition processes is investigated and a conventional model for an electrodeposition reaction is discussed. A new model that takes into account both electrode interfaces and the activity of ions participating in the deposition process is introduced. Before estimating the model it is desirable to examine the model identifiability, meaning that the model parameters can be uniquely recovered from input-output data. Such an examination is addressed in Chapter 3 of this thesis. This chapter also discusses the estimation methods for mass-transfer parameters and kinetic parameters that utilize the special shape of the current-potential curve. Chapter 4 focuses on the application of the Zakai filtering method for parameters identification of different electrode kinetics models in a voltammetric analysis. Issues related to computational effort, effectiveness and convergence are covered. Chapter 5 is devoted to the adaptive boundary control of the electroplating processes with simultaneous parameter identification. Boundary control schemes that track the desired current and concentration at the boundary are considered and the computational aspect is discussed. Finally, in Chapter 6 an identification method for the electrode kinetic parameters is presented for a specific case where the diffusion phenomena can be neglected. The

method is implemented with application to the electroless nickel deposition process model. A flowchart of the thesis is illustrated in Fig 1.2.

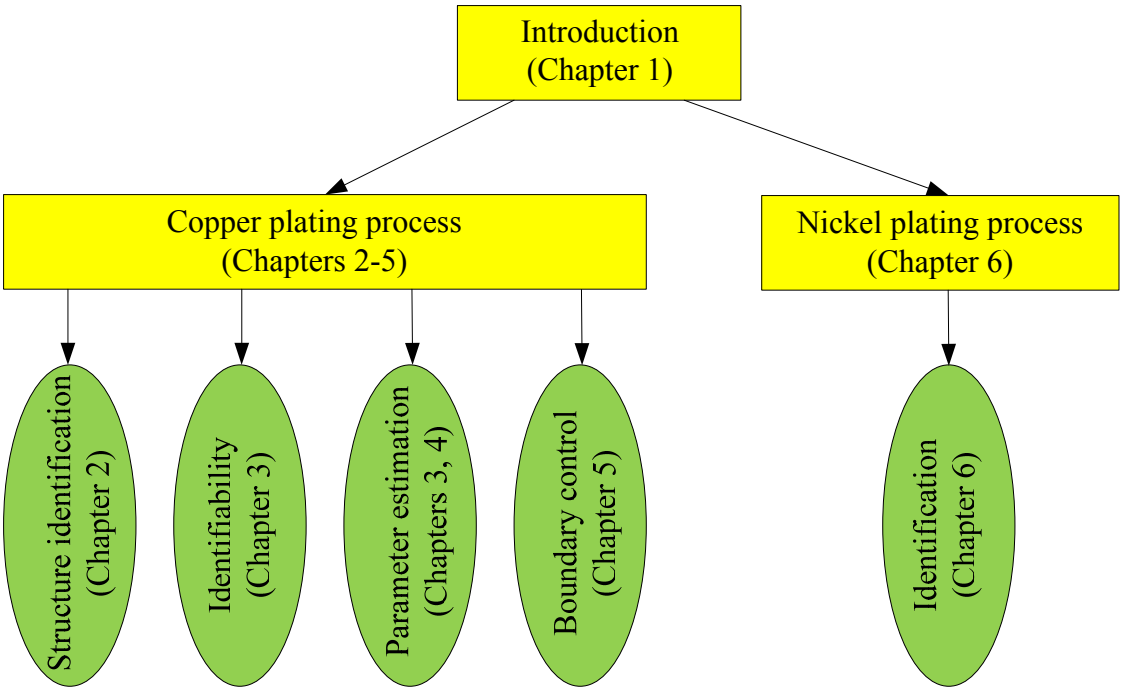

Figure 1.2: Flowchart of the thesis structure.

1.3 Contribution of the thesis

The contributions of this thesis can be summarized as follows:

- A model for an electrochemical cell that takes into account both electrode interfaces and the activity of ions participating in the deposition process is developed. A method for taking into account uncompensated resistance is proposed.
- The created model is simulated and verified against measurements in application to a Cu-Cu electrodeposition process. Electrode kinetic parameters are estimated by fitting measurements to the model with a direct search method.
- Identifiability of the model for agitated electrochemical cell is analyzed under a constant electrode voltage applied. It is proven that the model is globally identifiable. The method of identifying electrode kinetic parameters based on a series of voltage step experiments is proposed.
- A method for identifying mass-transfer parameters as well as kinetic parameters for a model of an unstirred electrochemical cell is proposed for a specific case of constant diffusivity.
- The Zakai filtering and pathwise filtering methods are applied to a nonlinear in the parameters electrochemical cell model to identify the electrode kinetics and mass-

transfer parameters of the copper electrodeposition process. Convergence of the estimates is analyzed and compared with the direct search method.

- Equations of the Zakai filtering and pathwise filtering methods are simplified for the case of constant parameter estimation and an analytical solution is obtained.
- The feedforward controllers that force the concentration at the boundary to follow the desired reference concentration are designed for finite-length diffusion and semi-infinite diffusion processes for the case of known parameters.
- The Zakai filtering is applied to a nonlinear in the parameters electrode kinetic model to control current in the electrochemical cell and its performance is compared with that of PI controller.
- The problem of adaptive boundary concentration control in the electrochemical cell is solved using the Zakai filtering method and several simplified computational schemes are introduced to save computational effort.
- An identification method for identifying kinetic parameters and a time-varying mixed potential process of the nonlinear electroless nickel plating model is proposed. The method converts the original nonlinear time-varying identification problem into a time-invariant quadratic optimization problem solvable by conventional least squares.

1.4 List of related publications

A total of 4 journal and 6 conference articles have been published on the topic of this thesis. They are listed below.

1. Tenno R. and *Mendelson A.* Adaptive boundary concentration control using Zakai equation. *International Journal of Control* (In press).
2. Pohjoranta A., *Mendelson A.,* and Tenno R. A Copper electrolysis cell model including effects of the ohmic potential loss in the cell. *Electrochimica Acta,* 2010, 55(3), pp. 1001-1012.
3. *Mendelson A.* and Tenno R. Identification of uncertainties of electrode kinetics using factorized Zakai equation. *Proceedings of the International Automatic Control Conference CACS 2009*, Taipei, Taiwan, 2009, 6 pp.
4. *Mendelson A.* and Tenno R. Electrode kinetics parameters estimation using Zakai equation. *Journal of Process Control*, 2009, 19(10), pp. 1698-1706.
5. *Mendelson A.* and Tenno R. Application of Zakai equation in parameter identification of electrode kinetics. *Preprints of the 15th IFAC Symposium on System Identification SYSID2009*, Saint-Malo, France, 2009, pp. 1423-1428.

6. *Mendelson A.* and Tenno R. Modelling and parameter identification of electrochemical Cu-Cu cell. *Proceedings of the UKACC International Conference on Control 2008*, Manchester, UK, 2008, 6 pp.

7. *Mendelson A.* and Tenno R. Model for electrode kinetics of copper-copper system. *Proceedings of the 17th IASTED International Conference on Applied Simulation and Modelling*, Corfu, Greece, IASTED, 2008, pp. 271-276.

8. *Mendelson A.* and Tenno R. Identification of the mass-transfer and kinetic parameters from voltammograms. *IEEE International Symposium on Industrial Electronics*, Vigo, Spain, 2007, pp. 142-146.

9. *Mendelson A.* and Tenno R. Identification of time-varying mixed potential processes. *Proceedings of the 9th WSEAS International Conference on Automatic Control, Modeling and Simulation*, *ACMOS '07,* Istanbul, Turkey, 2007, pp. 278-283.

10. *Mendelson A.M.*, Benderskaya E.N., and Tenno R.A. Genetic based identification of electrochemical processes. *Information and Control Systems*, 2006, №2, pp. 53-56 (in Russian).

Chapter 2

Modeling of the electrode kinetics of Cu-Cu system

2.1 Introduction

Studying of the electrode kinetics goes back to the works of Butler and Volmer, who investigated the hydrogen evolution reaction and derived an equation to describe the rate of electrode reaction as a function of electrode potential (Bamford and Compton, 1986; Bockris et al., 2000; Bard and Faulkner, 2001). Modern electrode kinetics theory utilizes a similar relationship with mass-transfer effects at the interface included to the model (see, e.g., Bard and Faulkner, 2001). This relationship is based on several fundamental assumptions. We introduce the relationship and illustrate the assumptions considering a one-step n-electron electrode process, wherein oxidized species (O) converse to a reduced form (R)

$$O + ne^- \rightleftarrows R\,. \tag{2.1}$$

The basic relation between the cell current and the voltage applied for the electrode reaction (2.1), where both oxidized and reduced species are soluble in the solution, is given by the current-overpotential equation (Christensen and Hamnett, 1994; Bard and Faulkner, 2001) as follows

$$I = I_0\left[\frac{c_R(0,t)}{c_R^b}e^{k\alpha_a\eta} - \frac{c_O(0,t)}{c_O^b}e^{-k\alpha_c\eta}\right], \tag{2.2}$$

where I is the total cell current, A, I_0 is the exchange current (constant), A, c_O is the concentration of oxidized species, mol/m^3, c_R is the concentration of reduced species, mol/m^3, c_O^b, c_R^b are the bulk concentrations of species, mol/m^3, α_a is the anodic apparent transfer coefficient, dim. less, α_c is the cathodic apparent transfer coefficient, dim. less, η is the surface overpotential of electrode, V, k is the temperature voltage, $k = nF/RT$, V^{-1}, n is the number of electrons, dim. less, F is the Faraday's constant, 96485 A·s/mol, R is the ideal gas constant, 8.314 J/(mol·K), T is the absolute temperature, K.

Equation (2.2) is the fundamental equation of electrochemical kinetics. Accompanied with concentration models for oxidized and reduced species, it underlies a numerical means for computing the current-potential curve for an electrochemical system. Such curves can provide valuable information about the system studied.

In the model (2.2) the reaction occurring in an electrode is considered to be a first-order process, meaning that the reaction rate is linearly proportional to the reaction species' concentration (Delahay, 1953).

ASSUMPTION A1. The reaction rate is linearly proportional to the reacting species' concentration at the reaction interface.

The surface overpotential of the electrode is defined as in (2.3)

$$\eta_e = \phi_e - \phi_{e,eq}, \tag{2.3}$$

where ϕ_e is the electrode potential with external voltage applied, V, and $\phi_{e,eq}$ is the electrode potential in equilibrium, V.

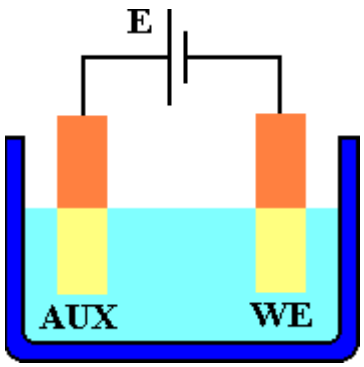

Figure 2.1: Electrochemical cell.

An electrochemical cell includes two electrodes (Fig. 2.1). When analyzed, one electrode, where the chemical reaction of interest occurs, is called the working electrode (WE) and, the other that completes the electric circuit, the auxiliary electrode (AUX). The electromotive force or cell voltage E, V is the algebraic sum of the cell electrodes' potentials and ohmic voltage drop due to the solution resistance

$$E = \phi_{WE} - \phi_{AUX} + IR. \tag{2.4}$$

Often the following assumptions are made.

ASSUMPTION A2. If the auxiliary electrode area is large enough ($A_{AUX} >> A_{WE}$) one can assume that $\phi_{AUX} = 0$.

ASSUMPTION A3. If a supporting electrolyte is used, the ohmic voltage drop in the cell is insignificant.

Following A1, species' concentration enters into (2.2) linearly. From A2 and A3 follows $\phi_{WE} = E$ and that the current-overpotential equation (2.2) can be written in terms of EMF rather than potentials:

$$I_e = I_{e,0}\left[\frac{c_R(0,t)}{c_R^b} e^{k\alpha_{e,a}(E-E_{eq})} - \frac{c_O(0,t)}{c_O^b} e^{-k\alpha_{e,c}(E-E_{eq})}\right]. \tag{2.5}$$

In the case of metal deposition (reduced species are not soluble in the solution) equation (2.5) takes the form

$$I_e = I_{e,0}\left[a_M e^{k\alpha_{e,a}(E-E_{eq})} - \frac{c_O(0,t)}{c_O^b} e^{-k\alpha_{e,c}(E-E_{eq})}\right], \tag{2.6}$$

where a_M is the activity of a metal at the electrode interface (White and Lawson, 1970).

Concentration of the oxidized species at the cathode surface is diffusion controlled and at the planar electrodes is governed by the following equation

$$\frac{\partial c_O(x,t)}{\partial t} = D_O \frac{\partial^2 c_O(x,t)}{\partial x^2}, \tag{2.7}$$

where D_O is the diffusivity coefficient of ions (m^2/s) that is assumed to be constant. The initial distribution of species is assumed to be homogeneous in the stagnation layer and equal to the bulk solution concentration

$$c_O(x,0) = c_O^b. \tag{2.8}$$

The boundary condition on the cathode is given by the first Fick law and states that the molar flux of ions is proportional to the cathode current density

$$D_O \frac{\partial c_O(x,t)}{\partial x}\Big|_{x=0} = -\frac{I(t)}{AnF}, \tag{2.9}$$

where A is the electrode area, m^2. A small ratio of electrode area to solution volume is assumed so that at larges distances from the electrode concentration of the species reaches bulk solution concentration

$$\lim_{x\to\infty} c_O(x,t) = c_O^b. \tag{2.10}$$

The benefit of equations (2.5)-(2.6) and, thus, the motives for the assumptions A1-A3 is that together with a linear, diffusion-controlled concentration model (2.7)-(2.10) at the cathode surface and sweep form of the applied voltage, it leads to a linear, first order Volterra integral equation, whose solution can be tabulated and utilized under any experimental conditions (Bard and Faulkner, 2001; Nicholson, 1965b). Then using this solution the electrode kinetics and mass-transfer parameters for the reversible, totally irreversible and quasi-reversible electrochemical reactions can be estimated. These knowledge-based identification methods are covered in Chapter 3 of this thesis. By reversibility we mean here that the electrode reaction is rapid compared with diffusion. Consequently, the reaction is said to be irreversible in the case the electrode reaction is slow, and quasi-reversible when both the anodic and cathodic processes have an impact on the current density (Bard and Faulkner, 2001).

The limitations of these equations also follow the assumptions A1-A3. Assumption A1 is reasonable only in dilute solutions, where the ion activity coefficient is close to unity and, thus, concentrations can be applied instead of activities. Generally, the ion activity coefficient dependence on concentration is nonlinear (Lide, 2006). Typically, voltammetric studies discuss only the working electrode and reactions on it, without considering the auxiliary electrode and the processes occurring there (Bamford and Compton, 1986). This is reasonable when areas of the electrodes differ significantly and the conductivity of the electrolyte is so good that the ohmic voltage drop can be neglected. In practical cases the AUX electrode is an essential part of the system and its area, material and corresponding electrochemical reactions affect the overall behavior of the electrochemical cell.

In this chapter we develop an electrode kinetics model of a Cu-Cu system which considers both electrodes of the system and the activity of copper(II) ions participating in the deposition process. Supplemented with a mass-transfer model, it will give an electrochemical cell model. Then we address the question of including uncompensated resistance into the model. An unstirred solution is presumed in contrast to the work of Pohjoranta and Tenno (2007), who proposed the model for well agitated solutions. The chapter focuses not on the modeling copper electrodeposition in great details, but on the choosing a simple model which forms the background for further parameter identification and control of the process.

The results of this chapter have been published in one journal and two conference papers (Mendelson and Tenno, 2008a, 2008b; Pohjoranta et al., 2010).

2.2 Contribution

The following contributions are covered in this chapter:

1. A model for an electrochemical cell with an unstirred solution that takes into account both electrode interfaces and the activity of copper(II) ions participating in the deposition process is developed, and a method for taking into account uncompensated resistance is proposed.
2. The created model is simulated and verified against measurements in application to a Cu-Cu electrodeposition process. The electrode kinetic parameters are estimated by fitting measurements to the model by a direct search method.

2.3 Electrochemical cell model

The electrode kinetics of copper electrodeposition has been studied in depth because of its technological importance (Mattson and Bockris, 1959; Hurlen et. al., 1978; Hinatsu and Foulkes, 1991; Pirogov and Zelinsky, 2004). The process is commonly modeled based on first principles. The only exception known to the author is work of Subramanian et al. (2009) where a functional relationship between deposition rate, current density, stirring rate and bath temperature was approximated using a second order polynomial model and a feed-forward back propagation neural network.

In experimental studies, copper deposition mechanism is usually investigated by means of voltammetry or chronopotentiometry (Mattson and Bockris, 1959; Hinatsu and Foulkes, 1991). The reaction mechanism of copper electrodeposition is generally supposed to include two consecutive charge-transfer steps, the reaction of disproportionation, adsorption, diffusion and dissolution processes (Chen and Wan, 1989; Tsai et. al., 2002). Two elementary reactions to occur at the interface are

$$Cu^{2+} + e^{-} \rightleftarrows Cu^{+}, \tag{2.11}$$

$$Cu^{+} + e^{-} \rightleftarrows Cu\,. \tag{2.12}$$

Treating reactions (2.11)-(2.12) as one elementary step with two electron transfers simplifies analysis considerably (Newman and Thomas-Alyea, 2004). This is reasonable because intermediate cupric ions are unstable, though their presence in the solution has been reported (Pirogov and Zelinsky, 2004; Gabrielli et. al., 2006). In addition, for simplicity in further development an adsorption phenomenon is assumed neglected.

The behavior of current in copper electroplating is given by the current-overpotential equation (2.6) (Reid, 2001). However, a commonly used relationship is based on the assumption of a dilute solution (Pirogov and Zelinsky, 2004). We remove this drawback from our model by considering the activity of the ions.

2.3.1 Electrode kinetics model

Consider an industrial Cu-Cu plating system which consists of two planar copper electrodes and copper sulphate solution (Fig. 2.2). In this system essentially the same reaction occurs on both electrodes, regardless of cell voltage polarity:

$$Cu^{2+} + 2e^{-} \rightleftarrows Cu\,. \tag{2.13}$$

Figure 2.2: Laboratory-scale Cu-Cu plating electrochemical cell consisting of two planar copper electrodes and acidic copper sulphate solution.

Copper ions will be produced at the anode, while copper is deposited at the cathode. We start from electrode current densities

$$i_e = i_{e,0}\left[a_M e^{k\alpha_{e,a}\eta_e} - \frac{a_{e,c}}{a_{e,c}^{b}} e^{-k\alpha_{e,c}\eta_e}\right], \tag{2.14}$$

where $i_{e,0}$ is the exchange current density, A/m^2, $a_{e,c}$ and $a^b_{e,c}$ are activities of the copper(II) ions at the electrode surface and at the bulk concentration, which are dimensionless. The apparent transfer coefficients and exchange current densities for both electrodes are assumed equal, because the material of the electrodes (copper) and the electrode reactions are essentially the same (but opposite in direction) $\alpha_{AUX,a} = \alpha_{WE,a} = \alpha_a$, $\alpha_{AUX,c} = \alpha_{WE,c} = \alpha_c$, $i_{AUX,0} = i_{WE,0} = i_0$. The subscript e denotes the electrode in question: WE or AUX.

Equations (2.14) involve electrode overpotentials, which can be calculated upon (2.3) when the electrode potentials and the electrode equilibrium potentials are known. The equilibrium potentials are given by the Nernst equation:

$$\phi_{e,eq} = U_e + k^{-1} \ln \frac{a^b_{e,c}}{a_M}, \tag{2.15}$$

where U_e refers to the reaction standard equilibrium potential equal for (2.13) to 0.337 V vs. standard hydrogen electrode (SHE).

The current densities are coupled by the total cell current and the electrode areas:

$$A_{AUX} i_{AUX} + A_{WE} i_{WE} = 0 . \tag{2.16}$$

Equation (2.16) enables the numerical calculation of the electrode overpotentials and the electrode current densities when the activity of copper(II) ions is known. Furthermore, for both of these, approximate analytical expressions can be derived for a specific case. Indeed, if it can be assumed that $A_{WE} \approx A_{AUX}$ the electrode current densities can be approximated by a single-directional model, which is valid if a large cell voltage is applied.

With a negative applied cell voltage ($\phi_{WE} < \phi_{AUX}$, WE cathode, AUX anode), the electrode current densities can be approximated by the single-directional models

$$i_{AUX} = i_0 a_M e^{k\alpha_a \eta_{AUX}} , \; i_{WE} = -i_0 \frac{a_{WE,c}}{a^b_{WE,c}} e^{-k\alpha_c \eta_{WE}} . \tag{2.17}$$

By substituting the electrode overpotentials (2.3) into (2.17) and then (2.17) into (2.16) we obtain

$$A_{AUX} i_0 a_M e^{k\alpha_a \left(\phi_{AUX} - \phi_{AUX,eq}\right)} - A_{WE} i_0 \frac{a_{WE,c}}{a^b_{WE,c}} e^{-k\alpha_c \left(\phi_{WE} - \phi_{WE,eq}\right)} = 0 . \tag{2.18}$$

Due to the assumption that $A_{WE} \approx A_{AUX}$, the electrode areas ratio $k_A = A_{AUX} / A_{WE}$ equal to 1. The activity of a metal deposited on an electrode made of the same metal is unity (Bard and Faulkner, 2002) and thus $a_M = 1$. Then based on the cell voltage definition (2.4), and still assuming A3 equation (2.18) can be solved for the electrode potentials:

$$\phi_{AUX} = \frac{\alpha_a \phi_{AUX,eq} + \alpha_c \phi_{WE,eq}}{\alpha_a + \alpha_c} - \frac{\alpha_c E - k^{-1} \ln\left(a_{WE,c} / a^b_{WE,c}\right)}{\alpha_a + \alpha_c}, \tag{2.19}$$

$$\phi_{WE} = \frac{\alpha_a \phi_{AUX,eq} + \alpha_c \phi_{WE,eq}}{\alpha_a + \alpha_c} + \frac{\alpha_a E + k^{-1} \ln\left(a_{WE,c} / a_{WE,c}^b\right)}{\alpha_a + \alpha_c}. \tag{2.20}$$

Substituting equations (2.19) and (2.20) into (2.3), an approximation for the electrode overpotentials is obtained, which is valid if a large negative cell voltage is applied

$$\eta_{WE} = \frac{\alpha_a E}{\alpha_a + \alpha_c} + \frac{k^{-1} \ln\left(a_{WE,c} / a_{WE,c}^b\right)}{\alpha_a + \alpha_c}, \tag{2.21}$$

$$\eta_{AUX} = -\frac{\alpha_c E}{\alpha_a + \alpha_c} + \frac{k^{-1} \ln\left(a_{WE,c} / a_{WE,c}^b\right)}{\alpha_a + \alpha_c}. \tag{2.22}$$

An approximation of the WE current density can be obtained by substituting equation (2.21) into (2.17)

$$i_{WE} = -i_0 \left(\frac{a_{WE,c}}{a_{WE,c}^b} \right)^{\frac{\alpha_a}{\alpha_a + \alpha_c}} e^{-k\beta E}, \tag{2.23}$$

where $\beta = \alpha_a \alpha_c / \left(\alpha_a + \alpha_c\right)$. By applying the equation (2.16), knowing WE current density (2.23) and taking into account that $k_A = 1$ we obtain the AUX current density as

$$i_{AUX} = i_0 \left(\frac{a_{WE,c}}{a_{WE,c}^b} \right)^{\frac{\alpha_a}{\alpha_a + \alpha_c}} e^{-k\beta E}. \tag{2.24}$$

Equations (2.21)-(2.24) compose an electrode kinetics model for a Cu-Cu system in the case of the identical electrode areas for the negative cell voltage. Using the technique presented above, one can obtain an approximation of the electrode overpotentials and current densities in the case of a positive applied voltage. The final expressions for an electrode kinetics model for both negative and positive cell voltage are summarized in Table 2.1.

The error, caused by approximating a bi-directional model (2.14) with a single-directional model is largest when the electrode current densities are close to zero. In such a case, the approximation error can be reduced in two ways. First, current density estimates in the case of negative and positive applied voltage can be summed which gives the following estimate

$$i_{WE} = i_0 \left[\left(\frac{a_{AUX,c}}{a_{AUX,c}^b} \right)^{\frac{\alpha_a}{\alpha_a + \alpha_c}} e^{k\beta E} - \left(\frac{a_{WE,c}}{a_{WE,c}^b} \right)^{\frac{\alpha_a}{\alpha_a + \alpha_c}} e^{-k\beta E} \right]. \tag{2.25}$$

Alternatively, the error can be reduced by substituting the electrode overpotentials (2.21) and (2.22) into (2.14). Consequently, the current density at WE is given by

$$i_{WE} = i_0 \left(\frac{a_{WE,c}}{a^b_{WE,c}} \right)^{\frac{\alpha_a}{\alpha_a+\alpha_c}} \left(e^{k\frac{\alpha_a^2}{\alpha_a+\alpha_c}E} - e^{-k\beta E} \right) \quad (E < 0), \tag{2.26}$$

$$i_{WE} = i_0 \left(\frac{a_{AUX,c}}{a^b_{AUX,c}} \right)^{\frac{\alpha_a}{\alpha_a+\alpha_c}} \left(e^{k\beta E} - \frac{a_{WE,c}}{a^b_{WE,c}} \frac{a^b_{AUX,c}}{a_{AUX,c}} e^{\frac{-k\alpha_c^2}{\alpha_a+\alpha_c}E} \right) \quad (E > 0). \tag{2.27}$$

Equation (2.25) is preferable, because in contrast to equations (2.26) and (2.27) it produces a smooth curve when the voltage is changed from negative to positive values.

Table 2.1: The electrode kinetics model

$E < 0$	$E > 0$
$\eta_{WE} = \frac{\alpha_a E}{\alpha_a+\alpha_c} + \frac{k^{-1}\ln\left(a_{WE,c}/a^b_{WE,c}\right)}{\alpha_a+\alpha_c}$	$\eta_{WE} = \frac{\alpha_c E}{\alpha_a+\alpha_c} + \frac{k^{-1}\ln\left(a_{AUX,c}/a^b_{AUX,c}\right)}{\alpha_a+\alpha_c}$
$\eta_{AUX} = -\frac{\alpha_c E}{\alpha_a+\alpha_c} + \frac{k^{-1}\ln\left(a_{WE,c}/a^b_{WE,c}\right)}{\alpha_a+\alpha_c}$	$\eta_{AUX} = -\frac{\alpha_a E}{\alpha_a+\alpha_c} + \frac{k^{-1}\ln\left(a_{AUX,c}/a^b_{AUX,c}\right)}{\alpha_a+\alpha_c}$
$i_{WE} = -i_0 \left(\frac{a_{WE,c}}{a^b_{WE,c}} \right)^{\frac{\alpha_a}{\alpha_a+\alpha_c}} e^{-k\beta E}$	$i_{WE} = i_0 \left(\frac{a_{AUX,c}}{a^b_{AUX,c}} \right)^{\frac{\alpha_a}{\alpha_a+\alpha_c}} e^{k\beta E}$
$i_{AUX} = i_0 \left(\frac{a_{WE,c}}{a^b_{WE,c}} \right)^{\frac{\alpha_a}{\alpha_a+\alpha_c}} e^{-k\beta E}$	$i_{AUX} = -i_0 \left(\frac{a_{AUX,c}}{a^b_{AUX,c}} \right)^{\frac{\alpha_a}{\alpha_a+\alpha_c}} e^{k\beta E}$

The developed model, presented by the equations in Table 2.1 and (2.25), gives a way of calculating an electrode current density which is dependent on the applied voltage and the activity of species. To obtain these activities we specify a mass-transfer model for the system.

2.3.2 Mass-transfer model

There are three forms of mass transfer: diffusion, convection and migration. The situation when all three forms occur simultaneously complicates analysis of the system. Because of this the experimental conditions in electrochemistry commonly employed in such a way that the convection and migration phenomena are suppressed. Convection is eliminated by preventing stirring of the electrochemical cell, and migration by adding a supporting electrolyte to the solution (see, e.g. eds Smyth and Vos, 1992; Wang, 2000; Bard and Faulkner, 2001). Then according to Fick's second law for one-dimensional mass transfer the concentration of ions at the cathode surface is diffusion-controlled along the *x*-axis (normal to cathode surface) as

$$\frac{\partial c(x,t)}{\partial t} = \frac{\partial}{\partial x}\left(D(c)\frac{\partial c(x,t)}{\partial x} \right), \tag{2.28}$$

where $D(c)$ is the concentration-dependent diffusivity coefficient, m^2/s. In dilute solutions, considered in voltammetric theory, such dependence is modest, and by assuming constant diffusivity, one can come to (2.7). However, in a general case this dependence can be very marked (Crank, 1975).

The initial concentration distribution of species is assumed to be uniform in the stagnation layer and equal to the bulk solution concentration

$$c(x,0) = c_b\,. \tag{2.29}$$

The condition on the cathode is given by the first Fick law and states that the molar flux of Cu(II) ions is proportional to the cathode current density

$$D(c)\frac{\partial c(x,t)}{\partial x}\Big|_{x=0} = -\frac{i_{WE}(t)}{2F}\,. \tag{2.30}$$

The condition at the outer boundary is given by

$$c(\infty,t) = c_b\,. \tag{2.31}$$

Similarly, the concentration of ions at the anode surface is diffusion-controlled, with the condition at anode

$$D(c)\frac{\partial c(x,t)}{\partial x}\Big|_{x=0} = -\frac{i_{AUX}(t)}{2F}, \tag{2.32}$$

For computational purposes, instead of two diffusion equations one can be solved where the position of cathode is set to 0 with a boundary condition (2.30) and position of anode is set to d, where d is the distance between the electrodes (m) with a boundary condition (2.32). In such a statement the concentration at the middle point along the finite-length interval of the x-axis is supported to be equal to the bulk solution concentration

$$c\left(\frac{d}{2},t\right) = c_b\,. \tag{2.33}$$

Noulty and Leaist (1987) have determined conductimetrically the diffusivity of Cu(II) ions in aqueous copper sulphate and copper sulphate with sulfuric acid solutions. They have presented their results numerically in tabled form as a dependence of diffusivity on the Cu(II) ions concentration. Based on this data in this thesis the following formula has been derived and utilized further in process modeling:

$$D(c) = 8.27\cdot 10^{-10} - 6.03\cdot 10^{-11}\ln(c)\,. \tag{2.34}$$

Solving the mass-transfer equation (2.28) with appropriate boundary conditions (2.29)-(2.31) and the diffusivity given by (2.34) yields a concentration curve and successively,

the Cu(II) ion activity on the copper electrode can be calculated as follows (Pohjoranta and Tenno, 2007) :

$$a_{Cu} = \frac{c}{c_0}\left(\frac{c+3.5}{c_0+3.5}\right)^{-0.5554}, \tag{2.35}$$

where c_0 is the standard concentration, 1000 mol/m^3. Figure 2.3 illustrates the relationship (2.35). One can observe that this dependence is nonlinear, meaning that using concentrations instead of activities brings a certain inaccuracy to the model.

In further text we will consider only oxidizing species. Consequently, the subscript O will be omitted for convenience.

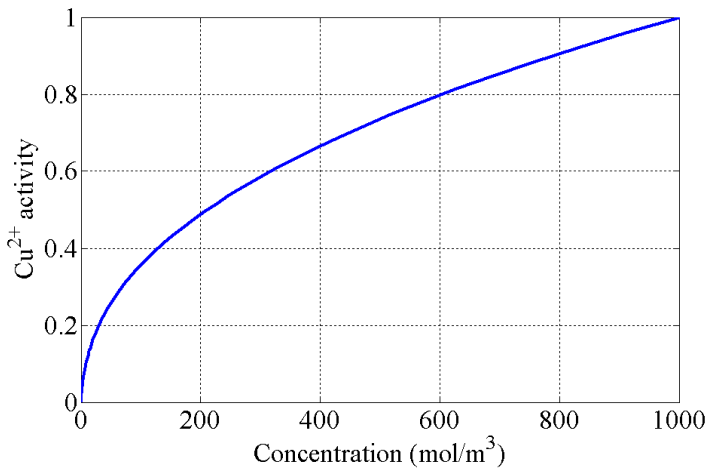

Figure 2.3: The relationship between Cu^{2+} activity a_{Cu} and concentration of the Cu^{2+} ions.

2.3.3 Ohmic potential drop

Ohmic potential drop, also known as iR drop, is a potential drop caused by the flow of current through the solution resistance. The problem of compensating the cell solution resistance in voltammetric analysis has been extensively studied by many researchers (Nicholson, 1965a; Britz, 1978; Wipf, 1996; Myland and Oldham, 2000). Even a sufficiently small uncompensated resistance can significantly distort electrochemical measurements when the cell current is high. The effects of ohmic drop on linear and cyclic sweep voltammetry, indicated in the literature, include displacement of the voltammograms along the voltage axis, which leads to a shift in peak potential, and flattening, which leads to a decrease of peak current (Nicholson, 1965a; Britz, 1978; Brett and Brett, 1993; Bard and Faulkner, 2001).

The theoretical basis for analysis of uncompensated resistance is addressed in the works of Nicholson (1965a) and White and Lawson (1970) in connection with a metal deposition case. Considering uncompensated resistance complicates the analysis since, being initially linear, boundary value problems take the form of nonlinear integral or integro-differential equations (Nicholson, 1965a). Therefore, correct compensation of the cell solution resistance becomes an important aspect of modeling electrode kinetics.

In the above model derivation, the influence of the ohmic potential drop was not taken into account. This question is treated below.

Due to cell resistance, the effective power of the electrolysis cell decreases on value of ohmic drop U_d, V. Then, with a negative applied cell voltage the electrode overpotential equations (2.21)-(2.22) have to be corrected as follows

$$\eta_{WE,U_d} = \frac{\alpha_a \left(E - U_d\right)}{\alpha_a + \alpha_c} + \frac{k^{-1} \ln\left(a_{WE,c} / a_{WE,c}^b\right)}{\alpha_a + \alpha_c}, \tag{2.36}$$

$$\eta_{AUX,U_d} = -\frac{\alpha_c \left(E - U_d\right)}{\alpha_a + \alpha_c} + \frac{k^{-1} \ln\left(a_{WE,c} / a_{WE,c}^b\right)}{\alpha_a + \alpha_c}. \tag{2.37}$$

In equations (2.36) and (2.37), subscript U_d means that in the electrode overpotentials effect of the ohmic drop is taken into account. Because analysis of the AUX electrode is similar to that of the WE electrode, in the coming text we proceed only with the WE electrode and then give only a final result for AUX. Comparing equations (2.21) and (2.36), one can find the correction term for WE overpotential as

$$\eta_{WE,U_d} = \eta_{WE} - \frac{\alpha_a U_d}{\alpha_a + \alpha_c}. \tag{2.38}$$

Substituting equation (2.38) into (2.17), an approximation for the WE electrode current density is obtained, which takes into account the ohmic losses

$$i_{WE} = -i_0 \frac{a_{WE,c}}{a_{WE,c}^b} e^{-k\alpha_c\left(\eta_{WE} - \frac{\alpha_a U_d}{\alpha_a + \alpha_c}\right)}. \tag{2.39}$$

To go further and derive an analytical formula to compute the current density expression for the ohmic drop is required. In an electrochemical cell, the potential drop depends on solution conductivity, the geometry of the electrodes, their location and area. For the plane electrodes of the same geometry and area with uniform current density across their surface

$$U_d = \frac{d}{\sigma} i_{WE}, \tag{2.40}$$

where d is the distance between the electrodes, m, and σ is the solution conductivity, S. Then, substituting (2.40) into (2.39) and rearranging the terms we obtain

$$i_{WE} e^{-k\beta \frac{d}{\sigma} i_{WE}} = -i_0 \frac{a_{WE,c}}{a_{WE,c}^b} e^{-k\alpha_c \eta_{WE}}. \tag{2.41}$$

Equation (2.41) is a transcendental equation with regard to current density and cannot be solved in terms of elementary functions. However, more deep insight shows that the Lambert W function, known also as Omega function, can be used to solve (2.41).

The Lambert W-function is the inverse of $f(W) = We^W$ (Weisstein, 2009). Numerous examples of its application in pure and applied mathematics have been reported (Corless et al., 1996). Utilizing the Lambert function one can write the solution of (2.41) as follows

$$i_{WE} = \frac{W\left[k\beta\frac{d}{\sigma}i_0\frac{a_{WE,c}}{a_{WE,c}^b}e^{-k\alpha_c\eta_{WE}}\right]}{-k\beta\frac{d}{\sigma}}. \tag{2.42}$$

Equation (2.42) was derived under the assumption of the same electrodes areas and a uniform current density. When this assumption fails, using equation (2.42) can lead to marked errors in modeling. However, what only has to be changed is the ohmic potential drop expression (2.40). In the case of simple electrodes geometry and similar, but different areas, another analytical formula can be obtained. For planar circle electrodes with radiuses R_{WE} and R_{AUX} the current density can be assumed flowing through the conductor in the form of truncated cone as illustrated in Fig. 2.4. One can consider a cross-sectional disc of thickness Δx and radius r with resistance $R_{\Delta x}$ given by the following equation

$$R_{\Delta x} = \frac{1}{\sigma}\frac{\Delta x}{A}, \tag{2.43}$$

where A is the cross-sectional area, m^2.

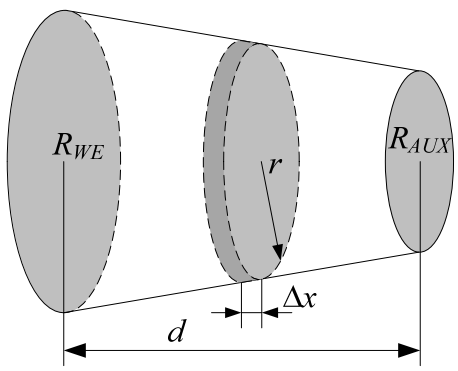

Figure 2.4: Conductor formed by two planar circle electrodes

The resistance of the overall cone composed of N such discs that are in a series connection

$$R = \sum_{i=1}^{N}\frac{1}{\sigma}\frac{\Delta x}{A_i}. \tag{2.44}$$

Approaching disc thickness Δx to zero, (2.44) takes the following form

$$R = \int_0^d \frac{1}{\sigma}\frac{dx}{A(x)}. \tag{2.45}$$

As mentioned above the electrodes were assumed to be circles, therefore

$$A(x) = \pi r^2(x). \tag{2.46}$$

It can be easily established that the relationship between disc radius and the location along the x-axis is given by

$$r(x) = R_{WE} + \frac{R_{AUX} - R_{WE}}{d}x. \tag{2.47}$$

Substituting (2.47) into (2.46) and then into (2.45), and then further calculating the integral in (2.45) one can find an expression for the cell solution resistance as

$$R = \frac{d}{\sigma} \frac{1}{\sqrt{A_{WE} A_{AUX}}} . \tag{2.48}$$

Therefore, for planar circle electrodes

$$U_d = \frac{d}{\sigma \sqrt{k_A}} i_{WE} = \frac{d\sqrt{k_A}}{\sigma} i_{AUX} . \tag{2.49}$$

Thus, utilizing (2.49) the WE current density takes a form similar to equation (2.42)

$$i_{WE} = \frac{W\left[k\beta \frac{d}{\sigma\sqrt{k_A}} i_0 \frac{a_{WE,c}}{a_{WE,c}^b} e^{-k\alpha_c \eta_{WE}} \right]}{-k\beta \frac{d}{\sigma\sqrt{k_A}}} . \tag{2.50}$$

Equation (2.50) is a general equation to find electrode current density and equation (2.42) is its particular case for the same electrode areas. It should be emphasized that the electrodes areas should not be very different. Otherwise, approximation of the solution by truncated cone conductor formed by two planar circle electrodes as illustrated in Fig. 2.4 will be inaccurate. In such a case one can use better approximation, where ohmic losses are estimated by the sum of the losses close to the electrodes and losses in the main electrolyte (Pohjoranta et al., 2010).

In a similar way, one can obtain an approximation of the electrode overpotentials and current densities in the case of positive cell voltage. The final expressions for an electrode kinetics model that takes into account the ohmic drop for both negative and positive cell voltage are summarized in Table 2.2 for the case of the same electrode areas.

Similar to fully compensated voltage drop the approximation error in the case of small voltages can be reduced by either substituting the electrode overpotential into a bi-directional model (2.14) an obtaining two different expressions for the current density at WE or by summing the estimates in the case of negative and positive applied voltage which leads to the following expression:

$$i_{WE} = \frac{W\left[k\beta \frac{d}{\sigma} i_0 e^{k\alpha_a \eta_{WE}^{(E>0)}} \right]}{k\beta \frac{d}{\sigma}} - \frac{W\left[k\beta \frac{d}{\sigma} i_0 \frac{a_{WE,c}}{a_{WE,c}^b} e^{-k\alpha_c \eta_{WE}^{(E<0)}} \right]}{k\beta \frac{d}{\sigma}} . \tag{2.51}$$

The current density equations in Table 2.2 use the WE electrode overpotential without the voltage drop being taken into account. This is computed according to the expressions listed in Table 2.1.

Table 2.2: The electrode kinetics model with the ohmic drop taken into account

$E < 0$	$E > 0$
$i_{WE} = \dfrac{W\left[k\beta\dfrac{d}{\sigma}i_0\dfrac{a_{WE,c}}{a_{WE,c}^b}e^{-k\alpha_c\eta_{WE}}\right]}{-k\beta\dfrac{d}{\sigma}}$	$i_{WE} = \dfrac{W\left[k\beta\dfrac{d}{\sigma}i_0 e^{k\alpha_a\eta_{WE}}\right]}{k\beta\dfrac{d}{\sigma}}$
$i_{AUX} = \dfrac{W\left[k\beta\dfrac{d}{\sigma}i_0\dfrac{a_{WE,c}}{a_{WE,c}^b}e^{-k\alpha_c\eta_{WE}}\right]}{k\beta\dfrac{d}{\sigma}}$	$i_{AUX} = \dfrac{W\left[k\beta\dfrac{d}{\sigma}i_0 e^{k\alpha_a\eta_{WE}}\right]}{-k\beta\dfrac{d}{\sigma}}$
$\eta_{WE,U_d} = \dfrac{\alpha_a(E-U_d)}{\alpha_a+\alpha_c} + \dfrac{\ln\left(a_{WE,c}/a_{WE,c}^b\right)}{k(\alpha_a+\alpha_c)}$	$\eta_{WE,U_d} = \dfrac{\alpha_c(E-U_d)}{\alpha_a+\alpha_c} + \dfrac{\ln\left(a_{AUX,c}/a_{AUX,c}^b\right)}{k(\alpha_a+\alpha_c)}$
$\eta_{AUX,U_d} = \dfrac{\alpha_c(U_d-E)}{\alpha_a+\alpha_c} + \dfrac{\ln\left(a_{WE,c}/a_{WE,c}^b\right)}{k(\alpha_a+\alpha_c)}$	$\eta_{AUX} = \dfrac{\alpha_a(U_d-E)}{\alpha_a+\alpha_c} + \dfrac{\ln\left(a_{AUX,c}/a_{AUX,c}^b\right)}{k(\alpha_a+\alpha_c)}$

2.4 Model validation

To verify the electrode kinetic model presented in Table 2.1, the simulation model under the COMSOL Multiphysics 3.3 software package was built and linear sweep voltammetry (LSV) experiments were performed on a laboratory-scale Cu-Pt electrochemical cell. The experimental setup shown in Fig. 2.5 consists of the electrochemical cell, data acquisition (DAQ) board and a personal computer (PC). The input voltage was set in the PC and applied to the electrochemical cell. Then the cell current and the voltages caused by the applied voltage were measured and transferred into the PC by using the DAQ board. The data were collected and visualized using the MATLAB Data Acquisition Toolbox.

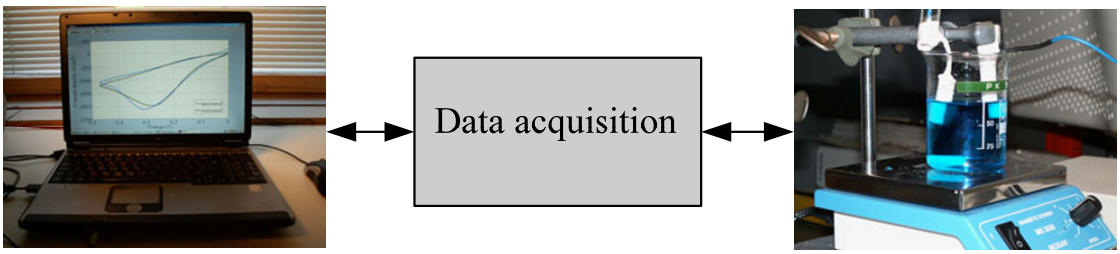

Figure 2.5: Experimental setup.

While the experimental setup shown in Fig. 2.5 is 3-dimensional, the assumption of one-dimensional diffusion was utilized in the modeling. This assumption is commonly

used in practice and reasonable if the electrodes are of the planar form and so thin that an amount of the diffusing substance entering through the edges is negligible compared with substance entering through the plane faces (Crank, 1975). The picture on the geometry of the model looks as shown in Fig. 2.4. In such a case, a concentration gradient occurs only along x-axis. Though this assumption is not strictly valid, it can be considered as certain simplification in the modeling.

A cylindrical glass of approximately 150 ml in volume is used as the electrochemical cell. The cell consists of copper WE electrode and platinum AUX electrode immersed in an aqueous solution, the composition of which is listed in Table 2.3. The apparatus for voltammetric measurements is shown in Fig. 2.6. The shunt resistor is used to measure the current, because it cannot be measured directly using the DAQ board. A saturated copper electrode acting as a reference electrode was included into the system to reduce the effect of voltage drop.

Values of magnitude E_M and sweep rate ν of the input voltage, area of the WE electrode and the areas ratio utilized in the experiment are listed in Table 2.4.

Table 2.3: Solution composition

Component	Concentration
$CuSO_4$	0.8 mol/l
H_2SO_4	1.0 mol/l
HCl	1.0 mmol/l

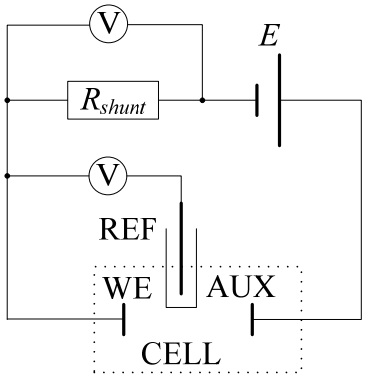

Figure 2.6: Apparatus for voltammetric measurements.

The least-square performance function continues to be most useful in estimation applications and, therefore, the model parameters were optimized to minimize the mean square error between the measured and predicted current densities on the WE electrode

$$J\left(i_0,\alpha_a,\alpha_c\right)=\frac{1}{N}\sum_{j=1}^{N}\left(\xi_{WE}(t_j)-i_{WE}(t_j,i_0,\alpha_a,\alpha_c)\right)^2 . \tag{2.52}$$

In equation (2.52), ξ_{WE} is the measured WE electrode current density, i_{WE} is the predicted by the model WE electrode current density and N is the number of measurements.

The current-density measurements were recorded with a sampling rate of 0.02 seconds and a total of $N = 470$ samples were collected. The kinetic parameters of the equivalent Cu-Cu model were estimated by a direct search method. The estimates are listed in Table 2.5. The performance criterion (2.52) at the optimum point was 9998 that corresponds to root mean square error equal to 100 A/m^2. No parameters were found

which give better value of the performance function. Therefore, we can conclude that the solution is unique.

Table 2.4: The values of parameters used in voltammetry experiment

Parameter	Unit	Value
ν	V/s	0.1
E_M	V	0.47
A_{WE}	m^2	$3.5 \cdot 10^{-6}$
k_A	-	10

The measured current-density-potential curve and its estimate, computed on the equivalent Cu-Cu model by minimizing the least-square performance function (2.52) is depicted in Fig. 2.7. Such curves are often referred to as voltammograms. They are known to be informative about the reactions occurring at the electrodes. Particularly, under certain assumptions the electrode kinetic and mass-transfer parameters can be easily estimated (Bard and Faulkner, 2001).

Table 2.5: The kinetics parameters used in simulation

Parameter	Unit	Value
i_0	A/m^2	150
α_a	-	0.84
α_c	-	0.16

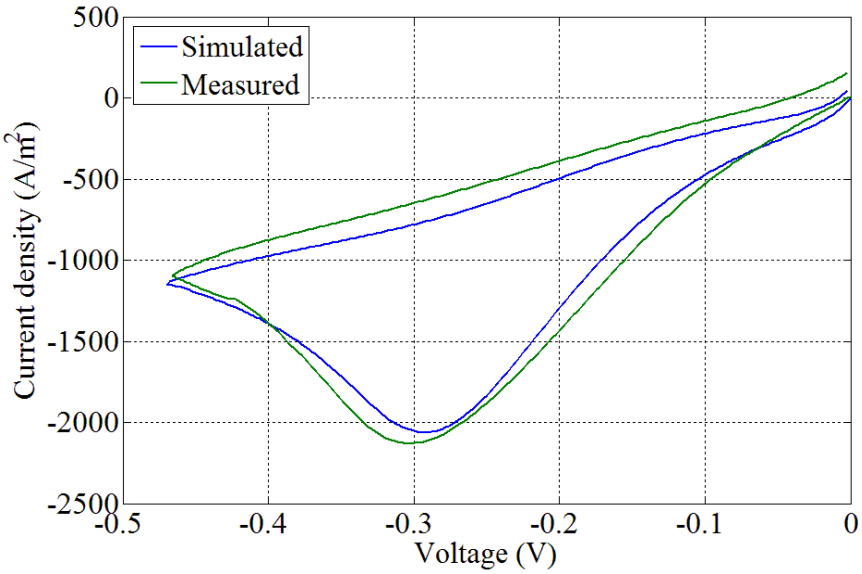

Figure 2.7: Measured current-density – potential curve and its estimate, computed on the Cu-Cu model by minimizing the least-square performance function (2.52).

Fig. 2.7 shows that the model is in relatively good agreement with the experimental data. This allows us to reconstruct physical quantities which are not directly available or cannot be measured, such as the concentration of copper ions on the electrode surfaces (Fig. 2.8), concentration profile (Fig. 2.9), the electrode overpotentials (Fig. 2.10) and the stagnation layer thickness (Fig. 2.11).

Fig. 2.8 shows that the more negative the applied cell voltage is, the lower the Cu(II) concentration is on the WE and, correspondingly, the higher the Cu(II) concentration is on the AUX. However, the WE concentration changes within a wider range than that on the AUX (Fig. 2.9). This indicates a difference in the areas of the electrodes, namely that the area of AUX is larger than that of the WE.

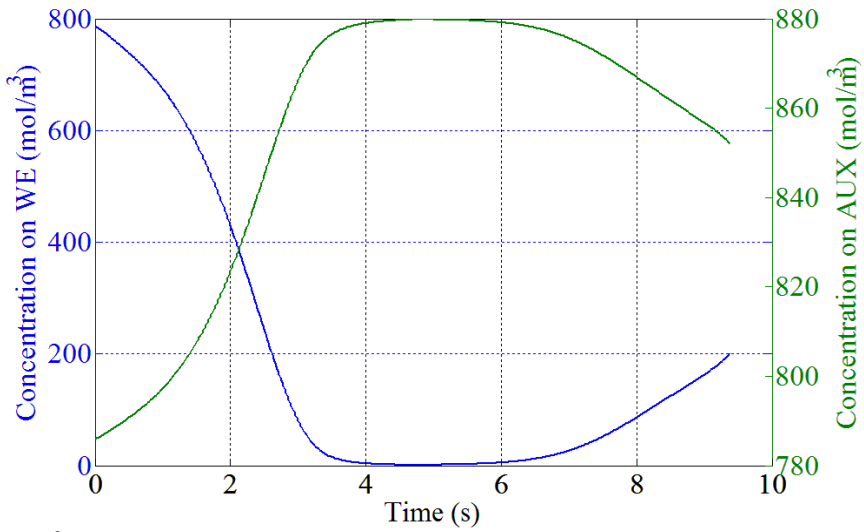

Figure 2.8: Cu^{2+} ion concentration at the WE and AUX electrode surfaces, reconstructed with the electrode kinetic model (2.21)-(2.24) and mass-transfer model (2.28)-(2.35).

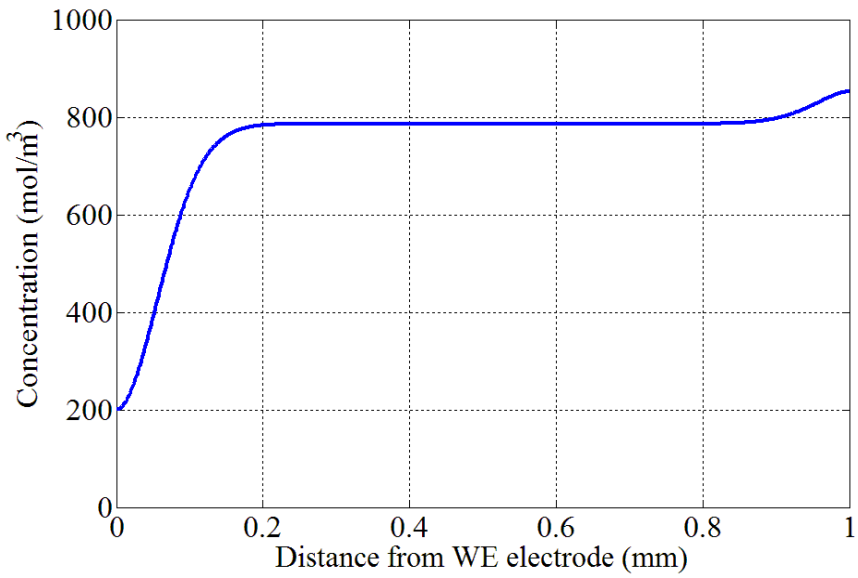

Figure 2.9: Cu^{2+} ion concentration profile $c(x, t)$ at time $t = 10$ s, reconstructed with the electrode kinetic model (2.21)-(2.24) and mass-transfer model (2.28)-(2.35).

A similar conclusion follows from Fig. 2.10 that clearly shows that the overpotential of the WE electrode is considerably smaller than that of the AUX electrode. Fig. 2.11 illustrates the growth of the stagnation layer thickness during the LSV experiment. The thickness was calculated as the distance from the WE electrode where the Cu^{2+} ion concentration is above 95% of the bulk solution concentration.

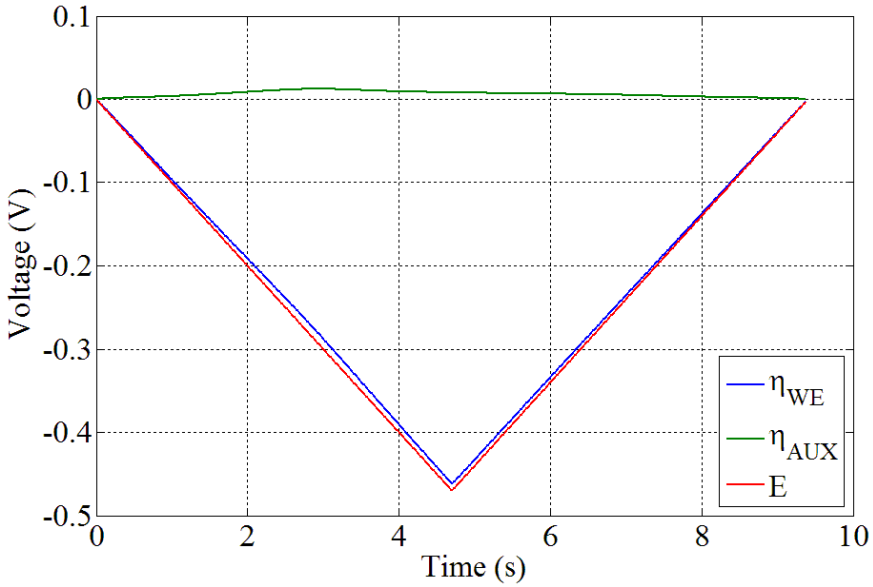

Figure 2.10: Electrode overpotentials and input voltage, reconstructed with the electrode kinetic model (2.21)-(2.24) and mass-transfer model (2.28)-(2.35).

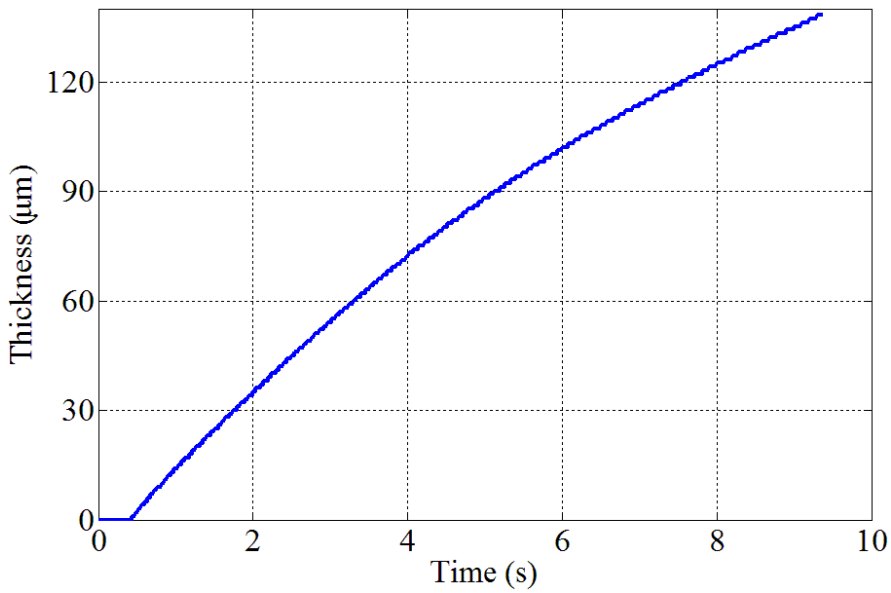

Figure 2.11: Stagnation layer thickness, reconstructed with the electrode kinetic model (2.21)-(2.24) and mass-transfer model (2.28)-(2.35).

For comparison, the Cu-Cu electroplating process was estimated using a model of irreversible electrochemical systems, whose current equation is a one-sided approximation of the electrode equation (2.6)

$$I_{WE} = -I_0 \frac{c(0,t)}{c_b} e^{-k\alpha_c(E-E_{eq})}. \tag{2.53}$$

The semi-infinite diffusion model (2.7)-(2.10) was used as a mass-transfer model as it is frequently used in the conventional LSV experiments. While the conventional estimation method of identifying the kinetic parameters as well as mass-transfer parameters of the electrochemical cell is known (Bard and Faulkner, 2001), it is based only on the measurements of the peak current, its position and position at half-peak current, while the rest of the curve is ignored. This method is discussed in more details in Chapter 3 of this thesis. And in this section to use the whole set of the measurements, the direct search method was utilized and the estimates are listed in Table 2.6.

Table 2.6: The kinetics parameters for irreversible model

Parameter	Unit	Value
i_0	A/m^2	42
α_c	-	0.25
D	m^2/s	$4.54 \cdot 10^{-10}$

The current-density-potential curve of the model is illustrated in Fig. 2.12 and the concentration evolution on the WE electrode is shown in Fig. 2.13.

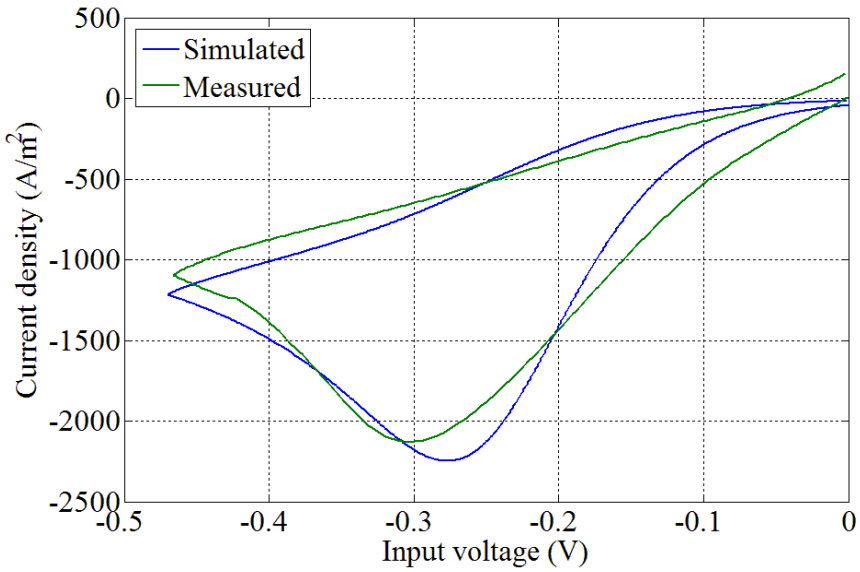

Figure 2.12: Measured current-density – potential curve and its estimate, computed based on the irreversible electrode kinetic model (2.53) and semi-infinite diffusion by minimizing the least-square performance function (2.52).

The performance criterion (2.52) at the optimum point was equal to J = 16470 that corresponds to root mean square error equal to 128 A/m^2.

Since conventional knowledge-based identification assumes constant diffusivity, this parameter was also estimated. The results shown in Figs 2.7 and 2.12 demonstrate that

the proposed model outperforms the conventional model for irreversible reactions in the case of saturated solution.

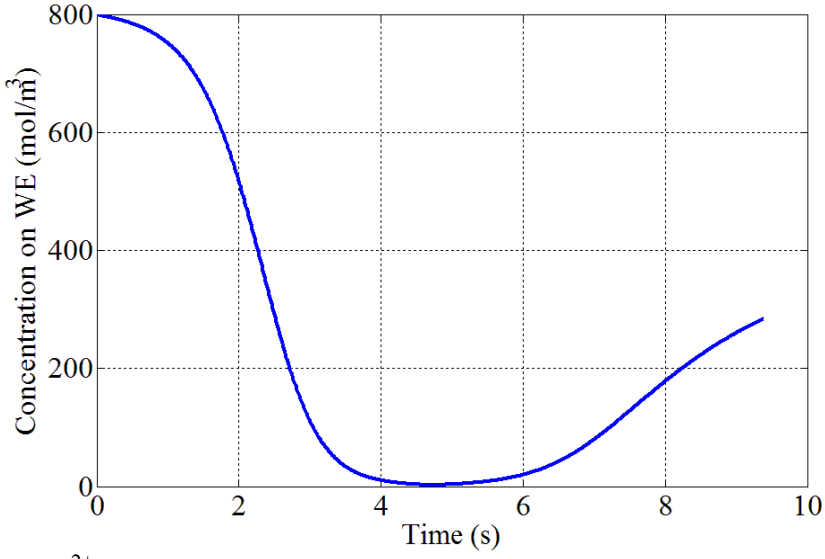

Figure 2.13: Cu^{2+} ion concentration at the WE electrode, reconstructed with the irreversible electrode kinetic model (2.53) and semi-infinite diffusion model (2.7)-(2.10).

2.5 Conclusions

A computational electrode kinetics model was developed for a Cu-Cu system. The system arises from plating chemistry where voltammetric measurements obtained during a sweep-shaped input voltage are commonly used for parameter estimation. The model enables monitoring the studied system, particularly, the concentration of copper ions on the electrode surfaces, the whole concentration profile, the electrode overpotentials and the stagnation layer thickness can be reconstructed. Therefore, the model-based control can be designed to maintain, for instance, the desired copper deposit thickness.

Chapter 3

Identifiability analysis and knowledge-based identification of electrochemical cells

3.1 Introduction

When one starts to fit the measured data to a physical model the following fundamental question arises: *can the model provide unique values of the model parameters under assumption of noiseless measurements?* This question is known as an identifiability question. If the model can be estimated uniquely then it is possible to understand its dependence on the physical parameters and to test hypotheses about the real process. In another case several sets of the parameters lead to an identical estimation quality with respect to measurements, so the model cannot be used to make unambiguous conclusions.

Berthier et al. (1996) have first introduced the concept of identifiability in the context of electrochemical models. It is mentioned that despite its importance identifiability is still widely ignored. There are several definitions of identifiability that all say the same: the model is identifiable if the model parameters can be uniquely recovered from input-output data (Walter and Pronzato, 1990; Ljung and Glad, 1994). More formally, the model structure $M(\theta^*)$ is said to be globally identifiable, if $M(\theta) = M(\theta^*)$ implies $\theta = \theta^*$ for almost any θ^* (Berthier et al.,1996; Ljung, 1999). One can also define local identifiability, requiring that $M(\theta) = M(\theta^*)$ implies $\theta = \theta^*$ for almost any θ^* in a neighborhood of θ^*. Bellman and Aström (1970) proposed another a method-oriented definition of identifiability. Following to that the structure M is said to be locally (globally) identifiable, if the cost function to be minimized in the identification algorithm has a local (global) minimum at $\theta = \theta^*$ (Nguyen and Wood, 1982).

Usually, the model is identifiable only under certain conditions known as the identification conditions. The identifiability is a challenging problem, especially for nonlinear models. Often all the parameters cannot be identified simultaneously. However, if a certain subset of the parameters can be estimated uniquely the model is still partially identifiable. Rarely, it is possible to prove unique estimation and find identifiability conditions analytically, and, therefore, numerical schemes are utilized to deal with it. One such numerical test for detecting parameters appearing in combinations was proposed by Rakitskii et al. (1982). Another numerical method for

examining the identifiability of the nonlinear models based on the numerical Jacobi matrix was developed by Gorskii et al. (1987).

There is a number of works studying the identifiability of the models that are nonlinear in the parameters with relevance for reaction kinetics (Klibanov et al., 1973, Lukashenok, 1979; Gorskii et al., 1987). However, voltammetric studies discuss only estimation of the kinetic and mass-transfer parameters without any investigation of identifiability.

In this chapter we will address the question of the identifiability of the electrochemical cell models. We should emphasize that we are concerned with the theoretical identifiability regardless of the estimation method employed. Basically, the identifiability issue involves the following aspects (Ljung, 1999): (i) Are the experimental conditions or data set informative enough? (ii) Is the model structure invertible with respect to the unknown parameters? We will discuss these questions under the step and sweep form of applied voltage.

In the latter case the current-potential curve is hysteresis-shaped. Methods for estimating the mass-transfer and kinetic parameters of conventional electrochemical cell models that utilize peak value and peak position of the curve have been developed (Matsuda and Ayabe, 1955; Nicholson and Shain, 1964; Bard and Faulkner, 2001). Because such parameter estimation methods are based on our knowledge about the shape of the plot where the output variable (current density) is plotted against input (applied voltage), we will refer to such methods as knowledge-based methods.

Two international conference papers have been published on the topic of this chapter (Mendelson and Tenno, 2007a, 2008a).

3.2 Contribution

The following contributions are covered in this chapter:

1. Identifiability of the model for an agitated electrochemical cell is analyzed under constant electrode voltage applied. It is proven that under the assumption of current density measurements the model is globally identifiable. The method of identifying electrode kinetic parameters based on a series of voltage step experiments is proposed.
2. A method for identifying the mass-transfer parameters as well as kinetic parameters for the electrochemical cell is proposed for a specific case of constant diffusivity and a semi-infinite boundary condition.

3.3 Identifiability under step form of applied voltage

Most of the electrochemical models are given in the form of partial differential equations to describe mass-transfer of reacting species. The identifiability problem of

parameters appearing in PDEs has been studied widely (Kitamura and Nakagiri, 1977; Pierce, 1979; Courdesses et al., 1981, Lahouaoula and Courdesses, 1989; Giudici, 1991; Orlov and Bentsman, 2000). Courdesses et al. (1981) have derived analytically a number of identifiability results for a one-dimensional linear diffusion equation. They considered the case of similar boundary conditions on different parts of the boundary. As a consequence, the eigenvalues of the problem they have examined are linear in the unknown parameters. Moreover, in their studies the parameters to be identified appear only in the PDE itself. Inspired by their work we extend the results to include the case of mixed boundary conditions which, as well as the diffusion equation, contain a number of the unknown parameters.

Consider the diffusion equation (2.7) with a uniform initial condition (2.8) and the condition at the cathode boundary (2.9). Assume that the solution is well stirred, that gives the second boundary condition as

$$c(\delta,t)=c_b\,, \tag{3.1}$$

where δ is the stagnation layer thickness, m. Assume a constant negative voltage applied. Then the current-overpotential equation (2.6) can be approximated by the single directional model

$$I_e=-I_{e,0}\frac{c(0,t)}{c_b}e^{-k\alpha_{e,c}(E-E_{eq})}. \tag{3.2}$$

Substituting (3.2) into (2.9) and taking into account a constant voltage, condition at the cathode can be rewritten as

$$D\frac{\partial c(x,t)}{\partial x}\Big|_{x=0}=k_c c(0,t)\,, \tag{3.3}$$

where the kinetic coefficient k_c is shorthand for the term $\frac{I_{e,0}}{c_b nFA}e^{-k\alpha_{e,c}(E-E_{eq})}$ (m/s).

The condition (3.1), specifying the value of the concentration at the boundary, is known as a Dirichlet boundary condition (Pinchover and Rubinstein, 2005). The condition (3.3), specifying a relation between the concentration and its derivative at the boundary, is known as a Robin boundary condition. Thereby, the studied equation is subject to mixed boundary conditions, because different conditions are involved on different parts of the boundary.

The objective of this section is to answer the identifiability question about the diffusivity, diffusion length and the kinetic coefficient. Because of the physical meaning, we look only for positive values of these parameters. Pursuing our goal, we consider the cases of concentration at the boundary and cell current measurements.

3.3.1 Concentration boundary measurements

Consider a pointwise measurement on the system

$$y(t) = c(0,t), \tag{3.4}$$

and study the question of the identifiability of the kinetic coefficient, diffusivity coefficient and stagnation layer thickness. The model of the system is given by

$$\frac{\partial c_m(x,t)}{\partial t} = D_m \frac{\partial^2 c_m(x,t)}{\partial x^2}, \tag{3.5}$$

where D_m is the diffusivity coefficient of the model (m^2/s) that is assumed to be constant. The initial distribution of the reacting species in the model is assumed to be homogeneous in the stagnation layer and equal to the bulk solution concentration

$$c_m(x,0) = c_b. \tag{3.6}$$

The boundary condition on the cathode is given by the first Fick law

$$D_m \frac{\partial c_m(x,t)}{\partial x}\Big|_{x=0} = k_{c,m} c_m(0,t), \tag{3.7}$$

Concentration on the stagnation layer outer boundary of the model equals to the bulk solution concentration

$$c_m(\delta_m,t) = c_b. \tag{3.8}$$

Under an assumption of pointwise measurement on the model

$$y_m(t) = c_m(0,t). \tag{3.9}$$

Following to Kitamura and Nakagiri (1977) and Courdesses et al. (1981) the parameters D, k_c and δ are said to be identifiable if $D = D_m$, $k_c = k_{c,m}$ and $\delta = \delta_m$ follows uniquely from the relation $e(t) = y(t) - y_m(t) = 0$ for all $t \geq 0$, where $e(t)$ is the error between the output of the process and output of the plant.

It is easy to establish that the parameters D, k_c and δ appear in combination and, therefore, are not identifiable. Indeed, designating new thickness as l (m) and by applying a change of variables

$$z = \frac{l}{\delta} x$$

with respect to the PDE (2.7) with the initial condition (2.8), boundary conditions (3.1), (3.3) and the pointwise measurements on the system (3.4) yields the following diffusion equation

$$\frac{\partial c(z,t)}{\partial t} = \frac{l^2 D}{\delta^2} \frac{\partial^2 c(z,t)}{\partial z^2}. \tag{3.10}$$

The initial condition and condition at the outer boundary for (3.10) remain similar to that of (2.7) while the boundary condition at the cathode is given by

$$\frac{l^2 D}{\delta^2}\frac{\partial c(z,t)}{\partial z}\Big|_{z=0} = \frac{lk_c}{\delta}c(0,t). \tag{3.11}$$

The system output is not affected by the change of variables and, therefore,

$$y(t) = c(0,t). \tag{3.12}$$

The system (2.8), (3.1), (3.10)-(3.12) given by the triple (l^2D/δ^2, lk_c/δ, l) produces the identical output as the original system (2.7), (2.8), (3.1), (3.3) and (3.4), and, because of that, the parameters D, k_c and δ are not identifiable simultaneously. Then the following question arises: *can the model provide unique value of one of the parameters or any pair of parameters?*

To answer the question, we utilize an analytical solution of the PDE (2.7) with the initial condition (2.8), and the boundary conditions (3.1), (3.3). Reducing the nonhomogeneous boundary condition (3.6) to the homogeneous case and applying the separation of variables method (Pinchover and Rubinstein, 2005) yields the solution

$$c(x,t) = \frac{c_b(D+k_c x)}{D+k_c\delta} + \sum_{n=1}^{\infty}\frac{2k_c^2 c_b}{\delta k_c^2 + k_c D + \lambda_n^2 \delta D^2}\left[\frac{1}{\lambda_n}\sin(\lambda_n x) + \frac{D}{k_c}\cos(\lambda_n x)\right]e^{-\lambda_n^2 Dt},$$

where $\{\lambda_n\}$ is the set of the problem eigenvalues given as a solution of the transcendental equation

$$D\lambda_n + k_c \tan(\lambda_n \delta) = 0. \tag{3.13}$$

In contrast to the problem examined by Courdesses et al. (1981), in our case there is no simple way to calculate the eigenvalues and numerical methods must be employed.

Since only pointwise measurement is available we are interested not in the concentration profile, but only in the concentration at the boundary

$$c(0,t) = \frac{c_b D}{D+k_c\delta} + \sum_{n=1}^{\infty}\frac{2c_b D k_c}{\delta k_c^2 + k_c D + \lambda_n^2 \delta D^2}e^{-\lambda_n^2 Dt}. \tag{3.14}$$

To obtain the identifiability results, the following lemma is useful (Courdesses et al., 1981)

Lemma 1. Let γ_i and $\gamma_{i,m}$, $i = 1,2,..$ be strictly monotone decreasing sequences tending to minus infinity and let

$$\sum_{i=1}^{\infty}\left(\alpha_i e^{\gamma_i t} - \alpha_{i,m} e^{\gamma_{i,m} t}\right) = 0 \quad \forall t \in [0,\infty).$$

Assume $\sum_{i=1}^{\infty}|\alpha_i|$ and $\sum_{i=1}^{\infty}|\alpha_{i,m}|$ to be convergent.

1) if α_i and $\alpha_{i,m} \neq 0$ for all $i = 1,..,N$, then $\gamma_i = \gamma_{i,m}$ and $\alpha_i = \alpha_{i,m}$.
2) if α_i and $\alpha_{i,m} \neq 0$ for all i, then $\gamma_i = \gamma_{i,m}$ and $\alpha_i = \alpha_{i,m}$.

Proof of this can be found in Courdesses et al. (1981).

To utilize Lemma 1 one should show that the assumptions for this lemma are valid for the series studied. In other words one should investigate whether the series

$$\sum_{n=1}^{\infty} \frac{2c_b D k_c}{\delta k_c^2 + k_c D + \lambda_n^2 \delta D^2} \tag{3.15}$$

converges. In (3.15) the operator of absolute value is taken away from the series, because due to the positive parameters we deal with the positive term series. The investigation of the convergence can be done by comparing the series (3.15) with the series

$$\sum_{n=1}^{\infty} \frac{1}{(2n-1)^2}. \tag{3.16}$$

Since D, k_c and δ are positive, we have

$$\frac{2c_b D k_c}{\delta k_c^2 + k_c D + \lambda_n^2 \delta D^2} < \frac{2c_b D k_c}{\lambda_n^2 \delta D^2}. \tag{3.17}$$

To proceed further, some information about the eigenvalues is required. Though equation (3.13) cannot be solved analytically, using the intermediate value theorem (Pinchover and Rubinstein, 2005) it can be verified that

$$\lambda_n \in \left(\frac{2n-1}{2\delta}\pi, \frac{n\pi}{\delta} \right). \tag{3.18}$$

Substituting the lower bound for λ_n into (3.17) gives

$$\frac{2c_b D k_c}{\delta k_c^2 + k_c D + \lambda_n^2 \delta D^2} < \frac{8c_b k_c \delta}{(2n-1)^2 \pi^2 D}. \tag{3.19}$$

The series in the right side of (3.19) is known to be convergent (Gradshteyn and Ryzhik, 1963). Therefore, according to the comparison test (Riley et al., 2006) the series (3.15) is convergent, since the general term in the series (3.15) is less than the general term in (3.16) multiplied to $8c_b k_c \delta / (\pi^2 D)$. As the consequence, it directly follows that the second condition of Lemma 1 is fulfilled in our case, because D, k_c and c_b are strictly positive constants.

Now it can be established that the diffusivity coefficient is identifiable under pointwise boundary measurements. Indeed, the relation $e(t) = 0$ implies

$$\begin{aligned} &\frac{c_b D}{D + k_c \delta} + \sum_{n=1}^{\infty} \frac{2c_b D k_c}{\delta k_c^2 + k_c D + \lambda_n^2 \delta D^2} e^{-\lambda_n^2 D t} \\ &\quad - \frac{c_b D_m}{D_m + k_c \delta} + \sum_{n=1}^{\infty} \frac{2c_b D_m k_c}{\delta k_c^2 + k_c D_m + \lambda_{n,m}^2 \delta D_m^2} e^{-\lambda_{n,m}^2 D_m t} = 0. \end{aligned} \tag{3.20}$$

Utilizing Lemma 1 gives

$$\frac{c_b D}{D + k_c \delta} = \frac{c_b D_m}{D_m + k_c \delta}, \tag{3.21}$$

$$\frac{2c_b D k_c}{\delta k_c^2 + k_c D + \lambda_n^2 \delta D^2} = \frac{2c_b D_m k_c}{\delta k_c^2 + k_c D_m + \lambda_{n,m}^2 \delta D_m^2}, \tag{3.22}$$

$$\lambda_n^2 D = \lambda_{n,m}^2 D_m . \tag{3.23}$$

From (3.21) it directly follows that $D = D_m$. Substituting (3.23) into (3.22) and reducing the fractions to a common denominator the same result is obtained. Therefore, the diffusivity is an identifiable parameter. Additional information we have used here is a known kinetic coefficient and the stagnation layer thickness. Similarly, it can be shown that the kinetic parameter and stagnation layer thickness are separately identifiable under concentration at the boundary measurements.

Though the parameters of interest are identifiable separately, starting from the analytical solution for the concentration at the boundary (3.14) a stronger result about the identifiability of any pair of the unknown parameters can be obtained. Assuming, for instance, the diffusivity and thickness to be unknown parameters, the relation $e(t) = 0$ then implies

$$\begin{aligned} &\frac{c_b D}{D + k_c \delta} + \sum_{n=1}^{\infty} \frac{2c_b D k_c}{\delta k_c^2 + k_c D + \lambda_n^2 \delta D^2} e^{-\lambda_n^2 D t} \\ &\quad - \frac{c_b D_m}{D_m + k_c \delta_m} + \sum_{n=1}^{\infty} \frac{2c_b D_m k_c}{\delta_m k_c^2 + k_c D_m + \lambda_{n,m}^2 \delta_m D_m^2} e^{-\lambda_{n,m}^2 D_m t} = 0. \end{aligned} \tag{3.24}$$

Utilizing Lemma (1) gives again (3.23) and

$$\frac{c_b D}{D + k_c \delta} = \frac{c_b D_m}{D_m + k_c \delta_m}, \tag{3.25}$$

$$\frac{2c_b D k_c}{\delta k_c^2 + k_c D + \lambda_n^2 \delta D^2} = \frac{2c_b D_m k_c}{\delta_m k_c^2 + k_c D_m + \lambda_{n,m}^2 \delta_m D_m^2} . \tag{3.26}$$

From (3.25) directly follows the next relationship

$$D \delta_m = D_m \delta . \tag{3.27}$$

Substituting (3.23) into (3.26), reducing the fractions to a common denominator and then using (3.27) gives $\delta = \delta_m$ and, consequently, from (3.27) $D = D_m$. Therefore, the diffusivity and stagnation layer thickness are simultaneously identifiable. In a similar manner, it can be established that any pair of the parameters in the model (2.7), (2.8), (3.1), (3.3) and (3.4) is simultaneously identifiable.

The results obtained make it possible to conclude, that the data collected from a single step voltage experiments are not informative enough to estimate all the parameters

uniquely under concentration at the boundary measurements and only any pair of the parameters is simultaneously identifiable.

3.3.2 Current measurements

Under concentration boundary measurements the model (2.7), (2.8), (3.1), (3.3) is partially identifiable. However, this case is unrealistic since, in practice, the current flowing through electrochemical cell is measured. It turns out that under current measurements the model is identifiable. Indeed, consider pointwise measurement on the system

$$y(t) = k_c c(0,t). \tag{3.28}$$

Under the assumption of pointwise measurement on the model

$$y_m(t) = k_m c_m(0,t) \tag{3.29}$$

the relation $e(t) = 0$ implies

$$\begin{aligned} &\frac{k_c c_b D}{D + k_c \delta} + \sum_{n=1}^{\infty} \frac{2 c_b D k_c^2}{\delta k_c^2 + k_c D + \lambda_n^2 \delta D^2} e^{-\lambda_n^2 D t} \\ &\quad - \frac{k_m c_b D_m}{D_m + k_m \delta_m} + \sum_{n=1}^{\infty} \frac{2 c_b D_m k_m^2}{\delta_m k_m^2 + k_m D_m + \lambda_{n,m}^2 \delta_m D_m^2} e^{-\lambda_{n,m}^2 D_m t} = 0. \end{aligned} \tag{3.30}$$

Utilizing Lemma (1) gives (3.23) and

$$\frac{k_c c_b D}{D + k_c \delta} = \frac{k_m c_b D_m}{D_m + k_m \delta_m}, \tag{3.31}$$

$$\frac{2 c_b D k_c^2}{\delta k_c^2 + k_c D + \lambda_n^2 \delta D^2} = \frac{2 c_b D_m k_m^2}{\delta_m k_m^2 + k_m D_m + \lambda_{n,m}^2 \delta_m D_m^2}. \tag{3.32}$$

Rearranging (3.31) gives the following relationship

$$D D_m (k_c - k_m) = k_c k_m (D_m \delta - D \delta_m). \tag{3.33}$$

Substituting (3.23) and (3.31) into (3.32) gives

$$k_c^2 \delta_m = k_{c,m}^2 \delta. \tag{3.34}$$

It should be emphasized that (3.23) must be fulfilled for all eigenvalues of the problems. Therefore, to prove uniqueness it is enough to show that it is not fulfilled at least for one equation of (3.23). This can be done in the following way. Consider the eigenvalues of the problem (3.5)-(3.8)

$$D_m \lambda_{n,m} + k_m \tan(\lambda_{n,m} \delta_m) = 0. \tag{3.35}$$

Expressing $\lambda_{n,m}$ from (3.23) and substituting into (3.35) one can get

$$D_m\sqrt{\frac{D}{D_m}}\lambda_n + k_m \tan\left(\sqrt{\frac{D}{D_m}}\lambda_n\delta_m\right) = 0\,. \tag{3.36}$$

The solution of the transcendental equation (3.13) can be found graphically as an intersection of tangent plot $y_1(\lambda_n) = k_c\tan(\lambda_n\delta)$ and linear plot $y_2(\lambda_n) = -D\lambda_n$ (see Fig. 3.1).

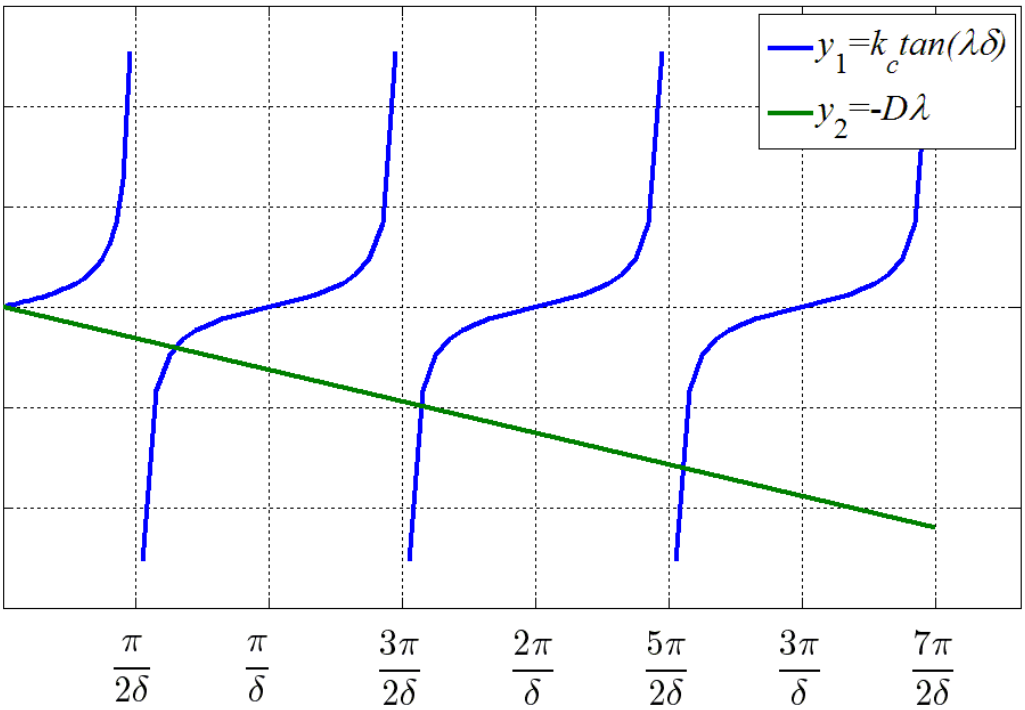

Figure 3.1: An illustration of the graphical solution of the transcendental equation (3.13). The eigenvalues are obtained as points of intersection of tangent plot $y_1(\lambda_n) = k_c\tan(\lambda_n\delta)$ and linear plot $y_2(\lambda_n) = -D\lambda_n$. The zero eigenvalue is not considered, since it provides no information.

Similarly, the solution of the equation (3.36) can be found. We consider only positive eigenvalues, because the negative eigenvalues have the same values, but opposite in sign, and have been taken into account in the Fourier coefficients of the series (3.14). Due to negative slope of the linear plot the nth eigenvalue of (3.13) lies in the interval given by (3.18). Similarly, due to (3.36) the same nth eigenvalue also lies in

$$\lambda_n \in \left(\sqrt{\frac{D_m}{D}}\frac{2n-1}{2\delta_m}\pi, \sqrt{\frac{D_m}{D}}\frac{n\pi}{\delta_m}\right). \tag{3.37}$$

Assume $\delta\sqrt{D_m/D} \neq \delta_m$. Then the relation

$$\sqrt{\frac{D_m}{D}}\frac{2n-1}{2\delta_m}\pi > \frac{n\pi}{\delta} \tag{3.38}$$

implies

$$n > \frac{\delta\sqrt{D_m/D}}{2\left(\delta\sqrt{D_m/D}-\delta_m\right)}. \tag{3.39}$$

The meaning of the inequalities (3.38) and (3.39) is that for any integer n satisfying to (3.39) the nth eigenvalue of (3.13) lies simultaneously in two non-overlapping intervals (3.18) and (3.37). This is not possible and, therefore,

$$\delta^2 D_m = \delta_m^2 D. \tag{3.40}$$

Now expressing δ_m from (3.40) and $\lambda_{n,m}$ from (3.23) and substituting them into (3.35) gives

$$\lambda_n + \frac{k_m}{\sqrt{DD_m}}\tan\left(\lambda_n\delta\right) = 0. \tag{3.41}$$

Equations (3.41) and (3.13) should produce the same set of eigenvalues. It is possible if and only if

$$k_m^2 D = k_c^2 D_m. \tag{3.42}$$

From equations (3.42) and (3.34) follows that

$$D\delta_m = D_m\delta. \tag{3.43}$$

Substituting equation (3.43) into (3.33) leads to $k_m = k_c$. Then from equation (3.34) it follows that $\delta_m = \delta$ and from (3.43) it follows that $D = D_m$. Therefore, the model (2.7), (2.8), (3.1), (3.3) is identifiable under current measurements (3.28).

3.3.3 Parameter identification

The previous section states that the model is identifiable. However, it does not give a method to find the estimates. The parameters can be estimated using gradient optimization techniques (Seinfeld and Chen, 1971). Alternatively, the estimates can be found by a direct search method (Hooke and Jeeves, 1961; Nelder and Mead, 1965) accompanied with a prior model reduction of the PDE. The finite-difference method and collocation methods are useful for this purpose (Boyd, 2001; Bhikkaji and Söderström, 2004).

In contrast to gradient optimization techniques that require evaluations of the derivative of the function to be minimized, direct search methods need only evaluations of this function. To verify the obtained identifiability results the direct search method was utilized. The algorithm converged to the given parameters irrespective of the different initial values chosen. An example of convergence an initial point $D = 5\cdot10^{-10}$ m^2/s, $\delta =$ 60 μm and k_c = 10 μm/s to the given parameters $D = 10^{-10}$ m^2/s, δ = 100 μm and k_c = 1 μm/s obtained with the Nelder-Mead direct search method (Lagarias et al., 1998) is illustrated in Fig. 3.2.

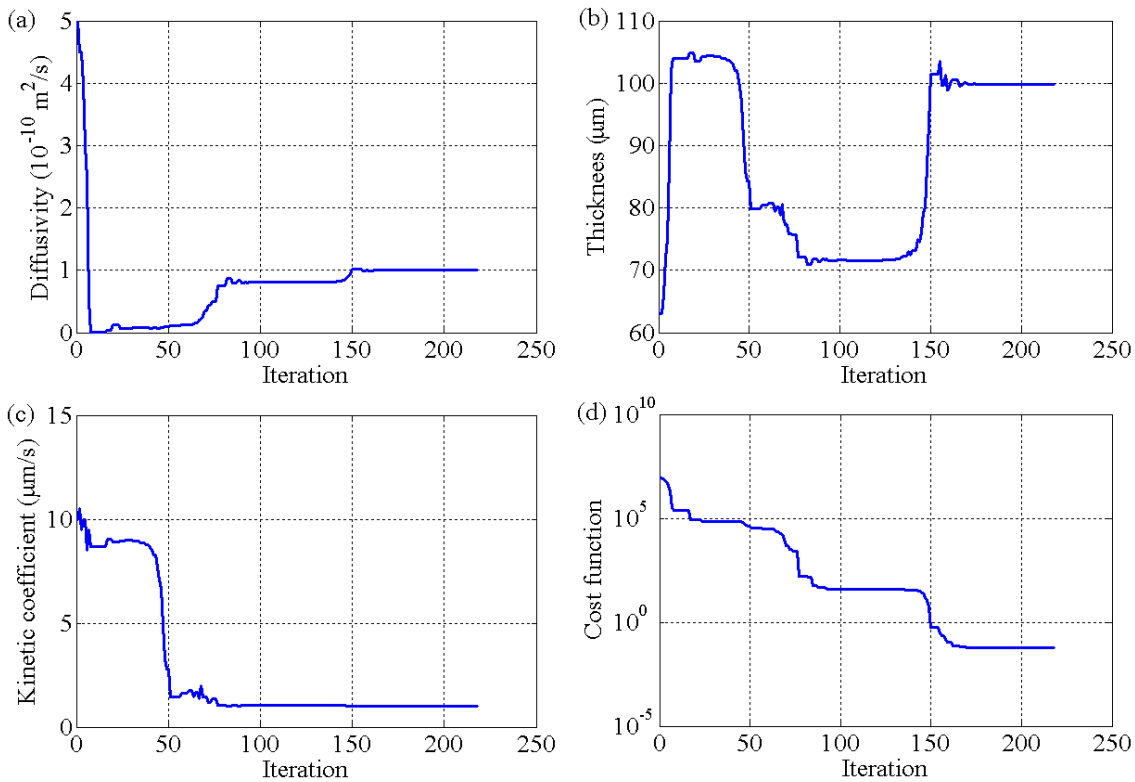

Figure 3.2: An illustration of convergence of the parameters using the Nelder-Mead direct search method. (a): Convergence of the diffusivity. (b): Convergence of the thickness. (c): Convergence of the kinetic coefficient. (d): Evolution of the cost function.

The convergence is non-monotonic and relatively slow: the algorithm terminated after 218 iterations when the termination tolerance of 10^{-8} on the cost function value was reached. The number of the function evaluation used was 400. However, the global optimal point was achieved.

It is interesting to note that even exchange current and apparent transfer coefficient are identifiable simultaneously. In one particular step voltage experiment, they appear in combination. However, by making several different step voltage experiments gives additional information for simultaneous identification. Let $E^{(1)}$ and $E^{(2)}$ be values of steps in two voltage step experiments and $k_c^{(1)}$ and $k_c^{(2)}$ be correspondingly estimated kinetic coefficients. Then substituting the voltage step and kinetic coefficient values into an expression for k_c produces a nonlinear system of two equations in two variables. This system can be solved analytically and its solution gives the following estimates for the exchange current and apparent transfer coefficient

$$\alpha = \frac{1}{k\left(E^{(2)} - E^{(1)}\right)} \log \frac{k_c^{(1)}}{k_c^{(2)}},$$

$$I_0 = -k_c^{(2)} c_b nFAe^{k\alpha\left(E^{(2)} - E_{eq}\right)}.$$

More accurately the kinetic parameters can be estimated under several different step test experiments by using the linear mean squares method (LMS). Therefore, the input-output data collected from a series of step voltage experiments are informative enough to estimate uniquely the diffusion coefficient, diffusion length and kinetic parameters simultaneously.

Summarizing, one can conclude that under step applied voltage and current measurements in well-stirred solutions the system is globally identifiable. However, the obtained result is not constructive, since stating that the system is identifiable does not give a way to estimate the parameters. In the following text we consider the cyclic voltammetry technique which gives as a primary result a simple way to estimate the electrochemical parameters from voltammograms, and, in addition, it shows that these parameters are identifiable.

3.4 Identifiability under sweep form of applied voltage

Cyclic voltammetry (CV) has become a standard technique in electrochemical experiments. The current-potential curve, measured by the instrumental in the experiments has a hysteresis shape. It is known and observed experimentally that when the voltage is swept the current rises until a peak occurs. Then under the assumption of one reaction, the current starts to decrease even if more voltage is applied into the system. When the sweep is reversed, the current falls off monotonically or another negative peak occurs. Then if the current is plotted against the voltage, it gives a hysteresis-shaped curve.

The relationship between the hysteresis shape and kinetic and mass transfer parameters have been studied extensively. It was established that the peak current is linearly proportional to the square root of the species' diffusivity. Considering, in addition to the peak current, the values of the potential at certain points allows estimating kinetic parameters. In general, three parameters of the curve have found their application in parameter estimation: peak current, peak potential and half-peak potential, where half-peak potential means a potential where the current reaches one half of its maximum. Utilizing these parameters makes it possible to show the identifiability of parameters for several analytical models of the electrochemical cells and gives a simple way of estimating the electrochemical parameters.

Voltammetry studies utilize several common assumptions. Particularly, the small ratio of electrode area to solution volume, the initial electrode potential, where no electrode reaction occurs and an unstirred solution are presumed. These assumptions imply semi-infinite linear diffusion (2.7)-(2.10). The methods of estimating kinetic and mass-transfer parameters for reversible, irreversible and quasi-reversible reactions have been developed based on an electrode kinetic model (2.5)-(2.6) together with semi-infinite diffusion (Bard and Faulkner, 2001). The nice feature of the semi-infinite diffusion model (2.7)-(2.10) is its simple analytical relationship between the concentration at the boundary and the cell current. This relationship can be derived using a Laplace transformation and is given by

$$c(0,t) = c_b + \frac{1}{nFA\sqrt{\pi D}} \int_0^t \frac{I(\tau)}{\sqrt{t-\tau}} d\tau . \tag{3.44}$$

Equation (3.44) can be written in terms of flux as

$$c(0,t) = c_b + \frac{1}{\sqrt{\pi D}} \int_0^t \frac{f(\tau)}{\sqrt{t-\tau}} d\tau , \tag{3.45}$$

where $f(\tau) = I(\tau)/(nFA)$ is the flux of the reacting species, mol/m^2/s. It should be emphasized that equation (3.44) was derived under no assumption of the electrode kinetic model. Therefore, it can be further utilized in identification of more complex models, particularly the model (2.23), (2.28)-(2.31) developed in Chapter 2.

3.4.1 Identification of models linear in the concentration

Consider the case of a totally irreversible reaction. In this case, the current-overpotential equation is approximated by the single-directional model

$$I = -I_0 \frac{c(0,t)}{c_b} e^{-\alpha \frac{nF}{RT}(E-E_{eq})} . \tag{3.46}$$

The applied voltage is swept linearly at a rate ν V/s so that the voltage at any time is given as

$$E(t) = E_i - \nu t , \tag{3.47}$$

where E_i is initial voltage of the electrode. Substituting (3.47) into (3.46) and by separating constant and time-dependent multipliers in forward of the concentration once can write flux at the electrode as follows

$$\frac{I}{nFA} = I_{fi} e^{bt} c(0,t) , \tag{3.48}$$

where $I_{fi} = -\frac{I_0}{nFAc_b} e^{-\alpha \frac{nF}{RT}(E_i - E_{eq})}$ and $b = \alpha \frac{nF}{RT} \nu$.

Substituting the concentration at the boundary (3.45) into (3.48), one can obtain the relationship between the cell current and the applied voltage that, in contrast to (3.46), does no longer include the time variant concentration

$$\frac{f(t)}{I_{fi}} e^{-bt} = c_b + \frac{1}{\sqrt{\pi D}} \int_0^t \frac{f(\tau)}{\sqrt{t-\tau}} d\tau . \tag{3.49}$$

Equation (3.49) is a linear, first-order Volterra integral equation and its solution cannot be found in a closed form and, therefore, numerical methods must be employed. The properties of the equation are well documented in voltammetric literature (Bard and Faulkner, 2001). Particularly, the equation can be deduced to a dimensionless form so

that numerically obtained solution can be useful under any experimental conditions. This can be done by the change of variables

$$f(\tau)=\sqrt{\pi Dbc_b}\chi(b\tau). \tag{3.50}$$

Then the desired equation in terms of dimensionless variables $\chi(z), \sqrt{\pi Db}/k_{fi}, bt$ takes the form

$$\int_0^{bt}\frac{\chi(z)}{\sqrt{bt-z}}dz=1-\chi(bt)e^{\ln\left(\sqrt{\pi Db}/I_{fi}\right)-bt}, \tag{3.51}$$

where $\chi(z)=\dfrac{I(bt)}{nFA\sqrt{\pi Dbc_b}}$ is the dimensionless current. The general result of solving (3.51) is the set of values of $\chi(bt)$ as a function of the dimensionless potential $u-bt$ (Bard and Faulkner, 2001), where $u=\ln\left[\sqrt{\pi Db}/I_{fi}\right]$ and

$$u-bt=\frac{\alpha nF}{RT}\left(E-E_{eq}\right)+\ln\left[nFAc_b\sqrt{\pi Db}/I_0\right].$$

Matsuda and Ayabe (1955) and Nicholson (1965b) studied equation (3.51) and found that the values of dimensionless current $\chi(bt)$ are independent of u provided that u is greater than 7.

The current flowing through an electrochemical cell under specific experimental conditions is related to dimensionless current as

$$I(t)=nFAc_b(\pi Db)^{1/2}\chi(bt). \tag{3.52}$$

To estimate the kinetic and mass-transfer parameters, it was proposed to utilize such specific parameters of the current-potential curve as peak current, peak potential and half-peak potential. It was found that the dimensionless current function $\sqrt{\pi}\chi(bt)$ reaches a maximum at -5.34 mV and $\sqrt{\pi}\chi(bt)$ = 0.4958. Then the peak current is:

$$I_p=0.4958Ac_b\left(\frac{n^3F^3}{RT}\right)^{1/2}D^{1/2}\alpha^{1/2}v^{1/2}. \tag{3.53}$$

The corresponding peak potential is

$$E_p=E_{eq}-\frac{RT}{\alpha nF}\left(0.7824+\ln\frac{nFAc_b\sqrt{D}}{I_0}+\ln\sqrt{\frac{\alpha nFv}{RT}}\right). \tag{3.54}$$

In electrochemical experiments, the potential correspondent to the point at the current-potential curve where the current reaches one half of its maximum, is commonly used for parameter estimation

$$E_{p/2} = E_{eq} - \frac{RT}{\alpha nF}\left(-1.0746 + \ln\left[nFAc_b\sqrt{Db}/I_0\right]\right). \tag{3.55}$$

Taking the difference between (3.54) and (3.55), one can find that the resulting value is inversely proportional to the apparent transfer coefficient of the system

$$\left|E_p - E_{p/2}\right| = 1.857\frac{RT}{\alpha nF} = \frac{47.7}{\alpha n}mV. \tag{3.56}$$

A similar dependence can be found by taking the difference between the peak or half-peak potentials at two different sweep rates

$$\left(E_{p/2}\right)_2 - \left(E_{p/2}\right)_1 = \left(E_p\right)_2 - \left(E_p\right)_1 = \frac{RT}{\alpha nF}\ln\sqrt{\frac{\nu_1}{\nu_2}}. \tag{3.57}$$

By combining equations (3.53) and (3.54), one can find the relationship between the peak current and peak voltage

$$I_p = 0.227 I_0 e^{-\frac{\alpha nF}{RT}\left(E_p - E_{eq}\right)}. \tag{3.58}$$

Equation (3.58) gives a straightforward way of estimating the kinetic parameters of the system. These can be found by calculating a slope and intercept of a plot of the logarithm of peak current against $E_p - E_{eq}$ determined at different scan rates.

Therefore, in order to identify the mass-transfer and kinetic parameters one can perform a series of sweep experiments with different sweep rates. Then, estimates can be obtained by utilizing (3.58) and (3.53). Alternatively, the parameters can be identified from one sweep experiment. Indeed, (3.53), (3.55) and (3.56) produce a nonlinear system of three equations in three variables that being solved gives the estimates.

Similar to (3.53)-(3.58) features were found for reversible and quasi-reversible reactions (Matsuda and Ayabe, 1955; Bard and Faulkner, 2001). Inspired by these results and similarities between the kinetic models (3.46) and (2.23), we develop an identification method for the kinetic model (2.23) that takes into account the activity of copper(II) ions.

3.4.2 Identification of models nonlinear in the concentration

Even though the approximation of the relationship between concentration and activity (2.30), that matches the estimate with concentration at infinite dilution, is known, it is strongly nonlinear and does not give the possibility to develop analytical methods suitable for analysis and identification of the overall system. To overcome this difficulty we will use another approximation given by the following expression

$$a_{WE,c} = \left(\frac{c(0,t)}{c_b}\right)^{\gamma}, \tag{3.59}$$

where $\gamma = 0.4446$ for copper(II) ions.

Substituting (3.59) into (2.23) and using (3.59) one can write the equation for cell current I as (3.60)

$$\frac{I}{nFA_{WE}} = -\frac{I_0}{nFA_{WE}}\left(\frac{c(0,t)}{c_b}\right)^{\alpha_1} e^{-k\alpha_2 E}, \tag{3.60}$$

where $\alpha_1 = \gamma\alpha_a/(\alpha_a+\alpha_c), \alpha_2 = \alpha_a\alpha_c/(\alpha_a+\alpha_c)$.

Based on (3.47) equation (3.60) takes the form

$$\frac{I}{nFA_{WE}} = -\frac{I_0 e^{-k\alpha_2 E_i}}{nFA_{WE}c_b^{\alpha_1}} c^{\alpha_1}(0,t)e^{k\alpha_2 \nu t}. \tag{3.61}$$

The left-hand side in (3.61) equals the flux of copper(II) ions per unit area $f(t)$

$$f(t) = I_{fi}c^{\alpha_1}(0,t)e^{bt}, \tag{3.62}$$

where

$$I_{fi} = -\frac{I_0 e^{-k\alpha_2 E_i}}{nFA_{WE}c_b^{\alpha_1}},\ b = k\alpha_2\nu. \tag{3.63}$$

Assuming diffusivity constant, substituting (3.45) into (3.62), by raising both sides to the power of $1/\alpha_1$ and by rearrangement, one obtains (3.64) a nonlinear second order Volterra integral equation that enables finding the current (and corresponding mass flux) at a given sweep voltage:

$$\int_0^t \frac{f(\tau)}{\sqrt{t-\tau}}d\tau = \sqrt{\pi D}\left(c_b - f^{\frac{1}{\alpha_1}}(t)e^{\frac{\ln(I_{fi})-bt}{\alpha_1}}\right). \tag{3.64}$$

Note that the structure of equation (3.64) would match that of the integral equation for the totally irreversible reactions (3.49), provided that $\alpha_1 = 1$. In this case, the nonlinear equation (3.64) becomes linear.

It is reasonable now to put the equation in a dimensionless form so that the numerically obtained results will be useful under any experimental conditions. This can be done by the change of variables

$$f(\tau) = \sqrt{\pi Db}c_b\chi(b\tau).$$

Then the desired equation in terms of dimensionless variables $\chi(z)$, u, bt takes the form

$$\int_0^{bt} \frac{\chi(z)}{\sqrt{bt-z}}dz = 1 - \chi^{\frac{1}{\alpha_1}}(bt)e^{\frac{u-bt}{\alpha_1}}, \tag{3.65}$$

where $u = \ln\left(\sqrt{\pi Dbc_b^{1-\alpha_1}}/I_{fi}\right)$.

Equation (3.65) can be solved numerically using the technique developed by Nicholson and Shain (1964). Then the current flowing through the electrochemical cell can be obtained as (3.66)

$$I(t) = nFA_{WE}c_b(\pi Db)^{1/2}\chi(bt). \tag{3.66}$$

Similar to the solution of (3.51), the solution function $\chi(bt)$ does not depend on parameter u provided that u is greater than 7. However, unlike in the totally irreversible reactions case, $\chi(bt)$ depends on α_1 as shown in Fig. 3.3, where it is plotted versus dimensionless voltage

$$E_d = \ln\left(\sqrt{\pi Dbc_b^{1-\alpha_1}}/I_{fi}\right) - bt.$$

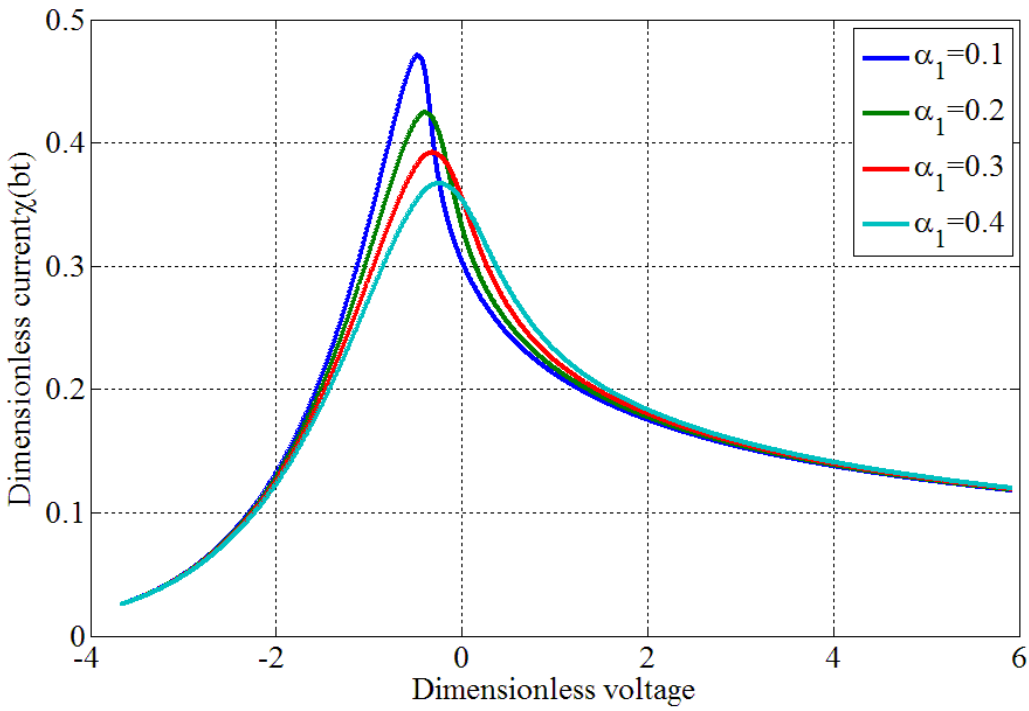

Figure 3.3: Dimensionless current-potential curve as function of α_1.

It is clearly observable that the larger α_1 is, the lower the dimensionless current peak, and the higher the peak potential is. These features are also observable from Fig. 3.4 where the dimensionless peak current and dimensionless peak voltage are illustrated as functions of the variable α_1.

According to the definition of b (3.63), the dimensionless voltage is related to cell voltage as

$$E_d = \ln\left(\sqrt{\pi Dbc_b^{1-\alpha_1}}/I_{fi}\right) - \frac{\alpha_2 nF}{RT}(E_i - E).$$

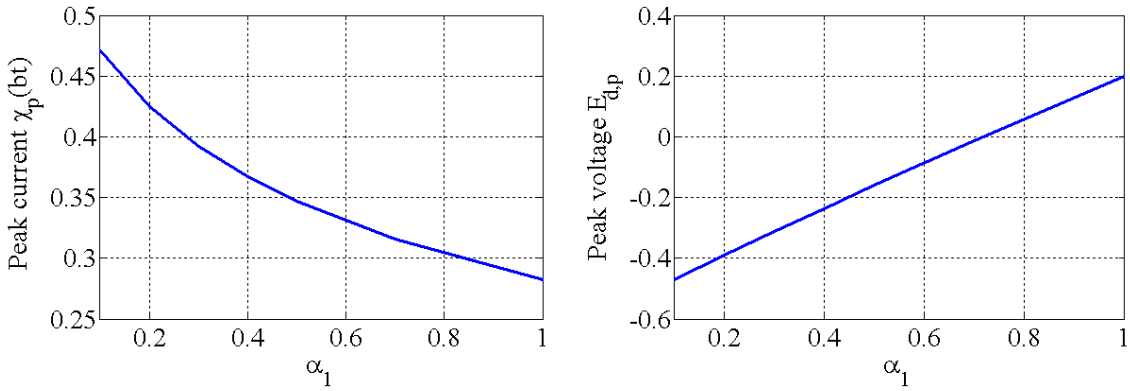

Figure 3.4: Left: Dimensionless peak current as function of α_1. Right: Dimensionless peak voltage as function of α_1.

The E_p corresponding to the peak current $\chi_p(bt)$ is a function of α_1 (see Fig. 3.4) and related to the dimensionless peak voltage $E_{d,p}$ as

$$E_{d,p} = \ln\left(\sqrt{\pi D b} c_b^{1-\alpha_1} / I_{fi}\right) - \frac{\alpha_2 nF}{RT}\left(E_i - E_p\right).$$

Solving for E_p and substituting b we obtain (3.67)

$$E_p = \frac{RT}{\alpha_2 nF}\left(E_{d,p}(\alpha_1) - \ln\frac{\sqrt{\pi D k \alpha_2 \nu} c_b nFA_{WE}}{I_0}\right). \tag{3.67}$$

According to (3.67), the peak voltage depends on the exchange current, apparent transfer coefficients and the diffusion coefficient. Considering the peak voltage at two different sweep rates and taking their difference yields (3.68)

$$E_{p,\nu_1} - E_{p,\nu_2} = \frac{RT}{\alpha_2 nF}\ln\sqrt{\frac{\nu_2}{\nu_1}}. \tag{3.68}$$

An estimate for α_2 can be created based on (3.68).

Still three parameters have to be identified (D, α_1 and I_0) but there are only two equations to utilize (χ_p and E_p). Therefore, one more equation is required. The voltage at half-peak of current can be considered, as is often done in cyclic voltammetry study. The expression for the half-peak voltage can be obtained similarly to that for the peak voltage

$$E_{p/2} = \frac{RT}{\alpha_2 nF}\left(E_{d,p/2}(\alpha_1) - \ln\frac{\sqrt{\pi D k \alpha_2 \nu} c_b nFA_{WE}}{I_0}\right). \tag{3.69}$$

The plot of the half-peak voltage versus α_1 is depicted in Fig. 3.5.

Setting the expressions for peak current, peak voltage and half-peak voltage to their measured values produces a nonlinear system of three equations in three variables, and

by solving the system one can estimate the mass-transfer parameters and kinetic parameters of the system. Particularly, taking the difference between (3.67) and (3.69), one can find that the resulting value is inversely proportional to the apparent transfer coefficient of the system

$$E_p - E_{p/2} = \frac{RT}{\alpha_2 nF}\left(E_{d,p}(\alpha_1) - E_{d,p/2}(\alpha_1)\right). \tag{3.70}$$

An estimate for α_1 can be created based on (3.70). This is justified in the right plot of Fig. 3.5 which clearly shows that this function depends uniquely on α_1. Consequently, the dimensionless peak current and peak voltage can be found (see Fig. 3.4). Then the diffusivity is evaluated from (3.66) and the exchange current by using (3.67). Alternatively, the exchange current can be estimated by using the dimensionless half-peak voltage and (3.69).

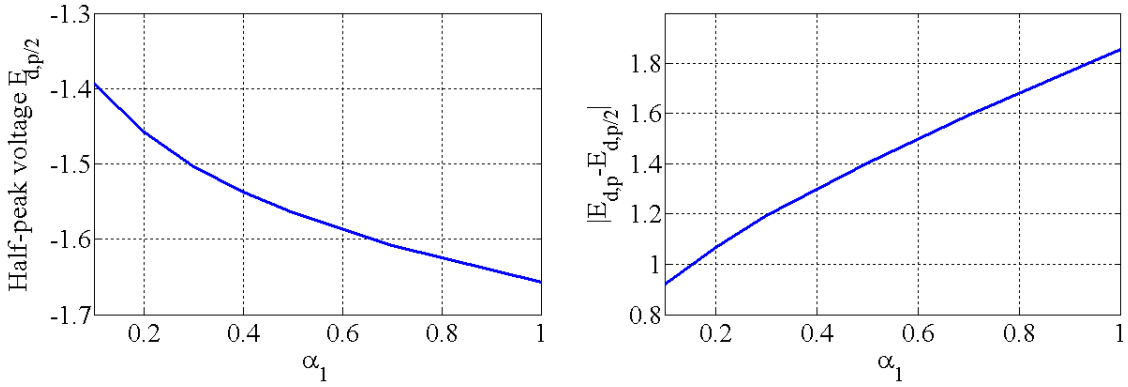

Figure 3.5: Left: Dimensionless half-peak voltage as function of α_1. Right: The difference between the dimensionless peak and half-peak potentials. This difference depends uniquely on α_1.

According to (3.68) the estimation algorithm above requires the experiments at two different sweep rates. It can be shown, that under the assumption that the sum of the apparent transfer coefficient equals to 1, all the electrochemical parameters can be uniquely estimated in a single LSV experiment. For that one may consider the voltage where the current reaches, for instance, 75% of its maximum ($E_{3/4p}$). This is justified in Fig. 3.6.

Therefore, it is possible to estimate the parameters of the nonlinear in concentration kinetic model (2.23) utilizing peak current, half-peak voltage and peak voltage from the current-potential curve. However, it should be emphasized that such an estimation instead of minimization of the cost function (3.71)

$$J(I_0, \alpha_a, \alpha_c, D) = \frac{1}{N}\sum_{j=1}^{N}\left(\xi_{WE}(t_j) - i_{WE}(t_j, I_0, \alpha_a, \alpha_c, D)\right)^2 \tag{3.71}$$

minimizes a cost function of the form

$$J\left(I_0,\alpha_a,\alpha_c,D\right)=\frac{1}{M}\sum_{j=1}^{M}\left(i_{\xi,p}^{(j)}-i_p^{(j)}(I_0,\alpha_a,\alpha_c,D)\right)^2+$$
$$\frac{1}{M}\sum_{j=1}^{M}\left(E_{\xi,p}^{(j)}-E_p^{(j)}(I_0,\alpha_a,\alpha_c,D)\right)^2+ \tag{3.72}$$
$$\frac{1}{M}\sum_{j=1}^{M}\left(E_{\zeta,p/2}^{(j)}-E_{p/2}^{(j)}(I_0,\alpha_a,\alpha_c,D)\right)^2,$$

where M is the number of sweep experiments, i_p is the modeled peak current density, E_p is the modeled voltage that correspond to the peak current density, $E_{p/2}$ is the modeled voltage at half-peak of current and subscript ξ stands for experimentally found values of these parameters.

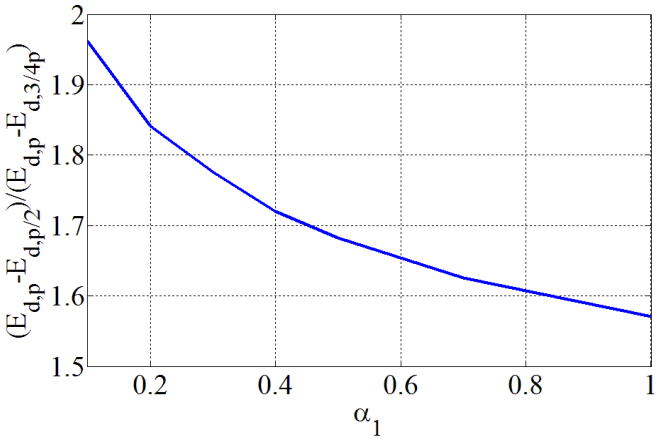

Figure 3.6: An illustration of the ratio to estimate α_1 in a single LSV experiment.

The drawback of (3.72) is that instead of considering all N measurements of the current-potential curve, only the special points are considered while the rest of the curve is ignored. Therefore, a model based on (3.72) will fit the measured data worse than (3.70) in root square mean, but the peak current, half-peak voltage and peak voltage will be closer to the measured values. Nevertheless, this knowledge-based identification can be useful to obtain good starting point for other more complex identification methods.

3.5 Conclusions

Identifiability of two models, the conventional model (2.6)-(2.9), (3.1) and the model (2.23), (2.28)-(2.31) further developed in Chapter 2, was investigated in this chapter. The results of this investigation show that the conventional electrochemical cell model can be identified uniquely using a series of step voltage experiments based on the measurements of cell current. The mass-transfer parameters can be estimated uniquely even under one step experiment. However, in such a case the kinetic parameters appear in combination and cannot be found. Indeed, in the mathematical sense, in one step experiment only one independent function depending on this combination is available

while in a series of step experiments several independent functions depending on this combination are available. In the case of measured concentration at the boundary a maximum of any two parameters of the model can be simultaneously estimated. On the contrary, in a single linear sweep voltammetry experiment the diffusivity and both the kinetic parameters are identifiable on the basis of the measurements of cell current. The mass-transfer parameters as well as kinetic parameters of the developed model can be estimated using linear sweep voltammetry with the values of peak current, its position and position of half-peak current. The limitation of this method lies in the fact that the rest of the measurements are ignored. Therefore, further development of the parameter identification methods is needed to utilize the whole set of the available current-potential measurements.

Chapter 4

Electrochemical parameters identification using Zakai equation

4.1 Introduction

Nonlinear filtering is an established theory extensively considered in the literature for a long period (see, e.g., Kushner, 1967; Zakai, 1969; Liptser and Shiryayev, 2000; Pardoux, 1981; Rozovsky, 1983 and references therein). Filtering theory addresses problems of estimating the state of a dynamical system on the basis of noisy measurements and separating a signal from a mixture of signal and measurement noise. It has found numerous applications in control engineering including robotics (e.g., Jetto et al., 1999; Briechle and Hanebeck, 2004), navigation systems (e.g., Kaminer et al., 2001; Dmitriyev et al., 1997), chemical plant control (e.g., Dondo and Marquers, 2003; Yoke Lin Tan, 1996; Li et al., 2004) and many others. Nonlinear filtering is also applied in stochastic control theory for transformation of a partially observable control problem into a complete data control problem (Fleming and Pardoux, 1982; Haussmann, 1986).

In addition to unknown states some of the system parameters are usually unknown or known with insufficient accuracy. The problem of estimating these parameters from measured data is called parameter identification. Parameter identification is easily reduced to the filtering problem for an extended state vector by treating the parameters as states. Consequently, the unknown parameters can be estimated using a nonlinear filter for the augmented system.

The solution to a nonlinear filtering problem for lumped parameter systems is given by a nonlinear stochastic partial differential equation for normalized probability density and is known as the Kushner equation (Ito and Rozovskii, 2000; Bain and Crisan, 2009). The Kushner equation is a nonlinear integro-differential equation and is difficult to solve. As a consequence, a majority of works deals with the Zakai equation which is stochastic partial differential equation for unnormalized probability density, but in contrast to the Kushner equation is a linear one (Zakai, 1969; Rozovsky, 1983; Ito and Rozovskii, 2000).

Several numerical methods have been developed to solve the Zakai equation. They are classified by the approximation method into several different categories: (1) the finite difference method (Kushner, 1977), (2) the finite element (Galerkin's) method (Ahmed and Radaideh, 1997), (3) the Markov chain method (Kushner, 1977), (4) the Monte-

Carlo branching partials method (Crisan *et al.*, 1998) and (5) the splitting-up approximation methods (Bensoussan et al., 1990; Ito and Rozovskii, 2000).

Although a theoretical framework for nonlinear filtering is well developed it is applied in practice only for the systems for which the optimal filter is finite-dimensional and for weakly nonlinear systems for which an approximate finite-dimensional filter can be derived via linearization. The first class of systems is very restricted. In addition to the linear case, where the solution is the Kalman-Bucy filter (see, e.g., Simon, 2006), only the Beneš type systems (Farina et al., 2002; Maybank, 1996) that satisfy a specific drift condition (Beneš, 1981) have been reported. The filters for the second class of the systems are not optimal due to the approximations used – like the extended Kalman filter, which makes a Taylor series expansion of the nonlinear terms up to the first or second orders (see, e.g., Simon, 2006), and like a particle filter for which the probability density is computed by Monte-Carlo simulations (Chen, 2003).

Optimal nonlinear filtering of distributed parameter systems has been studied by Kushner (1970), Balakrishnan and Lions (1967), Tzafestas and Nightingale (1968), Seinfeld (1969) and others. Similar to lumped parameter systems, it was found that exact nonlinear filters cannot be obtained in a general case. As a result, nonlinear filters are designed through approximation methods. One possible approach to obtain nonlinear filtering equations, used by Hwang et al. (1972), converts an estimation problem into optimal control problem and uses first order approximation of nonlinear terms.

In general, the nonlinear filtering problem has an infinite-dimensional solution and there are few examples where such a solution is applied. One of them is the volatility estimation problem (Aihara and Bagchi, 2006).

The lack of other applications is caused by the huge computational effort required to solve a nonlinear filtering problem. This problem consists in the exponential growth of computational effort as a function of the state vector dimension and is often called “the curse of dimensionality” due to Richard Bellman. In practice only problems that are low dimensional in unobservable components can be solved reasonably. Also, the lack of instructive case studies inhibits the development of applications.

In this chapter the Zakai filtering method is investigated when applied to a nonlinear system for which the estimation problem cannot be solved as a finite-dimensional filter. The chapter aims to gain specific knowledge from application of the Zakai equation to parameter estimation of the electrode kinetic model, known also as the Butler-Volmer equation (Bard and Faulkner, 2001; Newman and Thomas-Alyea, 2004). Questions that are answered: *How to apply the Zakai filtering method in a computationally effective mode? What is the estimation quality? Is there convergence to the true parameters and how fast is it? Is it possible to obtain similar results with the simpler direct search method?* The quality of the estimation is analyzed on different electrode kinetic models based on the results of identification of one, two or three parameters separately. The parameters to be estimated are the exchange current density, apparent transfer coefficient and diffusivity.

This chapter focuses less on the approximation of the data with some model and more on the estimation quality when using a model known in great detail. To have such a model, a known physical phenomenon is simulated using typical values of unknown parameters that are afterwards used as the references for comparison against the estimated values.

The results of this chapter have been published in one journal and two conference papers (Mendelson and Tenno, 2009a, 2009b, 2009c).

4.2 Contribution

The following contributions are covered in this chapter:

1. The Zakai filtering and pathwise filtering methods are applied to the nonlinear in the parameters electrochemical cell models to identify electrode kinetics and mass-transfer parameters of the electrochemical cells.
2. Equations of the Zakai filtering and pathwise filtering methods are simplified for the case of constant parameter estimation and an analytical solution is obtained.
3. The Zakai and pathwise filtering methods are applied for prediction of the measured data in the case of the copper electrodeposition process. Convergence of the estimates is analyzed and compared with the direct search method.

4.3 Estimation via Zakai equation

In this section the problem of estimating system parameters over nonlinear observation is formulated as a straightforward application of the Zakai and pathwise filtering methods. The unknown parameters are treated as if they were states and the estimation problem is solved by applying nonlinear filtering methods for the augmented system.

4.3.1 The estimation problem

In general the nonlinear filtering problem aims to estimate an unobserved state process ($\boldsymbol{\theta}_t$) on the basis of given measurements $\left(\xi_s : 0 \le s \le t\right)$ optimally in the mean square sense. The processes are driven by the following partially observable stochastic system (4.1)-(4.2)

$$d\boldsymbol{\theta} = \mathbf{a}\left(t, \boldsymbol{\theta}_t\right) dt + \mathbf{b} d\mathbf{W}, \quad \boldsymbol{\theta}(0) = \boldsymbol{\theta}_0 , \tag{4.1}$$

$$d\xi = \mathbf{A}\left(t, \boldsymbol{\theta}_t, \xi_{s \le t}\right) dt + \mathbf{B} d\mathbf{V}, \quad \xi(0) = \xi_0 , \tag{4.2}$$

where $\boldsymbol{\theta}$ is the state process, ξ is the measurements, $\mathbf{W}$, $\mathbf{V}$ are independent Wiener processes, $\mathbf{A}$ and $\mathbf{a}$ are piecewise smooth functions with derivatives bounded in a closed domain, $\mathbf{b}$ is non-negative and $\mathbf{B}$ is a positive definite matrix.

The initial condition $\boldsymbol{\theta}_0$ of the state process is specified by a Gaussian distribution $p_0(\mathbf{x})$ with a given mean $\mathbf{m}_0$ and covariance $\boldsymbol{\gamma}_0$; this reads in short notations as $\boldsymbol{\theta}_0 \sim N(\mathbf{m}_0, \boldsymbol{\gamma}_0)$.

The problem of estimating the unknown parameters can be interpreted as a filtering problem by augmenting the original system with additional differential equations which describe the evolution of parameters in time, i.e. by dealing with parameters as with states. If the parameters to be estimated are constant, the equations (4.1)-(4.2) take the following form

$$d\boldsymbol{\theta} = 0, \quad \boldsymbol{\theta}(0) = \boldsymbol{\theta}_0, \tag{4.3}$$

$$d\boldsymbol{\xi} = \mathbf{A}\left(t, \boldsymbol{\theta}, \boldsymbol{\xi}_{s \le t}\right) dt + \mathbf{B} d\mathbf{V}, \quad \boldsymbol{\xi}(0) = \boldsymbol{\xi}_0. \tag{4.4}$$

4.3.2 The solution to the estimation problem

A probability mass of all possible values of unknown parameters represented through an unnormalized distribution is an effective solution to the filtering problem (4.1)-(4.2). It satisfies the Zakai equation (see, e.g., Pardoux, 1981; Rozovskii, 1983; Ahmed and Radaideh 1997; Katzur et al., 1984)

$$dq = \left\{ \nabla \bullet \left(\frac{\mathbf{b}\mathbf{b}^T}{2} \nabla \right) q \; - \; \nabla \bullet (\mathbf{a} q) \right\} dt \; + \; \left\{ \mathbf{A}^T \left(\mathbf{B}\mathbf{B}^T \right)^{-1} q \right\} \bullet d\boldsymbol{\xi}, \quad q(0, \mathbf{x}) = p_0(\mathbf{x}). \tag{4.5}$$

In equation (4.5), q is the unnormalized probability density distribution $q = q(\mathrm{t}, \mathbf{x})$, $\mathbf{x}$ is the vector of all possible values of unknown parameters in a bounded closed subset $\mathbf{x} \in \Omega$ of Euclidean space and ∇ is a vector differential operator that designates the derivative in multi-dimensional space.

Estimation of the constant parameters

The Zakai equation is considerably simplified when specified for estimation of unknown constant parameters from the scalar-value measured process

$$dq = \frac{A}{B^2} q d\xi, \qquad q(0, \mathbf{x}) = p_0(\mathbf{x}). \tag{4.6}$$

Equation (4.5) and its simplification (4.6) are Ito stochastic partial differential equations (SPDE). Being solved with numerical methods the solutions of (4.5) and (4.6) do not converge to solutions of corresponding partial differential equations. It is more appropriate to use Stratonovich interpretation of SPDE (Mitter, 1982) which, for instance, admits ordinary calculus by the chain rule utilized further in the pathwise filtering. One can convert Ito SPDE to Stratonovich SPDE by adding the so-called Wong-Zakai correction term (Wong and Zakai, 1965). Being applied to equation (4.6) it results in the following Stratonovich SPDE utilized further in this chapter

$$dq = -\frac{1}{2}\left(\frac{A}{B}\right)^2 q dt \; + \; \frac{A}{B^2} q d\xi, \quad q(0, \mathbf{x}) = p_0(\mathbf{x}). \tag{4.7}$$

Equation (4.7) can be considered as a large-scale ODE system with respect to unnormalized probability density q and can be solved by direct integration of the sample path

$$q(t,\mathbf{x}) = p_0(\mathbf{x})\exp\left\{-\frac{1}{2}\int_0^t \left(\frac{A}{B}\right)^2 ds + \int_0^t \frac{A}{B^2} d\xi\right\}. \tag{4.8}$$

In practical applications, one is interested in computing the mean value and variance for an unknown parameter. These statistics are obtained by the integration of the unnormalized probability distribution (4.8) with respect to $\mathbf{x}$ and further normalization. Particularly, the conditional mean value of unknown parameters can be computed as

$$\mathbf{m}_t = \frac{\int_\Omega \mathbf{x} q(t,\mathbf{x})\, d\mathbf{x}}{\int_\Omega q(t,\mathbf{x})\, d\mathbf{x}}, \tag{4.9}$$

and the conditional covariance matrix as

$$\boldsymbol{\gamma}_t = \frac{\int_\Omega (\mathbf{x}-\mathbf{m}_t)(\mathbf{x}-\mathbf{m}_t)^T q(t,\mathbf{x})\, d\mathbf{x}}{\int_\Omega q(t,\mathbf{x})\, d\mathbf{x}}. \tag{4.10}$$

Statistics $\mathbf{m}_t$ and $\boldsymbol{\gamma}_t$ together will be further referred to in the text as the Zakai estimates, or pathwise estimates if considered with pathwise filtering. The Zakai filter allows also evaluation of the whole probability distribution in parameter space by normalization of the unnormalized distribution at every time step

$$p(t,\mathbf{x}) = \frac{q(t,\mathbf{x})}{\int_\Omega q(t,\mathbf{y})\, d\mathbf{y}}. \tag{4.11}$$

The prediction error, or the so called innovation process $d\overline{W}$ that gives a difference between observation process and its prediction obtained using parameters estimates, is evaluated as

$$d\overline{W} = \frac{1}{B}\left(d\xi - \frac{\int_\Omega A(t,\mathbf{x},\xi) q(t,\mathbf{x})\, dx}{\int_\Omega q(t,\mathbf{x})\, d\mathbf{x}} dt \right). \tag{4.12}$$

Estimation of the time-varying parameters

The case of practical interest is the estimation of the linear stochastic drift of unknown parameters. In such a case, equation (4.1), specified for estimation of one parameter, is

$$d\theta = (a_0 + a_1\theta)\, dt + b\, dW, \quad \theta(0) = \theta_0, \tag{4.13}$$

where a_0 and a_1 are given parameters. The unnormalized probability density for the drift $\theta(t)$ satisfies

$$dq = L^* q(t,x) + \frac{A(t,x)}{B^2} q(t,x) d\xi, \quad q(0,x) = p_0(x), \tag{4.14}$$

where L^* is the formal adjoint of the infinitesimal operator of drift $\theta(t)$

$$L^* q(t,x) = \frac{b^2}{2} \frac{\partial^2 q(t,x)}{\partial x^2} - (a_0 + a_1 x) \frac{\partial q(t,x)}{\partial x} - a_1 q(t,x). \tag{4.15}$$

Although the Zakai equation is a linear one, it suffers from such an undesired effect as fast growth of the unnormalized probability density. Another problem concerns the stability of solving the Zakai equation with the finite-difference method. As a result, a very fine grid must be used that is not computationally feasible. The Zakai equation (4.14) can be solved effectively using the factorization algorithm (Clark, 1978). According to this algorithm, we define a discrete mesh of points x_i with h being the distance between two consecutive grid points. Then the Zakai equation is approximated with the discrete-state equation

$$dq^i = \left(L^*\right)^i q^i dt + \frac{A^i}{B^2} q^i d\xi, \; q\left(0, x^i\right) = p_0(x^i), \tag{4.16}$$

where $q^i = q(t, x_i)$ is the unnormalized probability distribution in x_i and $A^i = A(t, x_i)$ is the measurement model in x_i.

Then the unnormalized probability density is decomposed into a product of two factors K^i and r^i

$$q^i = K^i r^i, \tag{4.17}$$

where the factor K^i is given by the following ordinary differential equation

$$dK^i = \frac{A^i}{B^2} K^i d\xi, \quad K^i(0) = p_0(x^i). \tag{4.18}$$

Its solution in the Stratonovich form can be expressed in a computationally effective manner as

$$K_t^i = p_0(x_i) \exp\left(\int_0^t \frac{A^i}{B^2} d\xi - \frac{1}{2} \int_0^t \frac{A^i}{B^2} dt \right). \tag{4.19}$$

The factor r^i depends on the drift model (4.13) and satisfies

$$dr^i = \left(K^i\right)^{-1} \left\{ \left(L^*\right)^i \left(K^i r^i\right) \right\}, \quad r^i(0) = 1. \tag{4.20}$$

The equation (4.20), when expanded with the finite difference approximation scheme (Dong and Krylov, 2007), gives the following calculation scheme

$$\frac{dr^i}{dt}=\frac{b^2}{2h^2}\left(r_t^{i+1}\frac{K_t^{i+1}}{K_t^i}-2r_t^i+r_t^{i-1}\frac{K_t^{i-1}}{K_t^i}\right)+\frac{\left|\left(a_0+a_1x_i\right)\right|+\left(a_0+a_1x_i\right)}{2h}\left(r_t^{i+1}\frac{K_t^{i+1}}{K_t^i}-r_t^i\right)$$
$$-\frac{\left|\left(a_0+a_1x_i\right)\right|-\left(a_0+a_1x_i\right)}{2h}\left(r_t^i-r_t^{i-1}\frac{K_t^{i-1}}{K_t^i}\right)-a_1r_t^i,\quad i=\overline{1,N}. \tag{4.21}$$

where N is a number of grid points in the mesh.

The infinite growth of unnormalized probabilities can be kept inside the computational range by partitioning the time interval [0, T] in a sequence of small intervals. In each subsequent interval the estimation process is reinitialized with the terminal probability density $p(t, x)$ taken from the previous interval.

Summarizing the algorithm consists of three steps. Firstly, the solution K_t^i of the factorized Zakai equation is computed as if the parameters to be estimated were constants according to equation (4.19). Then substituting the obtained solution K_t^i into the equation (4.21), the second factor r^i is computed. Finally, multiplication of both factors gives the unnormalized probability density distribution of θ. The distribution is further normalized and used to calculate the conditional mean (4.9) and variance (4.10). The whole calculation process is divided into several time intervals. At each interval the calculation process is reinitialized with probability density data from the previous interval.

If the parameter drift is without dynamics, i.e., a pure random walk

$$d\theta=bdW,\quad \theta(0)=\theta_0, \tag{4.22}$$

the finite difference approximation scheme (4.21) is simply

$$\frac{dr^i}{dt}=\frac{1}{2}\left(\frac{b}{h}\right)^2\left(r_t^{i+1}\frac{K_t^{i+1}}{K_t^i}-2r_t^i+r_t^{i-1}\frac{K_t^{i-1}}{K_t^i}\right).$$

Often the inadequacy of a model to a real process can be modeled by (4.22).

Pathwise filtering

If a standard routine developed for solving PDEs is applied for solving the Zakai equation, it must be represented through the time-derivative of measurements that is not well defined. To overcome this problem, the pathwise filtering technique was developed based on Doss's idea (Davis, 1981) to eliminate the derivative of the measurements from the Zakai equation and represent this equation in a parametric in the measurements form. The following change of variables was found to deal with such a problem

$$q=\rho e^{\xi\frac{A}{B^2}}. \tag{4.23}$$

Applying transformation (4.23) to the Zakai equation (4.7), one can come to the next SPDE

$$-\frac{\partial\rho}{\partial t}=\frac{1}{2}\left(\frac{A}{B}\right)^2\rho+\rho\frac{\xi}{B^2}\frac{dA}{dt},\quad \rho(0,\mathbf{x})=p_0\left(\mathbf{x}\right)e^{-\xi_0\frac{A(0,\mathbf{x},\xi)}{B^2}}. \tag{4.24}$$

Equation (4.14), similarly to the solution of the equation (4.7), can be presented in the following integral form (4.25)

$$\rho(t,\mathbf{x})=p_0\left(\mathbf{x}\right)e^{-\xi_0\frac{A(0,\mathbf{x},\xi)}{B^2}}\times e^{-\frac{1}{2}\int_0^t\left(\frac{A}{B}\right)^2 ds-\int_0^t\frac{\xi}{B^2}dA}. \tag{4.25}$$

The unnormalized probability density $q(t, \mathbf{x})$ can be calculated by backward substitution of the nonlinear transformation (4.23). Combining all the equations for pathwise filtering together one can derive the following equation for unnormalized probability density

$$q(t,\mathbf{x})=p_0\left(\mathbf{x}\right)e^{-\xi_0\frac{A(0,\mathbf{x},\xi)}{B^2}}\times e^{\xi\frac{A}{B^2}}\times e^{-\frac{1}{2}\int_0^t\left(\frac{A}{B}\right)^2 ds-\int_0^t\frac{\xi}{B^2}dA}. \tag{4.26}$$

Unlike to the equation (4.8) there is no derivative of measurements in equation (4.26) and, therefore, the mentioned computational problem is handled with the change of variables (4.23). Similarly, the transformation (4.23) can be applied to (4.14) to solve derivative-free with respect to the measurements problem.

In summary the Zakai and pathwise filtering methods for the identification of constant parameters consist of computing the unnormalized probability density by either equation (4.8) or (4.26) and then finding the mean value and variance of estimates by using (4.9) and (4.10).

4.3.3 Application to estimation of static models

Consider a general form static model to be estimated

$$y=h\left(u,\boldsymbol{\theta}\right), \tag{4.27}$$

where h is an arbitrary nonlinear function, u is the input signal and $\boldsymbol{\theta}$ is a vector of unknown constant parameters. Assume the process is corrupted by an additive white noise ε with zero mean and unit variance:

$$\zeta=y+B\varepsilon, \tag{4.28}$$

where ζ is the measurements and B is the measurements accuracy. The observation process (4.28) is static while the filter equations are derived for a dynamic model (4.4). The former can be converted to the latter either by operations of differentiation or integration.

It is well known that differentiation amplifies the noise unless certain smoothing is involved into the differentiation algorithm. Moreover, the differentiation changes noise distribution law and the system should be augmented by one additional state to satisfy the assumptions of (4.4). Integration is not subject to these problems and thus we define a new observation through the operation of integration as

$$d\xi = \zeta(t)dt\,. \tag{4.29}$$

Bearing in mind a relationship between the Wiener process and Gaussian noise $\varepsilon = dV / dt$, the new observation model takes the following form

$$d\xi = h(u, \boldsymbol{\theta})dt + BdV\,. \tag{4.30}$$

Treating the unknown parameter vector $\boldsymbol{\theta}$ as an unknown state and augmenting the observation process (4.30) with the corresponding differential equation (4.3) gives

$$\begin{aligned} d\boldsymbol{\theta} &= \mathbf{0} \\ d\xi &= h(u, \boldsymbol{\theta})dt + BdV. \end{aligned} \tag{4.31}$$

Similarly for the estimation of time-varying parameters the observation process (4.30) is augmented by the corresponding differential equation (4.13).

The electrode reaction models are given in the form of (4.27) and, therefore, they can be presented in the equivalent differential form (4.31) which admits application of the Zakai filtering theory for parameter identification. Further, the estimates (4.8) and (4.26) will be analyzed when applied for parameter identification of electrode reaction models.

4.4 Electrochemical parameters identification

In this section the Zakai filtering method is implemented for the estimation of different electrode kinetics models. The electrode kinetics models can be represented as a static relationship between the current density i (A/m^2), applied voltage or electrode potential E (V), and the concentration of species c (mol/m^3), involved in a reaction occurred in an electrochemical cell

$$i(t) = f\left(E(t), c(t), \boldsymbol{\theta}\right). \tag{4.32}$$

Equation (4.32) includes a number of unknown constant parameters $\boldsymbol{\theta}$, which should be estimated by fitting the measured data to a model. The data are generated by the CV method, i.e. the voltage is changed linearly versus time from a zero voltage to a set voltage and then swept back to zero. The voltage law is given as in (4.33)

$$E = \begin{cases} -\nu t, & 0 \le t \le T/2 \\ \nu(t-T), & T/2 < t \le T \end{cases}, \tag{4.33}$$

where E is the voltage between the working and reference electrodes, V, T is the sweep period, s and ν is the sweep rate, V/s.

Since the voltage is changed in a predetermined manner, it is natural to assume it to be completely known. The current density measurements ζ involve a certain measurement error depending on the equipment used and is assumed to be corrupted by an additive white noise

$$\zeta(t) = i(E(t), c(t), \boldsymbol{\theta}) + B\varepsilon(t) . \tag{4.34}$$

A number of current density models are known in electrochemistry (Bard and Faulkner, 2001; Newman and Thomas-Alyea, 2004). Further they will be considered in increased complexity starting from a linear model and going step by step to a highly nonlinear model in the unknown parameters.

4.4.1 Identification of single parameter

The simplest relationship between the current density and potential of a single electrode is prescribed by the single-directional Butler-Volmer equation (Newman and Thomas-Alyea, 2004)

$$i = -i_0 e^{-k\alpha E} , \tag{4.35}$$

where i is the current density, A/m^2, i_0 is the exchange current density, A/m^2, E is the potential of the electrode measured against a standard hydrogen electrode, V, α is the apparent transfer coefficient, dimensionless, k is the temperature voltage, 80 V^{-1}. The next two parameters will be used in simulation: i_0 = 42, α = 0.25 if not indicated otherwise.

If the exchange current density is assumed to be unknown $\theta \equiv i_0$ the equation (4.35) is linear in the unknown parameter, i.e.

$$d\xi = -\theta e^{-k\alpha E} dt + BdV , \quad \xi(0) = \xi_0 . \tag{4.36}$$

The initial distribution of the parameter is specified by normal distribution $\theta_0 \sim N(200, 9)$.

In the electrode kinetics models voltage acts as the input or perturbation of the system. Being applied to the system it produces the current density acting as output. A typical shape of voltage in a cyclic sweep test with the sweep rate 25 mV/s and the current density corrupted by additive white measurement noise with zero mean and standard deviation B = 10 A/m^2, are shown in Fig. 4.1. The corresponding Zakai equation derived from (4.7) and (4.35) is

$$dq = -\frac{1}{2}\left(\frac{\theta e^{-k\alpha E}}{B}\right)^2 qdt - \frac{\theta e^{-k\alpha E}}{B^2} qd\xi . \tag{4.37}$$

In the equations (4.1)-(4.2) of the general model for the Zakai filtering, the coefficients were assumed to be bounded. Though the coefficients in the equation (4.37) and further applied models are not bounded, the Zakai filtering method still can be used because all the calculations are carried out in a predefined bounded domain (Lototsky and Rozovskii, 1998).

Since the model is linear in the unknown parameter, a linear estimation technique such as the least mean square (LMS) estimation method (Liptser and Shiryayev, 1977) can also be used. The exchange current density estimated using and the Zakai filtering

method and the LMS is shown in Fig. 4.2. The mean values converge to the true value of the parameter, and the standard deviations of estimates approach zero value similarly, irrespective of the different initial values chosen. In this case both the estimates are optimal.

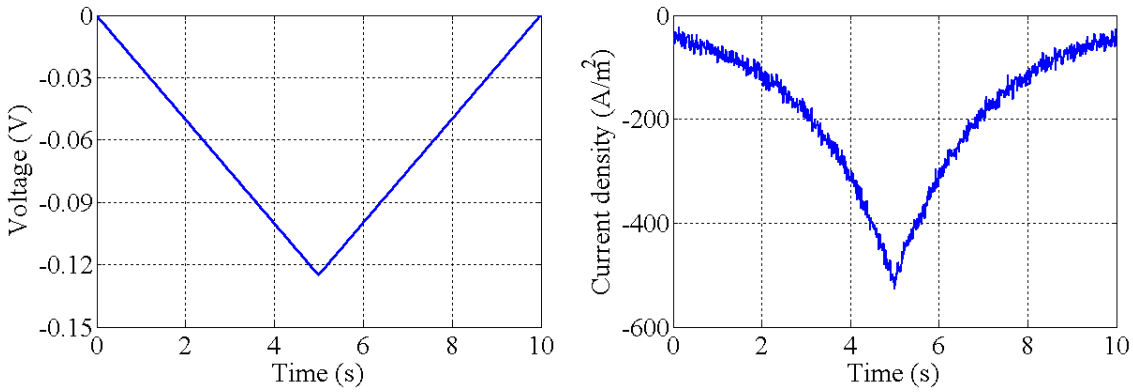

Figure 4.1: Left: An illustration of the voltage shape between the two electrodes in a cyclic sweep test. Sweep rate of 25 mV/s and magnitude 0.125 mV is used. Right: The simulated current density generated by the single directional Butler-Volmer equation (4.24).

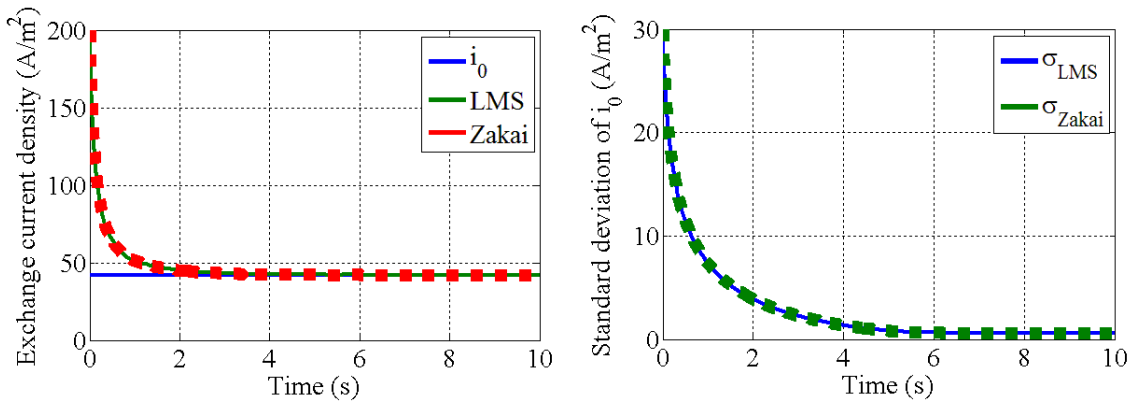

Figure 4.2: Left: The exchange current density estimate using the Zakai filtering and LMS methods. Right: Standard deviation of the exchange current density estimate using the Zakai filtering and LMS methods. Both the estimates converge identically to the true value of i_0.

The Zakai estimate is a random parameter characterized by a probability density. Evolution of the probability density distribution is shown in Fig. 4.3.

By examining the same model (4.35), but assuming the apparent transfer coefficient to be an unknown parameter, one can come to a nonlinear in the parameters estimation problem with the observable process given by (4.38)

$$d\xi = -i_0 e^{-k\theta E} + BdV, \quad \xi(0) = \xi_0. \tag{4.38}$$

The initial distribution of the parameter is specified by the normal distribution $\theta_0 \sim N(0.5, 0.09)$. Convergence of the estimate and evolution of the probability density are

illustrated in Figs 4.4 and 4.5 respectively. The Zakai estimate shows fast convergence of the estimated values to the true value.

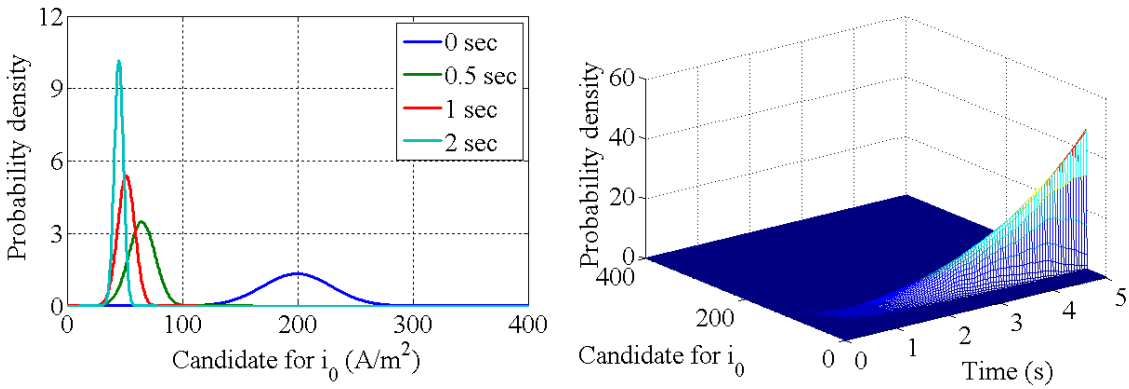

Figure 4.3: Left: Probability density distribution of the exchange current density estimate using the Zakai filtering method. Right: Evolution of the probability density in space and time.

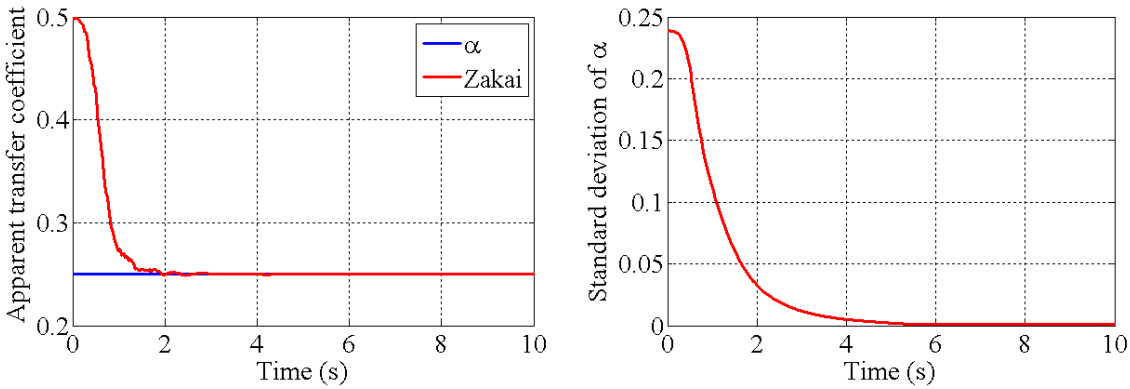

Figure 4.4: Left: The apparent transfer coefficient estimated using the Zakai filtering method. Right: Standard deviation of the apparent transfer coefficient estimate.

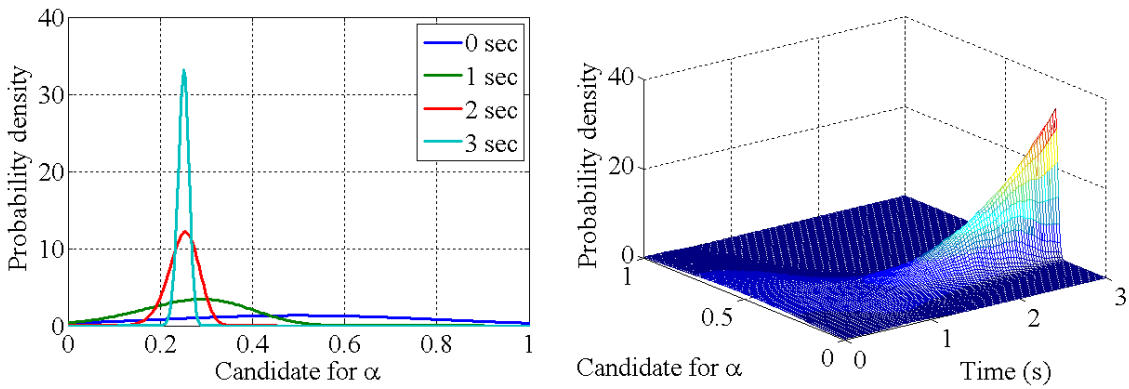

Figure 4.5: Left: Probability density of the apparent transfer coefficient estimate computed using the Zakai filtering method. Right: Evolution of the probability density in space and time.

It should be mentioned that the logarithmic change of variables can be applied in this case to make the model (4.35) linear in the parameters. This change of variables violates the assumption of the normally distributed noise, however, the least squares method

usually leads to satisfactory results (Cvetanovic and Singleton, 2004). Such a transformation is unquestionably impossible in the next two models.

In reversible reactions the electrode kinetics is represented by the bi-directional Butler-Volmer equation (Newman and Thomas-Alyea, 2004)

$$i = i_0 \left(e^{k(1-\alpha)E} - e^{-k\alpha E} \right). \tag{4.39}$$

The model (4.39) is more complicated as the apparent transfer coefficient appears in both exponents. The corresponding observable process (see Fig. 4.6) is given by (4.40)

$$d\xi = i_0 \left(e^{k(1-\theta)E} - e^{-k\theta E} \right) dt + BdV . \tag{4.40}$$

Convergence of the estimate is illustrated in Fig. 4.7. The convergence is slower as opposed to the single-directional model (4.35) when a low signal is applied to the system. Indeed, taking the Taylor series expansion of the equation (4.39) in the neighborhood of zero voltage and neglecting all the nonlinear terms yields the current density independent of α

$$i \approx i_0 kE .$$

The apparent transfer coefficient can also be estimated from the positive sweep; when instead of the former sweep rate of 25 mV/s and amplitude 125 mV, a slower sweep rate of 10 mV/s and less amplitude 50 mV is applied to remain similar to the range of the current density measurements obtained from the negative sweep. Convergence of the Zakai estimate to the true value of the parameter and standard deviation of the estimate is also shown in Fig. 4.7.

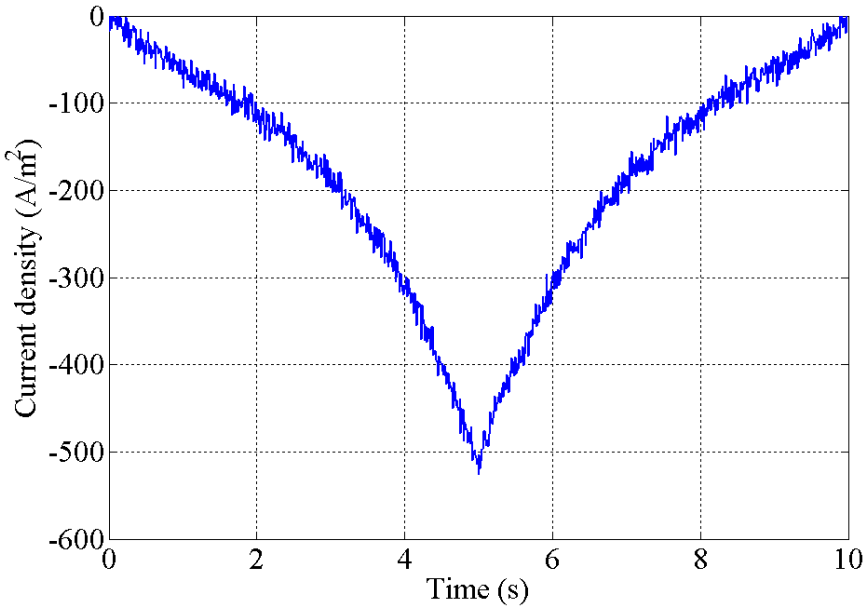

Figure 4.6: The simulated current density curve with the bi-directional Butler-Volmer equation (4.39).

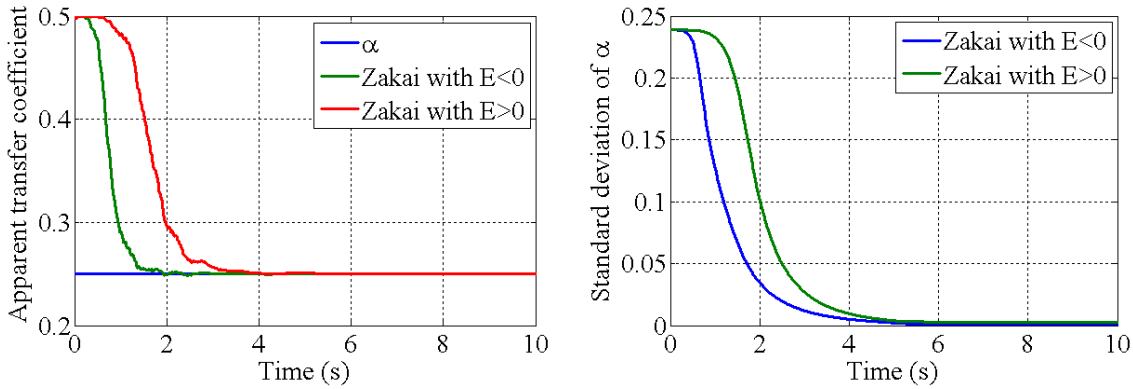

Figure 4.7: The apparent transfer coefficient estimated using the Zakai method in the case of bi-directional model with negative and positive sweep signals. Left: Conditional mean estimate. Right: Standard deviation of the estimate. The estimate converges slowly to the true value of α under a low input signal.

Results obtained under positive sweep voltage justify slow convergence under a low input signal which perturbs the system for a longer time than in the negative sweep case due to the slower sweep rate. However, as the signal grows, convergence of the bi-directional models tends to that of single-directional model. It becomes apparent when observing that the latter model is an approximation of the former model in a large signal case.

The previously considered single-directional model (4.35) and the bi-directional model (4.39) assume mass-transfer does not affect the electron transfer process. Otherwise concentration of species at the electrode surface should be taken into account. Particularly, under the assumptions A1 and A2 in Chapter 2 in unstirred solutions the concentration of species c affects the current density according to the following model (Bard and Faulkner, 2001)

$$i = i_0\left(e^{k(1-\alpha)E} - \frac{c(0,t)}{c_b}e^{-k\alpha E}\right). \tag{4.41}$$

Equation (4.41) has the form of (2.6) with $\alpha_c = \alpha$, $\alpha_a = 1 - \alpha$ and $E_{eq} = 0$. The ions concentration in the stagnation layer is a diffusion-controlled process (2.28)

$$\frac{\partial c(x,t)}{\partial t} = \frac{\partial}{\partial x}\left(D(c)\frac{\partial c(x,t)}{\partial x}\right)$$

with a uniform initial concentration (2.29), boundary conditions (2.30) and (2.31) or (3.1). In the simulations constant value of the diffusion coefficient $D = 4\cdot 10^{-10}$ m^2/s was used.

The concentration at the boundary (the left plot in Fig. 4.8) can be treated as measured as it always can be found from (2.28)-(2.30) and (2.31) or (3.1). Then the apparent transfer coefficient can be simply estimated using the Zakai filtering method. The current density-potential curve with the measurement errors is illustrated in the right plot of Fig. 4.8.

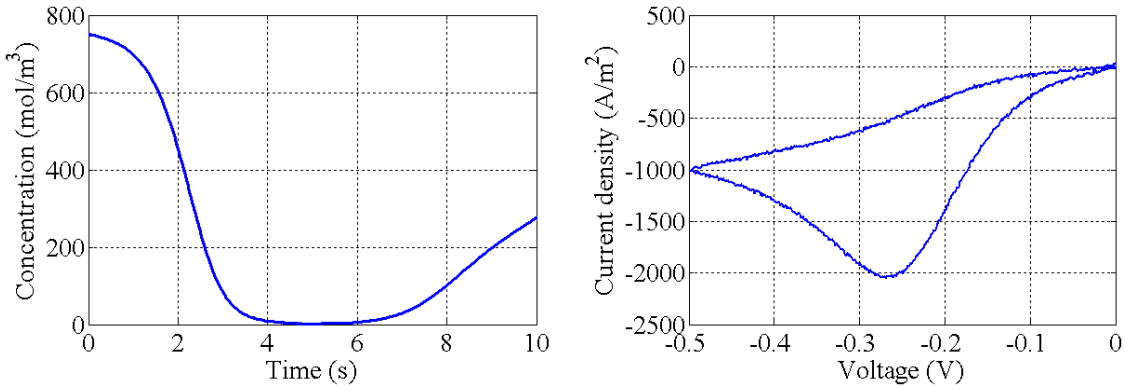

Figure 4.8: Left: An illustration of the ions concentration in near vicinity to the cathode surface (boundary) under sweep voltage experiment. Right: The current-density-potential curve under sweep voltage experiment.

The apparent transfer coefficient appears in both exponents with a time-varying coefficient in front of the second exponential term. The estimation problem is more time dependent and nonlinear than in the former case and requires solving the diffusion equation. The observed process is given by (4.42)

$$d\xi = i_0\left(e^{k(1-\theta)E} - \frac{c(0,t)}{c_b}e^{-k\theta E}\right) + BdV\ . \tag{4.42}$$

The convergence of the estimation process is still fast as illustrated in Figs 4.9-4.10.

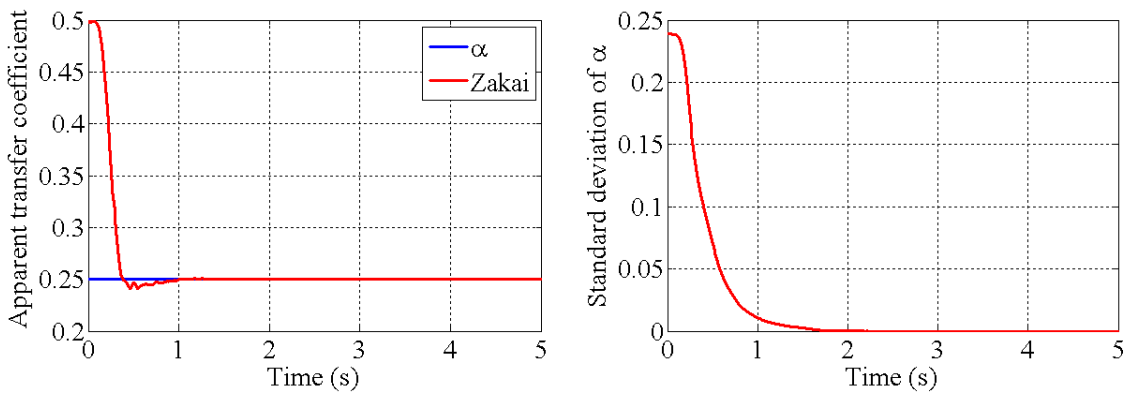

Figure 4.9: Left: The apparent transfer coefficient estimated from the mass-transfer limited electrode kinetic model (4.41) using the Zakai filtering method. Right: Standard deviation of the apparent transfer coefficient estimate.

As was mentioned in Chapter 2 the model (4.41) assumes the first order reaction at the reaction interface. As a consequence, the concentration of the species enters to the model (4.41) linearly. In general, the activity of species should be used instead of the concentration. The relationship between the activity and concentration can be, for instance, approximated though a power function of the concentration as in (3.59)

$$a = \left(\frac{c(0,t)}{c_b}\right)^{\gamma},$$

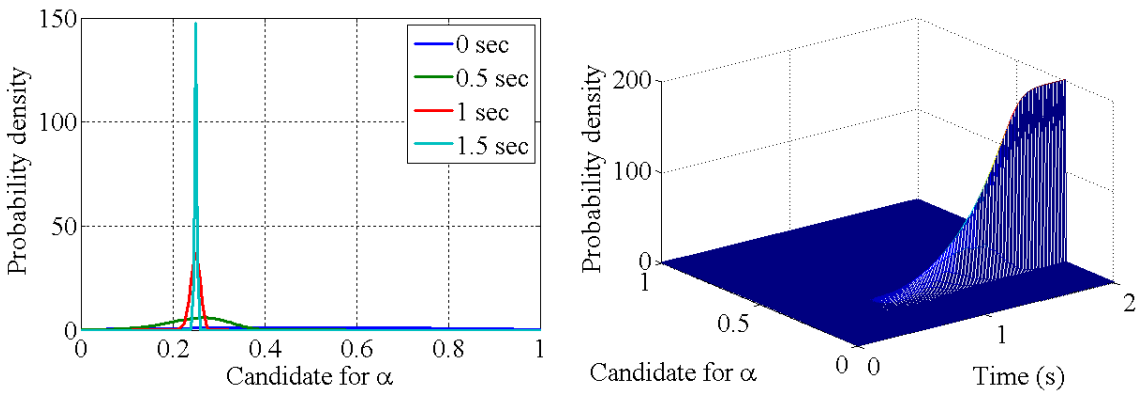

Figure 4.10: Left: Probability density of the apparent transfer coefficient from the mass-transfer limited electrode kinetic model (4.41) computed using the Zakai filtering method. Right: Evolution of the probability density in space and time.

where $\gamma = 0.4$ was used in the simulation. Changing concentration to activity in (4.41) yields the following electrode kinetics model

$$i = i_0 \left(e^{k(1-\alpha)E} - \left(\frac{c(0,t)}{c_b} \right)^{\gamma} e^{-k\alpha E} \right). \tag{4.43}$$

The estimation results are quite similar to the former case (Figs 4.9-4.10), but are rather different if a two-electrode system is used as is frequently applied in industrial plating processes. In this case the model of the working electrode with activity is the following (Mendelson and Tenno, 2008a)

$$i = i_0 \left(\frac{c(0,t)}{c_b} \right)^{\gamma(1-\alpha)} \left(e^{k(1-\alpha)^2 E} - e^{-k\alpha(1-\alpha)E} \right). \tag{4.44}$$

Equation (4.44), derived for a negative sweep voltage, follows from the equation (2.25) if the activity is approximated by a power function of the concentration (3.59) and $\alpha_c = \alpha$, $\alpha_a = 1 - \alpha$. A similar expression for a positive sweep can be obtained from (2.26). The corresponding (4.44) model, applied for estimation, is the following

$$d\xi = i_0 \left(\frac{c(0,t)}{c_b} \right)^{\gamma(1-\alpha)} \left(e^{k(1-\alpha)^2 E} - e^{-k\alpha(1-\alpha)E} \right) dt + BdV\,. \tag{4.45}$$

Convergence of the estimate for (4.45) with $i_0 = 150$, $\alpha = 0.16$ is illustrated in Fig. 4.11. Because of the more complex model the convergence is no longer exponential (Fig. 4.11). This is due to two observable peaks ($x = 0.2$; 0.6) in the initial phase ($t = 0.5$ s) of the probability density estimation (Fig. 4.12). In fact, the equations (4.9) and (4.10) cannot be applied to compute the mean value and variance of the estimated parameters without accounting high-order statistics. Such multi-modal densities may easily destroy the estimation. Therefore, a certain inspection of the probability density shape has to be done to prevent incorrect estimation with the Zakai filtering method.

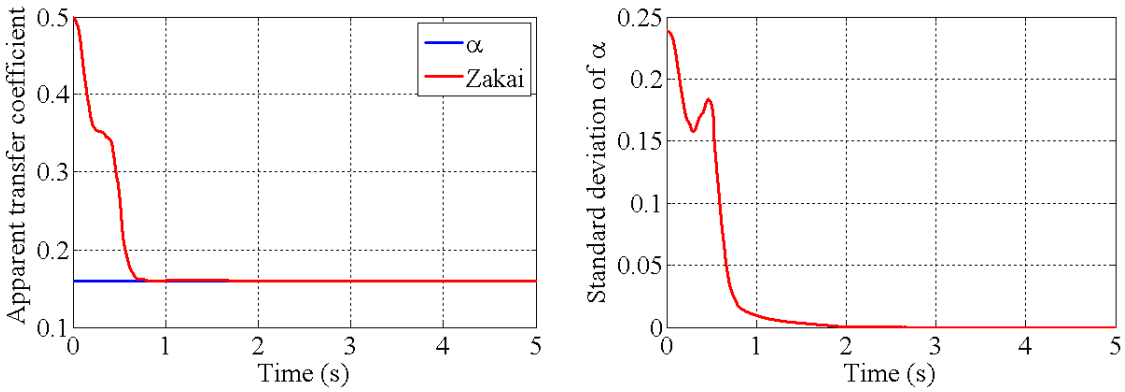

Figure 4.11: Left: The apparent transfer coefficient estimated from the mass-transfer limited electrode kinetic model (4.44). Right: Standard deviation of the apparent transfer coefficient estimate.

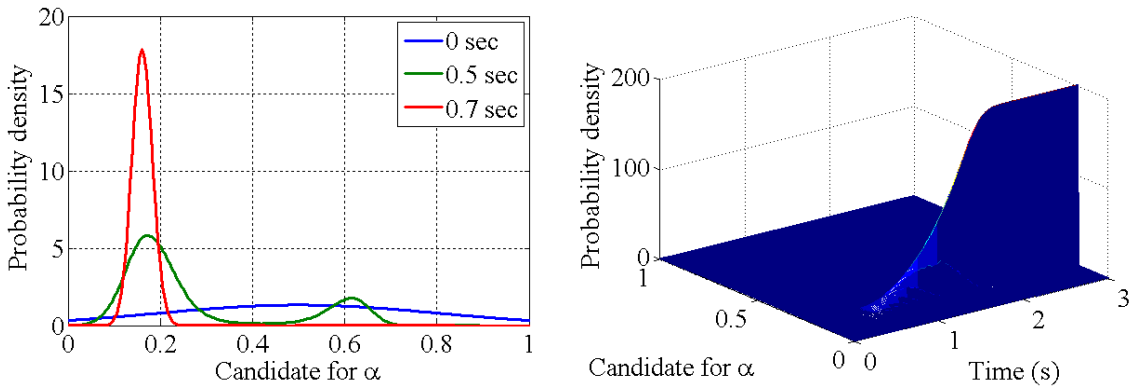

Figure 4.12: Left: Probability density of the apparent transfer coefficient estimated from the mass-transfer limited electrode kinetic model (4.44). Two peaks are clearly observable in the initial phase at $t = 0.5$ s. Right: Evolution of the probability density in space and time.

In the estimation presented before, the apparent transfer coefficient was assumed to be constant. This is reasonable if the potential range where current density measurements are collected is narrow (Bard and Faulkner, 2001). However, in general the apparent transfer coefficient is a potential-dependent factor. Moreover, in general both the exchange current density and apparent transfer coefficient are time-dependent. Moffat et al. (2001), for instance, modeled both the kinetic parameters as functions of the surface concentration of the used additives.

Consider the electrode kinetic model (4.42) and assume the following linear drift model for the apparent transfer coefficient

$$d\alpha = (0.25 - \alpha)\,dt + 0.05\,dW, \quad \alpha(0) = 0.25\,. \tag{4.46}$$

The current-density-potential curve with the measurement errors and estimation process calculated using the factorization algorithm (4.16)-(4.21) are illustrated in Fig. 4.13. The measured hysteresis is rather noisy in this case. After a short transient period of 1 second, the estimate follows the true value of the apparent transfer coefficient. The

corresponding evolution of the standard deviation and evolution of the probability density distribution that demonstrates the location of the Zakai estimates on the *x*-axis are shown in Fig. 4.14.

One can observe that even after removal of the initial uncertainty the tracking quality is not equally good in the remaining period. The quality deteriorates due to a small signal to noise ratio (Figs 4.13-4.14). The input signal (sweep voltage) should be large enough to achieve a small tracking error. The issue was tested in another sweep test where the input signal was set constant starting from t = 6 s further on as shown in Fig. 4.15. Unlike cyclic sweep voltage this signal supports about the same small tracking error everywhere in the remaining period after the initial uncertainty is removed.

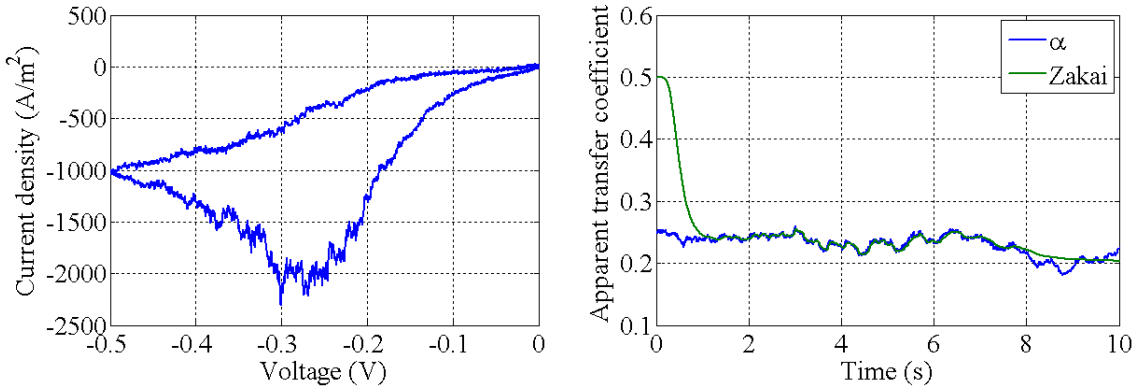

Figure 4.13: Left: The current-density-potential curve in the case of linear drift (4.46) of the apparent transfer coefficient. Right: The estimated apparent transfer.

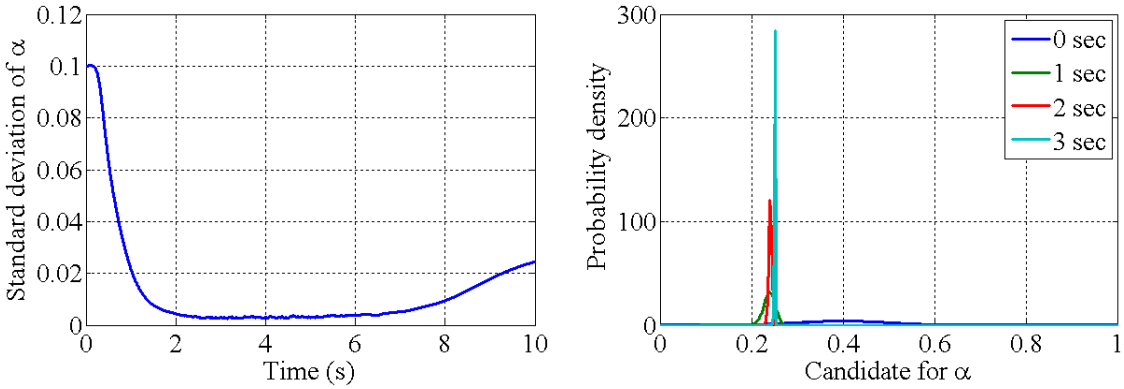

Figure 4.14: Left: Standard deviation of the estimate. Right: Evolution of the probability density.

4.4.2 Identification of two parameters

In the electrochemical reaction the exchange current density and the apparent transfer coefficient are kinetic parameters of a reaction. They are usually unknown, though their range is known to some extent. As regards the apparent transfer coefficient, it is known that its value lies between 0 and 1. Bard and Faulkner (2001) have argued that in most of the systems the apparent transfer coefficient lies between 0.3 and 0.7. However, a lot

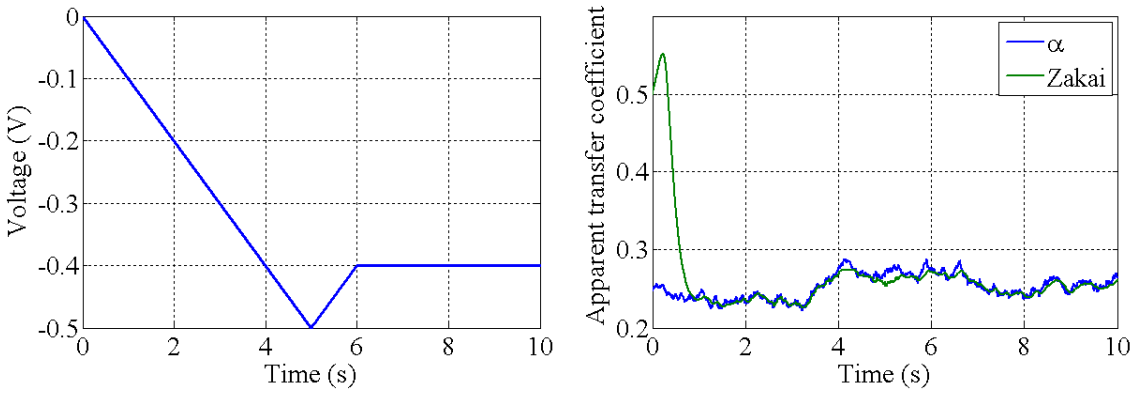

Figure 4.15: Left: The voltage that supports an equal tracking quality. Right: The apparent transfer coefficient estimated from the electrode kinetic model (4.42) and linear drift (4.46).

of studies in chemical and electrochemical literature suppose this coefficient to be equal to 0.5 (see, e.g., Pirogov and Zelinsky, 2004; Barbarisi et al., 2006). This presumption is used because it greatly simplifies the analysis excluding from consideration the nonlinear unknown parameter. In the following text we consider the identification of both kinetic parameters mentioned for the several bi-directional models. In addition, in this section the Zakai and pathwise filtering methods are compared.

The exponential model with concentration dependent on the finite-length diffusion process

Consider the bi-directional electrode kinetic model (4.41) together with the finite-length mass-transfer model (2.28)-(2.31). If diffusivity is assumed known beforehand, the boundary concentration on the cathode surface can be solved from (2.28)-(2.31) by substituting the current density (4.41) into the boundary condition (2.30). This solves the concentration profile everywhere in the domain and, particularly, on the boundary. The solved concentration on the cathode boundary $c(t,0)$ is designated below as $c^i(t)$. The superscript i is used to highlight the concentration dependence on the modeled current density. The solved concentration determines the current density model as the transient function (4.47)

$$i = i_0\left(e^{k\alpha E} - \frac{c^i(t)}{c_b}e^{-k(1-\alpha)E}\right). \tag{4.47}$$

The current density (4.47), corrupted with an additive white noise, is used to simulate the measured current density

$$\zeta(t) = i_0\left(e^{k\alpha E} - \frac{c^i(t)}{c_b}e^{-k(1-\alpha)E}\right) + B\varepsilon(t). \tag{4.48}$$

Then the corresponding concentration on the boundary $c^\zeta(t)$ can be found from (2.28)-(2.31) by substituting the measurements to the boundary condition (2.30). The superscript ζ is used to highlight the concentration dependence on the measured current

density. Therefore, the concentration can be treated as a measured process, because it is always can be found using the simulation procedure explained above.

One can use an initial guess of θ_0 with certain low accuracy for the unknown kinetic parameters, for instance

$$\theta_0 \sim N\left(\begin{bmatrix}100\\0.5\end{bmatrix}, \begin{bmatrix}8000 & 0\\0 & 0.09\end{bmatrix}\right) = p_0(x). \tag{4.49}$$

Since all the calculations are carried out in a predefined bounded domain, an uncertainty of unknown parameters is set by the truncated normal probability density distribution shown in Fig. 4.16.

The measurement function A is dependent on the candidates x and y of the unknown parameters i_0 and α

$$i = A(t,x,y,\zeta) = xe^{kyE}\left(1 - \frac{c^{\zeta}(t)}{c_b}e^{-kE}\right). \tag{4.50}$$

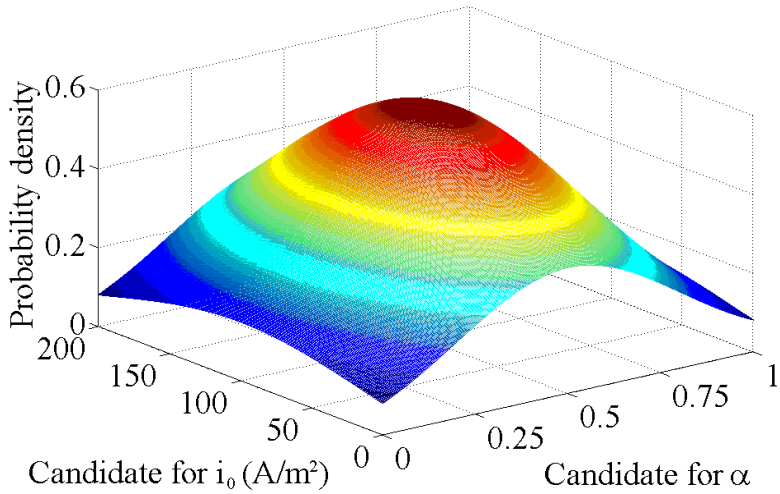

Figure 4.16: The initial guess of the unknown parameters is set by the truncated normal probability density.

It is not a smooth function of time because it includes the cyclic sweep function (4.33), whose time-derivative is a sign function

$$\frac{dE}{dt} = r\ \mathrm{sign}\left(t - \frac{T}{2}\right). \tag{4.51}$$

When solving the Zakai equation this pitfall is simply overcome by partitioning the time interval into two equal parts. Firstly, the solution is found on the first interval [0, T/2], and then, after a reinitialization of the unnormalized probability density q with $q(T/2,x,y)$, on the second interval [T/2, T]. The solution on the intervals is given by (4.52)

$$q(t,x,y)=p_0\left(x,y\right)\exp\left\{-\frac{x^2}{2}\int_0^t\frac{e^{-2kyrs}}{B^2}\left(1-\frac{c^{\zeta}(s))}{c_b}e^{krs}\right)^2ds+x\int_0^t\frac{e^{-kyrs}}{B^2}\left(1-\frac{c^{\zeta}(s)}{c_b}e^{krs}\right)d\xi\right\},$$

(4.52)

Pathwise filtering is more complicated than Zakai filtering. It includes the time-derivative of the model (4.50) which is a discontinuous function because of the sign function

$$\frac{dA}{dt}=xe^{kvE}\left(k\left(y+\left(1-y\right)\frac{c^{\zeta}(t)}{c_b}e^{-kE}\right)\frac{dE}{dt}-\frac{e^{-kE}}{c_b}\frac{dc^{\zeta}(t)}{dt}\right). \tag{4.53}$$

In addition, (4.53) includes the time derivative of the species' concentration. Nevertheless, the solution procedure for pathwise filtering can be treated similarly to the Zakai filtering by partitioning the time interval. The pathwise distribution on the intervals is

$$\rho(t,x,y)=p_0\left(x,y\right)e^{-\xi_0\frac{A(0,x,y,0)}{B^2}}\times$$

$$\exp\left\{\begin{array}{l}-\frac{x^2}{2}\int_0^t\frac{e^{-2kyrs}}{B^2}\left(1-\frac{c^{\zeta}(s)}{c_b}e^{krs}\right)^2ds+\\ x\int_0^t\frac{e^{-kyrs}}{B^2}\left(kr\left(y+\left(1-y\right)\frac{c^{\zeta}(s)}{c_b}e^{krs}\right)+\frac{e^{-kE}}{c_b}\frac{dc^{\zeta}(s)}{ds}\right)\xi(s)ds\end{array}\right\}. \tag{4.54}$$

The model structure allows effective computation of parameters by (4.52) and (4.54) by separation of the candidates x and y in the direct integration method (x is taken out of the integrals). The reason is that the model (4.47) is linear in the exchange current density.

Evolution of the current density and apparent transfer coefficient estimates is shown in Figs 4.17 and 4.18 respectively. From now on in the smaller boxes a zoomed portion of the plots will be illustrated to investigate differences in behavior between the Zakai and pathwise filtering methods.

The convergence of estimates is fast and unbiased. The Zakai filtering and pathwise filtering estimates are almost identical. However, in contrast to the Zakai estimate, certain small variations appear in the pathwise estimate. The reason for this larger variation is the time derivative of the concentration at the boundary that the pathwise estimate uses.

Evolution of the probability distributions is shown in three successive figures: Fig. 4.16, 4.19a and 4.19b. The probability density which is initially widely distributed (Fig. 4.16) is fairly concentrated at t = 1 second (Fig. 4.19a) and almost a delta function at t = 10 seconds (Fig. 4.19b).

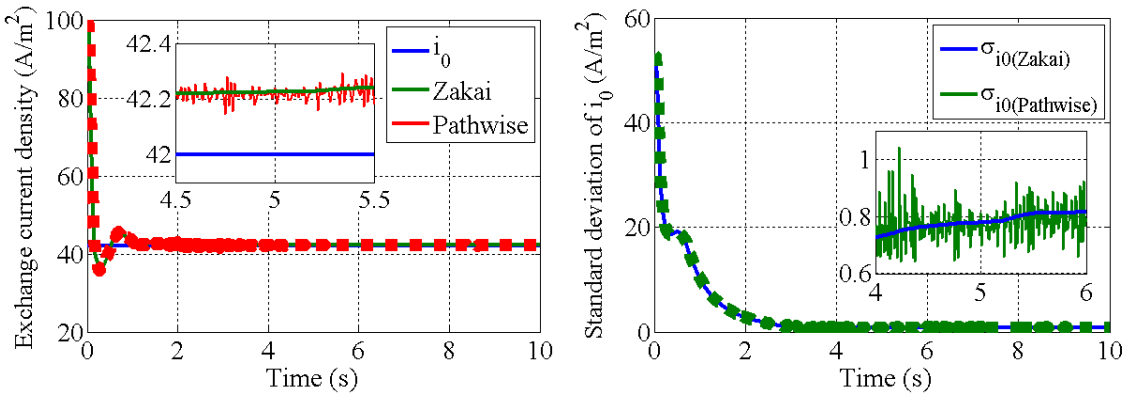

Figure 4.17: Left: The conditional mean of the exchange current density estimated simultaneously with apparent transfer coefficient from the bi-directional electrode kinetic model (4.41) using the Zakai filtering and pathwise filtering methods. Right: Standard deviation of the exchange current density.

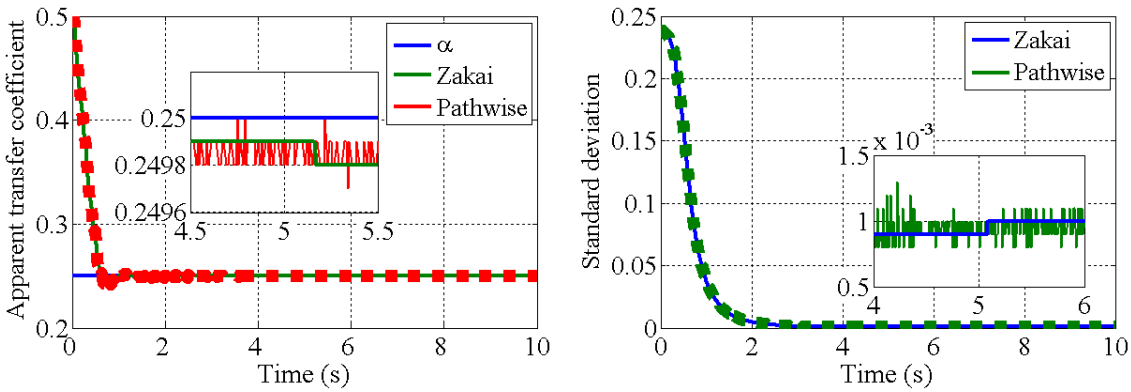

Figure 4.18: Left: The conditional mean of the apparent transfer coefficient estimated simultaneously with exchange current density from the electrode kinetic model (4.41) using the Zakai and pathwise filtering methods. Right: Standard deviation of the apparent transfer coefficient.

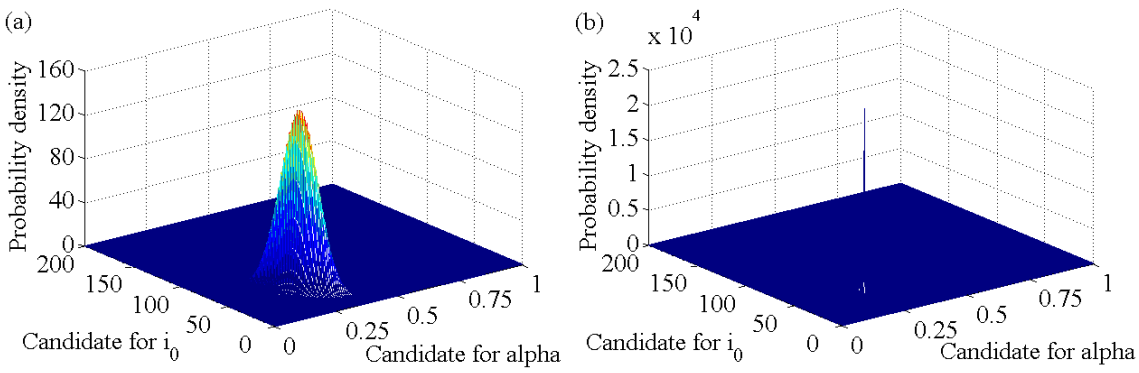

Figure 4.19: The probability density distribution in the case of the simultaneous estimation of two parameters from the electrode kinetic model (4.41). The Zakai filtering method is used. The distribution is shown at (a) $t = 1$ s and (b) $t = 10$ s.

Estimation of the two parameters simultaneously makes them dependent of each other. A strong correlation between the estimates is shown in Fig. 4.20a, as a narrow ellipse

build up in the form of equal value curves for the probability masses. This correlation is largest at about 1 second and eventually dies out. The corresponding circle-like curves at $t = 10$ seconds are shown in Fig. 4.20b.

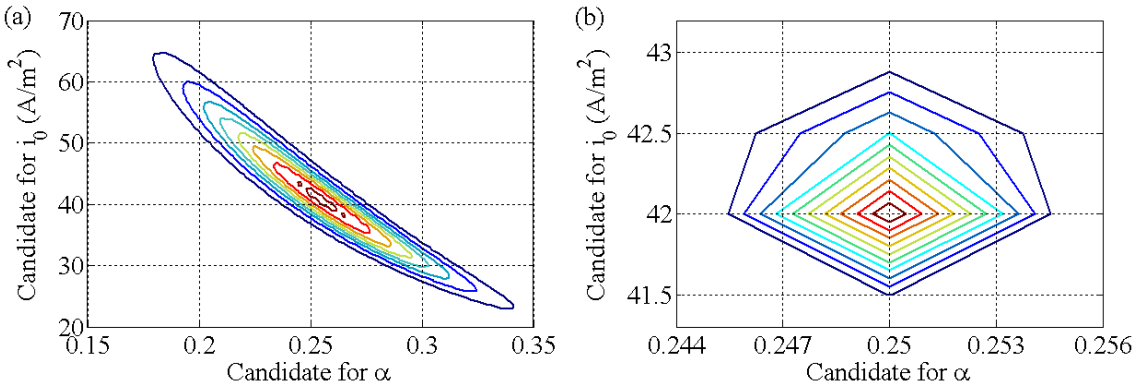

Figure 4.20: The correlation between the estimates in the case of the simultaneous estimation of two parameters from the electrode kinetic model (4.41). The Zakai filtering method is used. The correlation is shown at (a) $t = 1$ s and (b) $t = 10$ s.

The estimation of the two electrode model (4.44) leads to results similar to the case of single parameter estimation. Evolution of the estimates with $i_0 = 150$, $\alpha = 0.16$ is shown in Figs 4.21 and 4.22. In contrast to single parameter estimation, the convergence of the estimates is no longer exponential. The reason is the multivariate shape of the probability density distribution at the initial phase of the estimation. The local minimum degrades the estimation in the beginning, but disappears as more data comes, and equations (4.9) and (4.10) adequately give the mean value and variance of the exchange current density and apparent transfer coefficient.

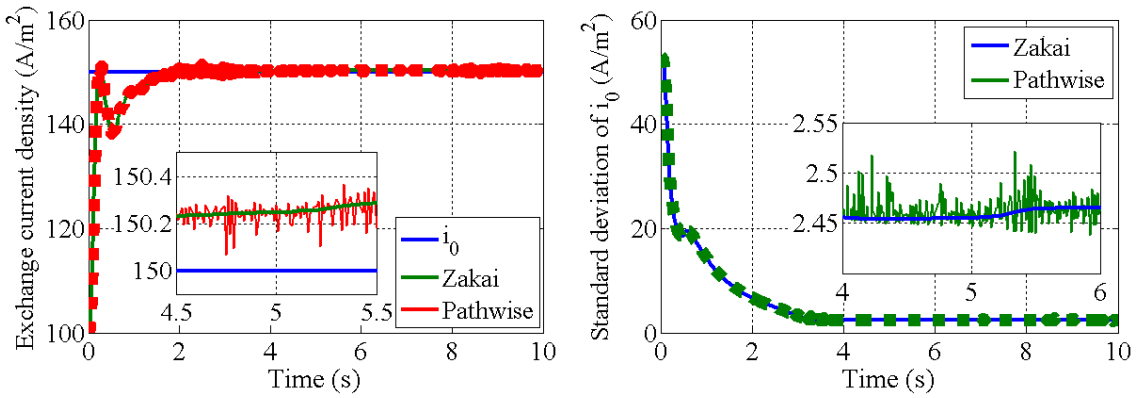

Figure 4.21: Exchange current density estimated simultaneously with apparent transfer coefficient from the electrode kinetic model (4.44) using the Zakai filtering and pathwise filtering methods. Left: Conditional mean. Right: Standard deviation.

Evolution of the probability mass densities is shown in three successive figures: Fig. 4.16, 4.23a and 4.23b. Similar to the results for the model (4.41), the probability mass widely distributed initially (Fig. 4.16) is fairly concentrated at $t = 1$ second (Fig. 4.23a) and almost a delta function at $t = 10$ seconds (Fig. 4.23b).

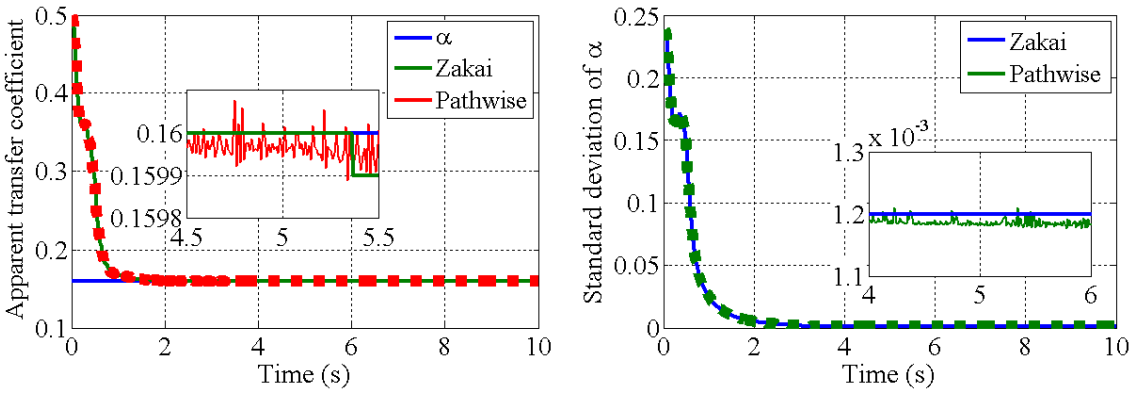

Figure 4.22: Apparent transfer coefficient estimated simultaneously with exchange current density from the bi-directional electrode kinetic model (4.44) using the Zakai filtering and pathwise filtering methods. Left: Conditional mean. Right: Standard deviation.

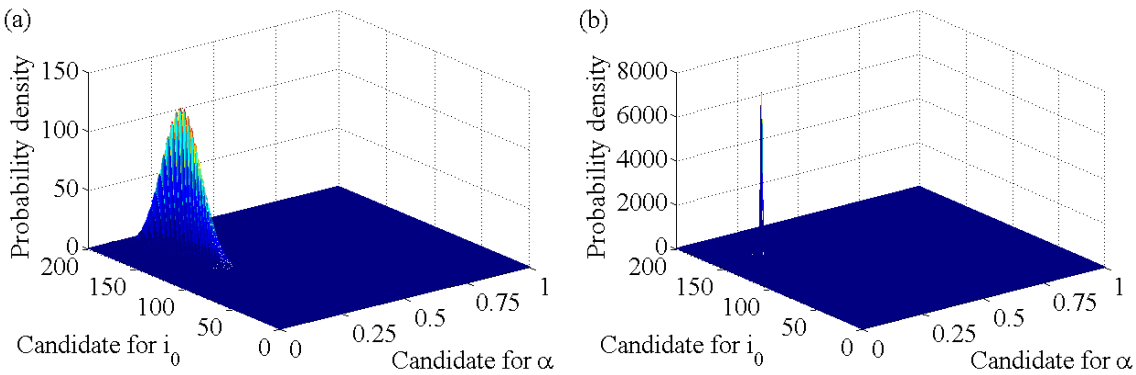

Figure 4.23: The probability density distribution in the case of the simultaneous estimation of two parameters from the bi-directional electrode kinetic model (4.44). The Zakai filtering method is used. The distribution is shown at (a) $t = 1$ s and (b) $t = 10$ s.

The evolution of the correlation between the estimates is shown in Fig. 4.24 starting from $t = 0.5$ seconds. The correlation is largest in the initial phase of the estimation process when a small amount of data with a small signal to noise ratio is available. As new data comes the correlations eventually dies out.

The exponential model with concentration dependent on the semi-infinite diffusion

Except for the kinetic parameters, one or several mass-transfer parameters can be unknown. This makes the problem fundamentally more complicated since the unknown parameters enter into the partial differential equation (2.28)-(2.31) or (2.28)-(2.30) and (3.1). However, by keeping the special conditions of the electrochemical experiment it is possible to remain the same level of complexity. For instance, in unstirred solutions a semi-infinite diffusion takes place with a stagnation layer whose thickness increases infinitely according to the boundary condition (3.1). In such a case the relationship between the concentration in the near vicinity of the cathode surface and the current measurements is given by (3.44) written in terms of current density as

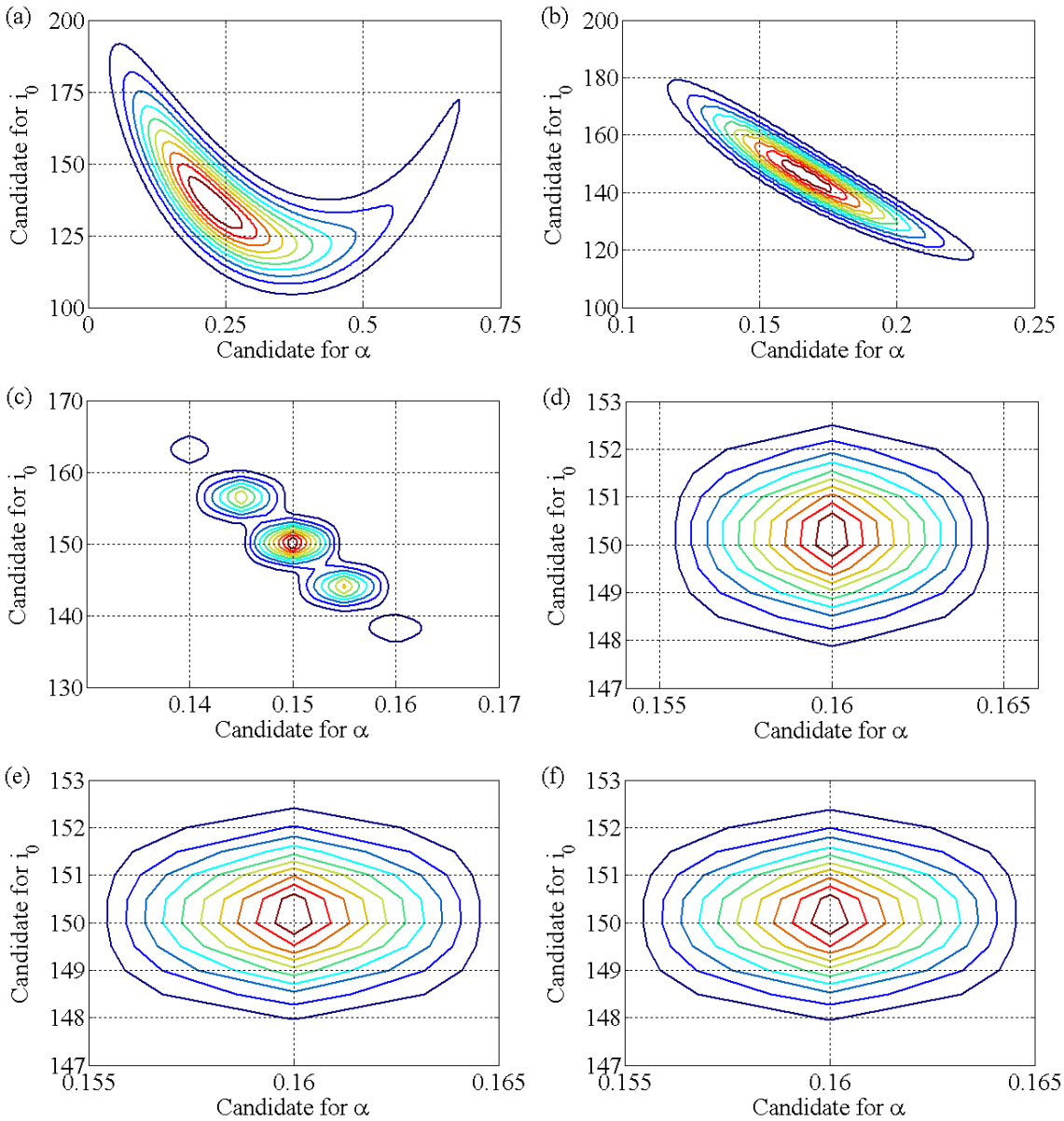

Figure 4.24: The correlation between the estimates in the case of the simultaneous estimation of two parameters from the electrode kinetic model (4.44). The Zakai filtering method is used. The correlation is shown at (a) $t = 0.5$ s, (b) $t = 1$ s, (c) $t = 2$ s, (d) $t = 3$ s, (e) $t = 5$ s and (f) $t = 10$ s.

$$c(0,t) = c_b + \frac{1}{nF\sqrt{\pi D}} \int_0^t \frac{i(s)}{\sqrt{t-s}} ds \,. \tag{4.55}$$

Equation (4.55) gives an approximation (4.56) of the concentration at the boundary when the current density is replaced with the noisy measurements

$$c(0,t) \approx c_b + \frac{1}{nF\sqrt{\pi D}} \int_0^t \frac{\zeta(s)}{\sqrt{t-s}} ds \,. \tag{4.56}$$

Equation (4.56) yields to the model (4.57) that, as opposed to the finite-length diffusion model, does not depend explicitly on the boundary concentration

$$d\xi = i_0 e^{k\alpha E}\left(1 - e^{-kE}\left(1 + \frac{1}{nF\sqrt{\pi D c_b}}\int_0^t \frac{\zeta(s)}{\sqrt{t-s}}ds\right)\right)dt + BdV\,. \tag{4.57}$$

The measurements function with the candidates *x, y, z* of the unknown parameters is given by (4.58)

$$A(t,x,y,z,\zeta) = xe^{kyE}\left(1 - e^{-kE}\left(1 - \frac{K}{\sqrt{z}}u(t)\right)\right). \tag{4.58}$$

In (4.58), z is a candidate of unknown diffusivity D, K is a known constant

$$K = \frac{1}{nF\sqrt{\pi c_b}}, \tag{4.59}$$

and $u(t)$ is the stochastic convolution of the current density measurements

$$u(t) = -\int_0^t \frac{\zeta(s)}{\sqrt{t-s}}ds\,. \tag{4.60}$$

The convolution integral (4.60) can be calculated using the fast computational scheme proposed by Nicholson and Shain (1964). The estimation of diffusivity can be performed using the same partitioning of the time interval as before to eliminate the sweep-related singularity of function (4.58). The unnormalized probability density in this case is given by

$$q(t,x,y,z) = p_0(x,y,z)\times$$

$$\exp\left\{-\frac{x^2}{2}\int_0^t \frac{e^{-2kyrs}}{B^2}\left(1 - e^{krs}\left(1 - \frac{K}{\sqrt{z}}u(s)\right)\right)^2 ds + x\int_0^t \frac{e^{-kyrs}}{B^2}\left(1 - e^{krs}\left(1 - \frac{K}{\sqrt{z}}u(s)\right)\right)d\xi\right\} \tag{4.61}$$

The pathwise estimation creates additional difficulties because it requires calculating the time derivative of the measurement function (4.58) that can be expressed through the derivative of the convolution integral as

$$\frac{dA}{dt} = xe^{kyE}\left(ky\left(1 - e^{-kE}\left(1 - \frac{K}{\sqrt{z}}u(t)\right)\right)\frac{dE}{dt} + e^{-kE}\left(k\left(1 - \frac{K}{\sqrt{z}}u(t)\right)\frac{dE}{dt} + \frac{K}{\sqrt{z}}\frac{du}{dt}\right)\right). \tag{4.62}$$

The last term of (4.62), if used for calculating distribution (4.26), can be expressed explicitly if multiplied by $\xi(s)e^{-k(1-y)E(s)}$ and integrated by parts over the interval [0, t]

$$\int_0^t \xi(s)e^{-k(1-y)E(s)}\frac{du}{ds}ds = \xi(t)e^{-k(1-y)E(t)}u(t) - \int_0^t e^{-k(1-y)E(s)}u(s)d\xi + k(1-y)\int_0^t \frac{dE}{ds}e^{-k(1-y)E(s)}\xi(s)u(s)ds \quad . \tag{4.63}$$

Using (4.63) the pathwise distribution can be estimated as follows

$$\rho(t,x,y,z) = p_0(x,y,z)e^{-\xi_0\frac{A(0,x,y,z,0)}{B^2}} \times \exp\left\{\begin{array}{l} -\frac{x^2}{2}\int_0^t \frac{e^{-2kyrs}}{B^2}\left(1-e^{krs}\left(1-\frac{K}{\sqrt{z}}u(s)\right)\right)^2 ds + xkr\int_0^t \frac{e^{k(1-y)rs}}{B^2}\left(1-\frac{K}{\sqrt{z}}u(s)\right)\xi(s)ds + \\ xykr\int_0^t \frac{e^{-kyrs}}{B^2}\left(1-e^{krs}\left(1-\frac{K}{\sqrt{z}}u(s)\right)\right)\xi(s)ds - x(1-y)\frac{K}{\sqrt{z}}kr\int_0^t \frac{e^{k(1-y)rs}}{B^2}\xi(s)u(s)ds \\ -x\frac{K}{\sqrt{z}}\xi(t)e^{k(1-y)rt}u(t) + x\frac{K}{\sqrt{z}}\int_0^t \frac{e^{k(1-y)rs}}{B^2}u(s)d\xi \end{array}\right\} . \tag{4.64}$$

Once again, because the electrode kinetic model (4.41) is linear in the exchange current density, effective computation of parameters by (4.61) and (4.64) by separation of the candidates x and y in the direct integration method (x is taken out of the integrals) is possible.

The Zakai and pathwise estimation results for the exchange current density and apparent transfer coefficient in the semi-finite diffusion are rather similar to that of the finite-length diffusion, and, therefore, are not reported here. Only an estimation of the diffusion coefficient is presented. At first it was estimated simultaneously with the exchange current density and then simultaneously with the apparent transfer coefficient using the Zakai filtering method (Fig. 4.25). In both cases the estimates converge to the true parameters. It is interesting to note that there is no movement towards the true diffusivity estimate in low voltage ranges. The reason for this is that the concentration at the boundary does not differ appreciably from the bulk solution concentration, and hence mass-transfer effects do not contribute to the current density. In other words, in low voltage ranges the current density is almost independent of the diffusivity coefficient.

The standard deviations of estimates present similar behavior as shown in the right plot of Fig. 4.25. The estimation accuracy did not change during the initial phase of estimation. Then it improved dramatically and reached a steady state. A non monotonic overshoot, clearly visible in the simultaneous estimation of the diffusivity with the apparent transfer coefficient, illustrates a nonlinear character of the estimation.

The correlation between estimates is weak during the initial period $t < 1$, strong during the period of rapid convergence and disappears after converging to the true values. The contour level lines of the probability density for the simultaneously estimated diffusivity

and apparent transfer coefficient in the middle of the rapid period (at t = 1.8) and after convergence are shown in Fig. 4.26. The behavior of correlation is again attributed to the manifesting of mass-transfer effects in the electrochemical cell.

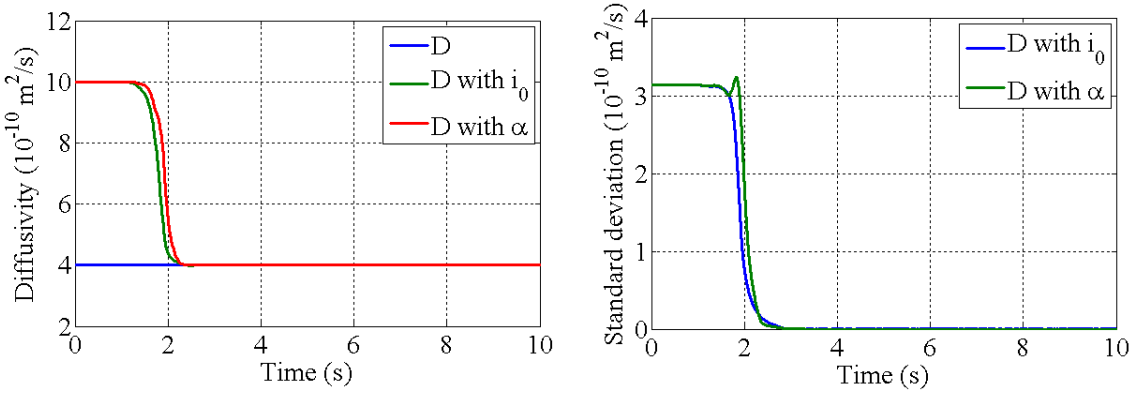

Figure 4.25: Left: Diffusivity estimated simultaneously with the unknown exchange current density or apparent transfer coefficient using the Zakai filtering method. Right: The standard deviations of the estimates.

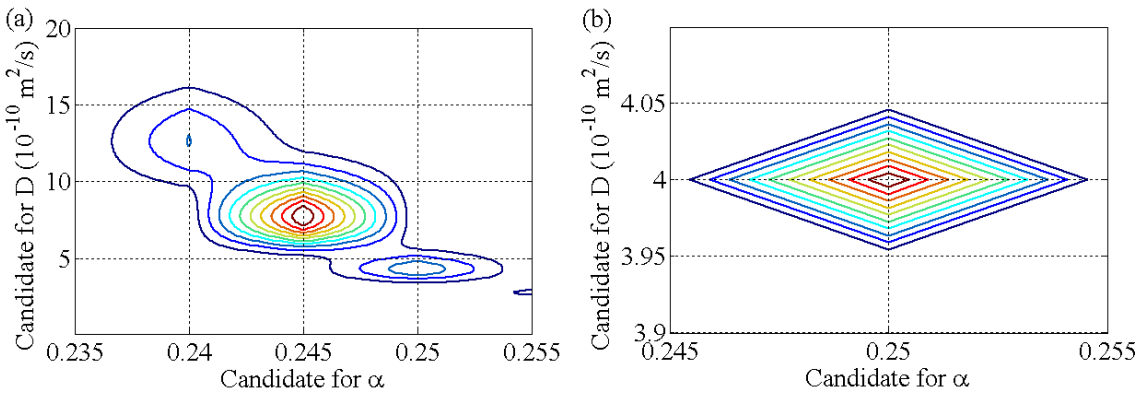

Figure 4.26: The correlation between simultaneously estimated diffusivity and apparent transfer coefficient evaluated at (a) t = 1.8 s and (b) t = 3 s. The Zakai filtering method is used.

4.5 Experimental study

As a practical test example, the Cu-Pt plating system was considered. It consists of two planar copper and platinum electrodes immersed in a non-agitated copper-sulphate solution. The bulk solution concentration of Cu(II) ions was 786 mol/m^3. Sulfuric acid was used in the solution to make the voltage drop in the system insignificant. The negative sweep voltage was applied to the system and the current-density measurements were recorded with a sampling rate of 0.02 seconds. The measured current-density–potential curve is depicted in Fig. 4.27.

The reaction, taking place at the copper electrode, is a copper deposition reaction. Such a reaction is usually considered as a two-step reaction and each elementary step is

described by its own set of kinetic parameters. Therefore, this is a more complex reaction than considered in (4.41). Because it is known that one of the reactions is much faster than the other, the whole reaction can be approximated as a one-step reaction with certain accuracy. Generally, the electrode reaction is not controlled so much by the concentration of species as by their activities. This is also a source of certain inaccuracy in the electrode reaction model (4.41) that is used for approximation of the experimental data. Because of the lack of agitation, the semi-infinite diffusion (2.28)-(2.30) and (3.1) is a proper model for the case.

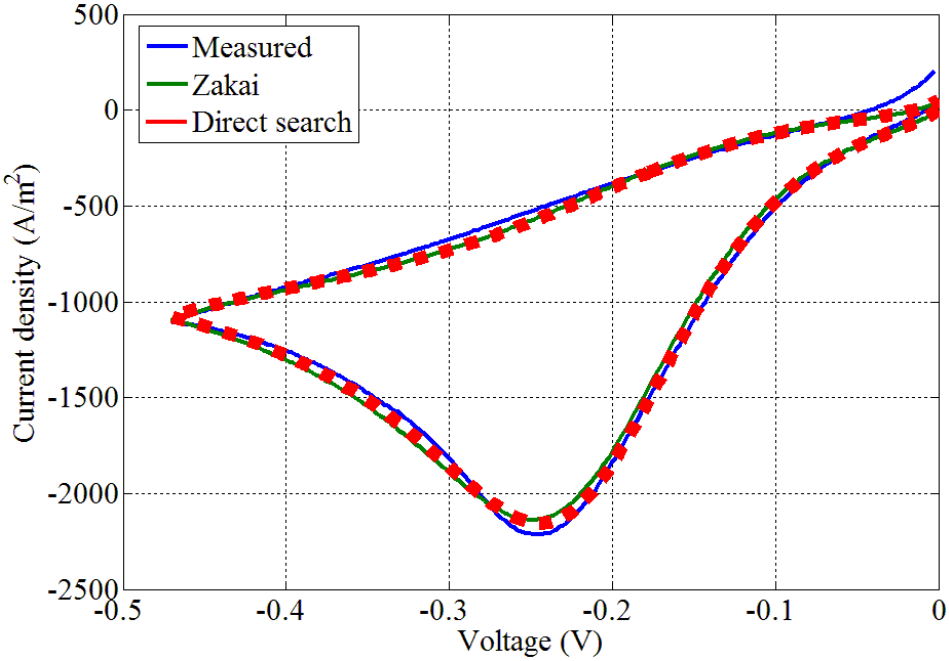

Figure 4.27: The experimental and estimated cyclic voltammetry curves of the Cu-Pt system. The estimates were obtained using Zakai filtering and direct search method.

The model parameters are typically unknown. According to the literature, the copper ion diffusivity may be assumed to be in the range of $10^{-9} - 10^{-10}$ m^2/s (Noulty and Leaist, 1987) while the exchange current density is not specified in a well defined range and the apparent transfer coefficient is in between 0 - 1 (Newman and Thomas-Alyea, 2004). This allows narrowing down the interval of admissible values for the parameters to be estimated. Particularly, in Zakai estimation the intervals 0–1, 0–200 A/m^2 and 10^{-9}–$2\cdot10^{-10}$ m^2/s were used for estimation of the apparent transfer coefficient, exchange current density and diffusivity respectively. In spite of all the inaccuracies, pointed out above, the applied model gave a reasonably good fit with the experimental data shown in Fig. 4.27.

The same dataset was then used to estimate the parameters of the model with the direct search method using MATLAB. The estimates produced by both the direct search method and the Zakai filtering method are listed in Table 4.1. The results of the approximation are similar to those of the Zakai filtering. The performance criterion (2.52) at the optimum point was equal to $J = 993$ that corresponds to root mean square error equal to 31.5 A/m^2.

Table 4.1: The estimates of parameters obtained by two methods.

Method	i_0	α	D
Zakai filtering	74.50	0.250	$4.140 \cdot 10^{-10}$
Direct search	74.51	0.255	$4.136 \cdot 10^{-10}$
	A/m^2	-	m^2/s

There are two benefits of using the Zakai filtering method. Firstly, it has the advantage of involving the whole probability density which helps to find global estimates of the parameters while direct search methods can drive the estimation process into a local minimum. And secondly, the structure of the Zakai filter admits recursive implementation of the estimation. Therefore, an identification of slow-varying parameters can also be captured by the latter method.

4.6 Conclusion

This study has shown that the Zakai filtering method is computationally feasible and effective in estimation of the nonlinear models in the case of 2-3 unknown constant parameters. Both the Zakai and pathwise filtering methods show a fast and unbiased convergence of estimates to the given values of unknown parameters. Time-varying parameters can also be estimated using the Zakai equation with the computationally effective factorization algorithm. Compared with linear estimates, the nonlinear estimates behave rather differently in terms of non-monotonic convergence of the conditional mean and variance as well as strong correlation between estimates. A capability of the Zakai filtering method to deal with these problems has been demonstrated in the conventional electrode kinetics examples (4.35), (4.39), (4.41), (4.43)-(4.44) and in the laboratory-scale copper electrodeposition process.

Chapter 5

Adaptive boundary tracking control of electrochemical cells

5.1 Introduction

Trajectory tracking control systems force the output to follow asymptotically a reference signal. The problem of tracking control design is closely related to model following where a reference signal is generated by a model. Effective trajectory tracking algorithms guarantee that system output accurately tracks the desired trajectory. The tracking and model following problem has been widely investigated over recent decades. The methods based on feedback linearization and the back-stepping technique have been proposed for the systems described by nonlinear ordinary differential equations in the case when the model to be exactly known (Khalil, 2002). Usually the system parameters are unknown or known with insufficient accuracy. In such a case robust control methods or sliding-mode control should be used. Alternatively, adaptive control can be used along with the certainty equivalent approach that replaces the unknown parameters with their estimates. A number of results for solving the adaptive tracking control problem have been obtained for lumped parameter systems (see, e.g., Marino et al., 2008; Zhao and Chen, 2009; Wu, 2009; Bresch-Pietri and Krstic, 2009). However, for distributed parameter systems trajectory tracking control is a challenging problem (Krstic, 2009). One possible approach that will be used in this chapter is to use the stochastic control theory.

The stochastic control theory allows converting a partially observed control system into a completely observed one. In the case of linear systems with incomplete state information and additive Gaussian noise the solution of the stochastic control problem with quadratic performance criterion leads to a Linear-Quadratic-Gaussian controller (LQG-controller) which consists of a Kalman filter and a linear-quadratic regulator (LQR). The problems of designing a Kalman filter and LQR can be decoupled. This fact is known as the separation principle. The separation principle can be used to compute optimal control for nonlinear systems. However, instead of a Kalman filter a nonlinear filtering problem (see, e.g., Bain and Crisan, 2009; Rozovskii, 1990) has to be solved. The resulted filter, which can be the Kushner filter (Kushner, 1967) or Zakai filter (Zakai, 1969), is used as an estimator of the probability density of unknown state and the controller has to be designed to minimize the given criterion. In stochastic control theory such a problem is known as the separated control problem (Fleming and Pardoux, 1982). The optimality conditions for such a system are known as the

Mortensen equation and its solution is analyzed to some extent in Beneš (1983), Gozzi and Swiech (2000) and more deeply in Beneš et al (2004) for the predicted miss problem, which remains the only specific problem considered so far. Alternatively, the optimality conditions can also be represented as a Bellman equation by discrete approximations of the state-space. However, practically a numerical solution of such a representation is unreachable due to a large dimension of the system required to be solved, if the infinite-dimensional system is approximated with the finite-dimensional one. Moreover, the separated control system is degenerate and one must deal with a singular part of a Bellman equation as well, i.e., to deal with the Bellman equation in the lattice of measures (Krylov, 1980; Pragarauskas, 1981, 1982). The probabilistic method (Kushner, 1977) that approximates the ordinal system with a Markov chain allows solving the Bellman equation numerically through its finite-difference approximation in time and state-space, if the system is non-degenerate and low in dimension (say, 1 or 2). However, in a nonlinear process case the separated control system is neither non-degenerate nor low dimensional.

The existence of optimal controls is another difficult issue. The existence is shown for so called wide sense controls (Fleming and Pardoux, 1982) when the admissible controls allow a weak solution (Liptser and Shiryayev, 1977) of the controlled system. The existence of optimal controls is not shown for controls in the usual strict sense and that they allow a strong solution of the system. Therefore, the practical problem, if solved, should be proven to be relevant to any Wiener process.

Regardless of the established theories, few applications are known: the linear regulator problem and some problems in finance, e.g., risk-sensitive control, portfolio selection and mean-variance hedging (Pham, 2005) are the only ones solved with the stochastic control theory. The aim of this chapter is to enlarge this list solving an electroplating process control problem. This process is nonlinear and certain simplifications are inevitable.

The specific minimum variance problem solved in this chapter stems from an industrial plating process, where the production maximization is an operational target. This is closely related to the plating rate maximization and this in turn means maximization of the current density. However, a large increase of the current density ends up with depletion of the oxidizing species. Therefore, the species' concentration control is a more relaxed control problem that helps to avoid the depletion while maximizing the current density through a carefully chosen reference concentration.

The results of this chapter have been accepted for publication in the International Journal of Control (Tenno and Mendelson, in press).

5.2 Contribution

The following contributions are covered in this chapter:

1. The feedforward controllers that force the concentration at the boundary to track the desired reference concentration are designed for finite-length diffusion and

semi-infinite diffusion processes and different electrode kinetic models in the case of known parameters.

2. The Zakai filtering is applied to a nonlinear in the parameters electrode kinetic model to control current in the electrochemical cell and its performance is compared with that of PI controller.
3. The problem of adaptive boundary concentration control for the electrochemical cell with simultaneous parameter identification is solved using the Zakai filtering method.
4. Several simplified computational schemas are introduced to save the computational effort required to solve the adaptive current and concentration boundary control problems.

5.3 Tracking control of electrochemical systems

When the parameters of a partial differential equation are known, the controller to track the desired reference is designed using series-expansion and back-stepping techniques (Dunbar et al., 2003a, 2003b; Krstic and Smyshlyaev, 2008). We consider the electrochemical cell model (2.7)-(2.9) and (3.1) with an arbitrary electrode kinetic model. The goal is to design such a control that the concentration at the boundary follows a certain specified trajectory. Even in a deterministic case this is a challenging problem. However, for a specific case of reference signal the problem can be easily solved. Let the reference trajectory be given as

$$c_{ref}(t) = A + (c_b - A)e^{-\gamma t}, \tag{5.1}$$

where c_{ref} is the reference trajectory of the concentration at the boundary and A and γ are the positive-valued constants, that specify the desired concentration at the boundary at steady state and the rate of tracking to steady state respectively. To design the control we replace the boundary condition (2.9) with (5.2):

$$c(0,t) = c_{ref}(t), \tag{5.2}$$

where the reference trajectory c_{ref} is specified in (5.1). Now the diffusion equation (2.7) has the Dirichlet boundary conditions, since both (3.1) and (5.2) specify the values of a solution on the boundary. In contrast to the original problem, the new problem allows an analytical solution. Indeed, by making a change of variables

$$u(x,t) = c(x,t) - \left(A + (c_b - A)e^{-\gamma t}\right) - \left(c_b - A - (c_b - A)e^{-\gamma t}\right)\frac{x}{\delta} \tag{5.3}$$

the following problem is obtained

$$\frac{\partial u(x,t)}{\partial t} = D\frac{\partial^2 u(x,t)}{\partial x^2} + \gamma e^{-\gamma t}(c_b - A)\left(1 - \frac{x}{\delta}\right), \tag{5.4}$$

with zero initial condition

$$u(x,0)=0, \tag{5.5}$$

and zero boundary conditions

$$u(0,t)=0, \tag{5.6}$$

$$u(\delta,t)=0. \tag{5.7}$$

The problem (5.4)-(5.7) is a nonhomogeneous diffusion problem with a special form of source term. Due to homogeneous boundary conditions this problem can be solved by the separation of variables method (Strauss, 1992; Pinchover and Rubenstein, 2005) and the solution is given by

$$u(x,t)=\frac{2(c_b-A)\gamma}{\delta}\sum_{n=1}^{\infty}\left[\frac{e^{-\gamma t}-e^{-\lambda_n^2 Dt}}{\left(\lambda_n^2 D-\gamma\right)\lambda_n}\sin(\lambda_n x)\right]. \tag{5.8}$$

In (5.8) $\{\lambda_n\}$ is the set of the problem's eigenvalues $\lambda_n = n\pi/\delta$. Using (5.3) the desired profile of the concentration at the boundary is given as

$$c(x,t)=\frac{2(c_b-A)\gamma}{\delta}\sum_{n=1}^{\infty}\frac{e^{-\gamma t}-e^{-\lambda_n^2 Dt}}{\left(\lambda_n^2 D-\gamma\right)\lambda_n}\sin(\lambda_n x)+\left(A+(c_b-A)\left(e^{-\gamma t}+\left(1-e^{-\gamma t}\right)\frac{x}{\delta}\right)\right). \tag{5.9}$$

The expression (5.9) is the solution of the so called motion planning problem (Krstic, 2006). It provides the profile of the concentration at the boundary that corresponds to the desired reference signal (5.1). Now the expression (5.9) can be used to design controls. However, for that one must specify the electrode kinetic model. First, we study the simplest single-direction model in the form of (3.2)

$$i=-i_0\frac{c(0,t)}{c_b}e^{-k\alpha E}. \tag{5.10}$$

Substituting (5.10) into (2.9), one can find that the input voltage E is given as

$$E=-\frac{1}{k\alpha}\ln\left[\frac{2Fc_bD}{i_0c(0,t)}\frac{\partial c(x,t)}{\partial x}\Big|_{x=0}\right]. \tag{5.11}$$

The meaning of the equation (5.11) is that given the concentration at the boundary and flux at the boundary it determines the voltage such that (2.9) holds.

To follow the prescribed reference trajectory we replace the concentration at the boundary with the reference concentration and find the flux from (5.9) and then substitute it into (5.10). This gives the controller as

$$E = -\frac{1}{k\alpha}\ln\left[\frac{2Fc_bD(c_b - A)}{i_0\delta c_{ref}(t)}\left(\left(1-e^{-\gamma t}\right)+2\gamma\sum_{n=1}^{\infty}\frac{e^{-\gamma t}-e^{-\lambda_n^2 Dt}}{\left(\lambda_n^2 D-\gamma\right)}\right)\right]. \tag{5.12}$$

This control has been simulated with the following values of parameters: $\alpha = 0.25$, $D = 4\cdot10^{-10}$, $i_0 = 42$, $c_b = 750$, $\delta = 1\cdot10^{-4}$, $A = 100$, $\gamma = 1$. The trajectory tracking and the control signal are illustrated in Fig. 5.1. The designed controller is a feedforward controller and to deal with uncertainties and unmodeled dynamics it should be accompanied with a feedback.

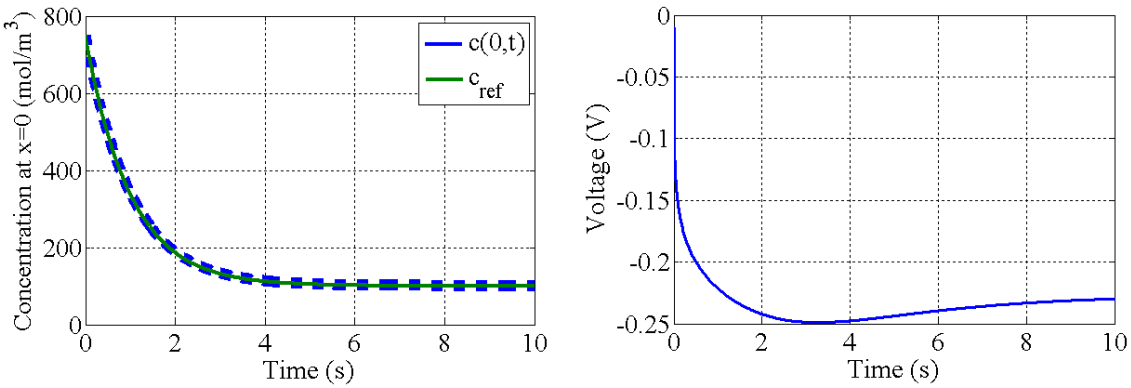

Figure 5.1: An illustration of trajectory tracking. Left: Concentration at the boundary tracking the desired reference concentration. Right: Input voltage, evaluated using (5.12).

The controller for the single-directional model (2.24), which takes into account the activity of species

$$i = -i_0\left(\frac{c(0,t)}{c_b}\right)^{\beta(1-\alpha)} e^{-k\alpha(1-\alpha)E}, \tag{5.13}$$

can be designed similarly to that of the model (5.10). Equation (5.13), derived for a negative sweep voltage, follows from the equation (2.24) if the activity is approximated by a power function of the concentration (3.59) and $\alpha_c = \alpha$, $\alpha_a = 1 - \alpha$. Substituting (5.13) into (2.9) and using the flux from (5.9) gives the controller as

$$E = -\frac{1}{k\alpha(1-\alpha)}\ln\left[\frac{2Fc_b^{\beta}D(c_b - A)}{i_0\delta c_{ref}^{\beta}(t)}\left(\left(1-e^{-\gamma t}\right)+2\gamma\sum_{n=1}^{\infty}\frac{e^{-\gamma t}-e^{-\lambda_n^2 Dt}}{\left(\lambda_n^2 D-\gamma\right)}\right)\right]. \tag{5.14}$$

While the analytical expressions for controls can be derived for single-directional models (5.10) and (5.13), this is unquestionably impossible for bi-directional models like (4.41), (4.43) and (4.44). However, the controls can be easily evaluated numerically. Let us define a function

$$y = F(x;a,b,c) = e^{ax} - ce^{-bx}. \tag{5.15}$$

In definition (5.15), a and b are the arbitrary nonnegative constants and c is the strictly positive constant. Denote the inverse function of (5.15) by

$$x = F^{-1}\left(y; a, b, c\right). \tag{5.16}$$

Given y, a, b, c and d, the inverse function (5.16) can be easily evaluated numerically. Then for a bi-directional electrode kinetic model (4.41) the control can be specified using (5.16) as

$$E = F^{-1}\left(-\frac{2FD}{i_0}\frac{\partial c(x,t)}{\partial x}\Big|_{x=0}; k(1-\alpha), k\alpha, \frac{c_{ref}(t)}{c_b}\right). \tag{5.17}$$

Calculating flux from (5.9) and then substituting it into (5.17) gives

$$E = F^{-1}\left(-\frac{2FD(c_b - A)}{i_0\delta}\left(\left(1-e^{-\gamma t}\right) + 2\gamma\sum_{n=1}^{\infty}\frac{e^{-\gamma t} - e^{-\lambda_n^2 Dt}}{\left(\lambda_n^2 D - \gamma\right)}\right); k(1-\alpha), k\alpha, \frac{c_{ref}(t)}{c_b}\right).$$

In a similar way, a tracking controller can be designed for the case of the semi-infinite diffusion model (2.7)-(2.10). Once again, the corresponding species concentration profile is constructed by replacing the boundary condition (2.9) with (5.2) and solving the problem obtained. Applying to the equation (2.7) the Laplace transform with respect to the variable t reduces the PDE into a solvable ODE (Riley et al., 2006). Incorporating the boundary conditions yields the solution

$$c(x,s) = (c_b - A)\left[\frac{1}{s+\gamma} - \frac{1}{s}\right]e^{-x\sqrt{\frac{s}{D}}} + \frac{c_b}{s}, \tag{5.18}$$

where $c(x, s)$ is the Laplace transform of $c(x, t)$. It should be pointed out that the controller can be derived without the analytical inverse transformation of (5.18). Indeed, according to the boundary condition (2.9) the controller is governed by the flux of species at the boundary. Differentiating (5.18) with respect to x and taking $x = 0$ yields

$$\frac{\partial c(x,s)}{\partial x}\Big|_{x=0} = \frac{(c_b - A)}{\sqrt{D}}\left[\frac{1}{\sqrt{s}} - \frac{\sqrt{s}}{s+\gamma}\right]. \tag{5.19}$$

Equation (5.19) is the Laplace transform of the desired flux at the boundary. The solution of (5.19) in time domain can be found from the tables of inverse Laplace transforms (Polyanin, 2005). Particularly, it is known that

$$L^{-1}\left(\frac{1}{\sqrt{s}}\right) = \frac{1}{\sqrt{\pi t}} \tag{5.20}$$

and

$$L^{-1}\left(\frac{\sqrt{s+a}}{s+b}\right) = \frac{e^{-at}}{\sqrt{\pi t}} + \sqrt{a-b}e^{-bt}erf\left(\sqrt{(a-b)t}\right). \tag{5.21}$$

Equation (5.21) written for $a = 0$ and $b = \gamma$ gives

$$L^{-1}\left(\frac{\sqrt{s}}{s+\gamma}\right) = \frac{1}{\sqrt{\pi t}} + j\sqrt{\gamma}e^{-\gamma t}erf\left(j\sqrt{\gamma t}\right), \tag{5.22}$$

where the symbol j stands for the imaginary unit. Combining the expressions (5.20) and (5.22) gives the desired flux at the boundary as

$$\frac{\partial c(x,t)}{\partial x}\Big|_{x=0} = \sqrt{\frac{\gamma}{D}}\left(c_b - A\right) je^{-\gamma t}erf\left(j\sqrt{\gamma t}\right). \tag{5.23}$$

It is known that $jerf(jz) = erfi(z)$ for any complex argument z (Lebedev, 1965), where the function *erfi* is the imaginary error function defined as

$$erfi(z) = \frac{2}{\sqrt{\pi}}\int_0^z e^{t^2}dt.$$

Consequently, taking $z = \sqrt{\gamma t} + 0j$ the desired flux at the boundary can be written in the terms of the imaginary error function as

$$\frac{\partial c(x,t)}{\partial x}\Big|_{x=0} = \sqrt{\frac{\gamma}{D}}\left(c_b - A\right)e^{-\gamma t}erfi\left(\sqrt{\gamma t}\right). \tag{5.24}$$

In contrast to the error function, the imaginary error function rapidly diverges to infinity as z grows (Lebedev, 1965). However, it is well known that the function $F(z) = e^{-z^2}erfi(z)$ is bounded for all real z (Lebedev, 1965). These issues are illustrated in Fig. 5.2. Therefore, the flux (5.24) is always bounded and can be utilized to design controls.

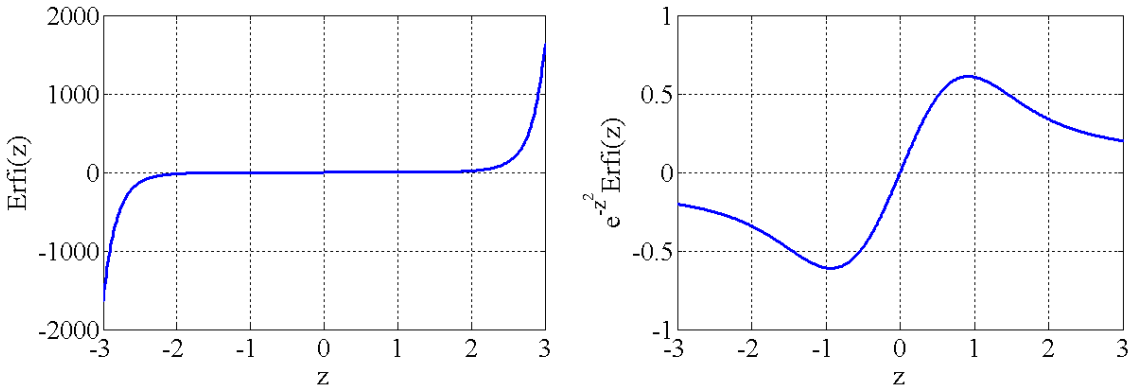

Figure 5.2: Left: The imaginary error function with real argument. Right: Bounded modification of the imaginary error function with real argument.

Assuming the bi-directional model (4.41), the control, that forces the concentration at the boundary to follow the prescribed reference trajectory (5.1), can be specified using (5.24) as follows

$$E = F^{-1}\left(-\sqrt{D\gamma}\,\frac{2F}{i_0}\left(c_b - A\right)e^{-\gamma t}erfi\left(\sqrt{\gamma t}\right); k\left(1-\alpha\right), k\alpha, \frac{c_{ref}\left(t\right)}{c_b}\right). \tag{5.25}$$

The control evaluated by using (5.25) is similar to that of finite-diffusion model shown in Fig. 5.1 and, therefore, is not reported here.

The family of the controllers (5.11), (5.17) and (5.25) has been derived because of the simple expression for the desired trajectory (5.1) which allows analytical solution of the diffusion equation. In the case of arbitrary reference trajectory the solution cannot be found in closed form and a numerical solution is required. Unlike finite-length diffusion for the semi-infinite diffusion model (2.7)-(2.10) the controller can be simply designed to follow an arbitrary reference trajectory. However, the controls still will be evaluated numerically using an inverse function of (5.15). Indeed, utilizing the analytical expression for the concentration at the boundary (4.56), the goal of control is specified as

$$c_b + \frac{1}{nF\sqrt{\pi D}}\int_0^t \frac{\zeta(s)}{\sqrt{t-s}}\,ds - \lambda\left(t\right) = 0\,. \tag{5.26}$$

In (5.26) $\lambda(t)$ is the tracking target, i.e. a reference concentration at the boundary in an electrochemical cell. Following Nicholson and Shain (1964) we will approximate the convolution integral in (5.26) as follows

$$\int_0^t \frac{\zeta(s)}{\sqrt{t-s}}\,ds = 2\sqrt{\Delta t}\sum_{j=1}^{n}\zeta\left(j\Delta t\right)\left(\sqrt{n-j+1} - \sqrt{n-j}\right), \tag{5.27}$$

where n is the number of measured current density samples during the experiment time t, s and Δt is the discretization interval, s. Assuming that the system is in tracking mode, (4.41) can be written as

$$i = i_0\left(e^{k(1-\alpha)E} - \frac{\lambda\left(t\right)}{c_b}e^{-k\alpha E}\right). \tag{5.28}$$

Replacing in (5.27) the unavailable measurement in the last interval by the model (5.28) and then substituting the resulted approximation into (5.26), one obtains the equation that after being solved determines the control signal to be applied into the electrochemical cell to force the concentration at the boundary to follow the reference signal $\lambda(t)$

$$e^{k(1-\alpha)E} - \frac{\lambda\left(t\right)}{c_b}e^{-k\alpha E} = \frac{nF\sqrt{\pi D}}{2\sqrt{\delta}i_0}\left(\lambda\left(t\right) - c_b\right) + \frac{1}{i_0}\sum_{j=1}^{n-1}\zeta\left(j\Delta t\right)\left(\sqrt{n-j+1} - \sqrt{n-j}\right). \tag{5.29}$$

Once again, the analytical expression for the control signal can not be derived from (5.29). However, this control can be easily evaluated numerically by using the inverse function of (5.15). This gives

$$E = F^{-1}\left(\frac{nF\sqrt{\pi D}}{2\sqrt{\delta}i_0}\left(\lambda(t)-c_b\right)+\frac{1}{i_0}\sum_{j=1}^{n-1}\zeta\left(j\Delta t\right)\left(\sqrt{n-j+1}-\sqrt{n-j}\right);k\left(1-\alpha\right),k\alpha,\frac{\lambda(t)}{c_b}\right). \tag{5.30}$$

The simulated trajectory tracking of (4.41) along with the control signal (5.30) are illustrated in Fig. 5.3. In the simulation the parameters of the model (4.41) were α = 0.25, $D = 4\cdot10^{-10}$, i_0 = 42 and c_b = 750. The reference trajectory was generated in the following way. Till t = 5 s the trajectory was taken as the solution of semi-infinite diffusion equation and the electrode kinetic model (4.41) with sweep form of the applied voltage and the parameters α = 0.5, $D = 5\cdot10^{-10}$, i_0 = 100 and c_b = 750. After t = 5 s the trajectory was taken to be constant with the same value as at t = 5 s. The function obtained is not analytic and, as a consequence, an irregular point at t = 5 s is clearly observed in the right plot of Fig. 5.3.

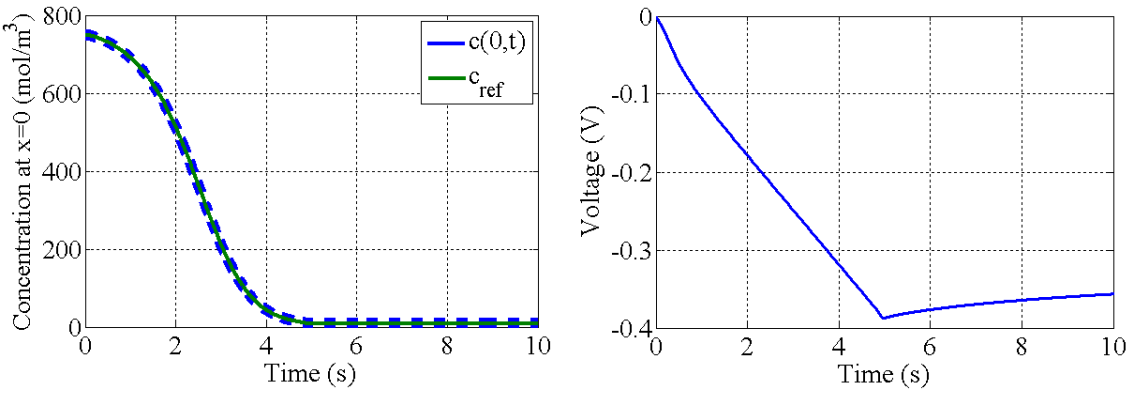

Figure 5.3: An illustration of trajectory tracking. Left: Concentration at the boundary tracking the desired reference concentration. Right: Input voltage, evaluated using (5.30).

5.4 Adaptive tracking control of electrochemical cells

The concentration profile in the whole domain cannot be found and adaptive boundary controls should be used, unless the model parameters are known. Among the existing adaptive control methods for PDEs, only the design with a swapping identifier can handle the output-feedback tracking problem. Moreover, even in a stabilization control problem the adaptive boundary controls are limited to the models that are linear in the unknown parameters (Krstic, 2006). Therefore, more advanced methods are required.

In this section the control problem of a system with unknown constant parameters over nonlinear observation is formulated. The unknown parameters are treated as if they were states and a nonlinear estimator is designed as a straightforward application of the Zakai filtering method. Firstly, the control problem is solved for cell current and performance of the controller is compared with that of PI controller. Then the tracking control problem for the unmeasured concentration at the boundary is solved.

5.4.1 Adaptive current control

The adaptive tracking cell current control problem is to design the voltage such that the cell current follows the desired reference trajectory. From a mathematical point of view, the problem is to minimize the current deviation from the target on average

$$v^E(t) = \mathbf{M}\left\{\left(i(t) - i_{ref}(t)\right)^2 + \mu E^2(t)\middle| F_{t-h}^{\xi}\right\} \tag{5.31}$$

subject to the partially observed system

$$d\theta = 0, \quad \theta(0) = \theta_0 \sim N(m_0, \gamma_0), \tag{5.32}$$

$$d\xi = i\left(t, c\left(t,0\right), E\left(t\right), \theta\right)dt + BdW, \quad \xi\left(0\right) = \xi_0, \tag{5.33}$$

where **M** is the conditional mean operator, $i_{ref}(t)$ is the tracking target, i.e. a reference current density in an electrochemical cell, A/m^2, $E(t)$ is the applied voltage between the working and auxiliary electrodes, V, μ is the control price, A/m^2/V^2, θ is the vector of unknown parameters, whose initial distribution is specified by a Gaussian distribution $N(m_0, \gamma_0)$ with given mean m_0 and covariance γ_0, $i(t)$ is the current density of an electrode reaction, A/m^2, $c(t,0)$ is the concentration of oxidizing species at the boundary, mol/m^3, $\xi(t)$ is the measured current density with an additive noise, which is modeled by a Wiener process $W(t)$, F_{t-h}^{ξ} is the natural filtration of the measured current density up to the moment $t - h$, where the delay h is applied to make the admissible controls causal.

The system (5.32)-(5.33) is obtained by treating the unknown constant parameters as if they were states similar to that in Chapter 4. Voltage $E(t)$ acts as control signal that has to be designed to minimize the performance criterion (5.31). The concentration of the species satisfies the semi-infinite diffusion equation (2.7) with the initial condition (2.8) and boundary conditions (2.9) and (3.1). It was mentioned in Chapter 4 that for such a model the concentration at the boundary is given by (4.55)

$$c(0,t) = c_b + \frac{1}{nF\sqrt{\pi D}}\int_0^t \frac{i(s)}{\sqrt{t-s}}ds .$$

Substituting (4.55) into an electrode kinetic model produces an integral equation in the unknown current density similar to that of Chapter 3. By replacing in the convolution integral (4.55) the modeled current densities with their measurements up to a delayed moment (t–h) makes the integral equation containing only one unknown current density at time t as function of applied voltage E

$$f\left(E, i^E\left(t\right)\right) = \int_0^{t-h} \frac{\xi(s)}{\sqrt{t-s}}ds + \int_{t-h}^{t} \frac{i^E(s)}{\sqrt{t-s}}ds , \tag{5.34}$$

where f is a function whose form depends on the electrode kinetic model used. We will refer to the unknown current density in (5.34) as the predicted current density $i^E(t)$. The predicted concentration $c^E(t)$ can be found from (4.55) or from the electrode kinetic

model. This scheme is equivalent to approximating the convolution integral in (4.55) by the sum of two integrals, one with the measured current density $\xi(s)$ up to a delayed moment (t–h) and another with the predicted current density between the moment (t–h) and the current moment t that gives

$$c(t,0) \approx c_b + \frac{1}{nF\sqrt{\pi D}} \left\{ \int_0^{t-h} \frac{\xi(s)}{\sqrt{t-s}} ds + \int_{t-h}^{t} \frac{i^E(s)}{\sqrt{t-s}} ds \right\} \equiv c^E(t) . \tag{5.35}$$

The nonlinear estimation problem can be solved in a similar manner as it was done in Chapter 4 using the Zakai filtering method (4.7)-(4.10). To design a controller we will use the certainty equivalence principle according to which the identified values will be used in the controller as if they were the real values. However, instead of the identified values as in linear case identified probability density of unknown parameters will act as controller input. The incomplete data control problem (5.31)-(5.33) can be converted to the complete data control problem that minimizes the square functional

$$v^E(t) = \int_{R^n} \left(i^E\left(t, E(t), \mathbf{x}\right) - i_{ref}(t) \right)^2 p(t, \mathbf{x}) d\mathbf{x} + \mu E^2(t) \tag{5.36}$$

subject to the completely observable system

$$dq = -\frac{1}{2}\left(\frac{i^E(t,\mathbf{x})}{B} \right)^2 q dt + \frac{i^E(t,\mathbf{x})}{B^2} q(t,\mathbf{x}) d\xi , \tag{5.37}$$

where $\mathbf{x}$ is the vector of candidates of the unknown parameters i_0, α, and D respectively and $p(t, \mathbf{x})$ is the probability density that can be obtained by normalizing the unnormalized probabilities q according to (4.11). We emphasize that the functional (5.36) does not depend explicitly on the boundary concentration.

The general architecture of the adaptive current tracking control system is depicted in Fig. 5.4. It includes an electrochemical cell, Zakai filter which computes the probability density $p(\mathbf{x})$ of the parameter candidates lying in the predefined set $\mathbf{x}$ based on input voltage E and measured current density ξ, a storage device RAM (random access memory), where past samples of the current density are kept, and a controller, which produces input voltage E based on the desired value of current density, probability density of parameter candidates and past samples of the current density.

The more parameters are unknown, the more computational effort is required to minimize (5.36). To save the computational effort several simplified computational schemes can be introduced.

- Tracking control based on concentration at a previous time instant

  Concentration at the boundary at a previous time instant is used to predict future current. This is the natural and, perhaps, the simplest approach. Indeed, since in this case there is no need to predict concentration at the boundary for all possible candidates of the unknown parameters, several operations of multiplication, integration and raising to the power are avoided. This simplification leads to a

visible delay in tracking because, evidently, an incorrect value of concentration is used.

- Tracking control based on instant values of the estimates

  The main difficulty of minimizing (5.36) is in taking the product of error with probability density and integrating after that. The more measurements in the minimization algorithm are used, the more operations of integration are required. To avoid a large number of integrations the estimates of the unknown parameters can be computed on every time step and then they can be used as if they were true to evaluate optimal control.

- Tracking control based on assumption that the system is already in steady state.

  Assuming that the system is already in perfect tracking mode leads to another simplification. Since the desired current trajectory is known in advance, the desired concentration at the boundary can be computed also in advance. In contrast to the first simplification schema this method does not suffer from delay, i.e. it does not reduce control performance.

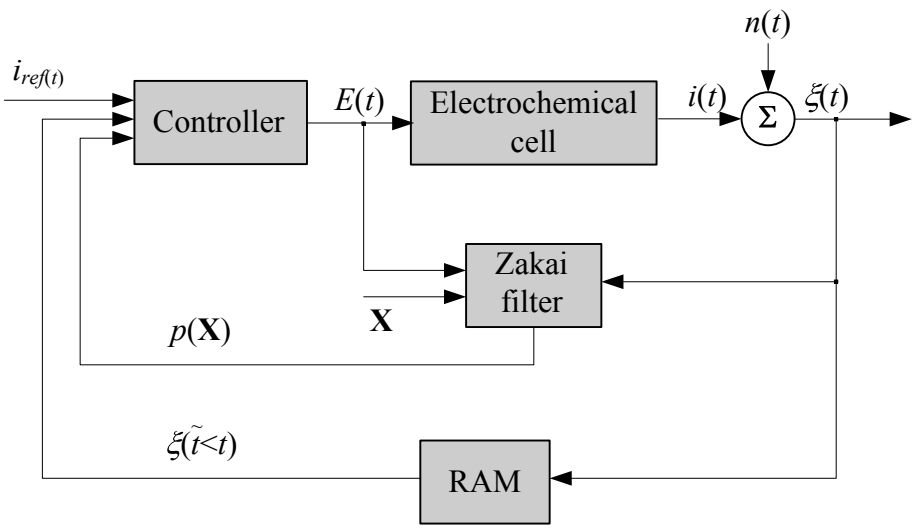

Figure 5.4: General architecture of the adaptive current control system.

The current tracking problem can be solved with a conventional PID control as the current is measured in the electrochemical cell (see Fig. 5.5). It should be mentioned that the electrochemical cell model is nonlinear in the parameters and in the input. Because of that, the performance of a PID-controller can be poor. However, usually the potential range where the cell is operated is relatively narrow and then the PID-control is expected to produce satisfactory results. Otherwise gain-scheduling PID controls can be used (Rugh, 1991; Aström and Wittenmark, 1994). Therefore, the benefit of adaptive control in this case is computing the estimates of the unknown parameters. The expected improvement in performance is insignificant compared with the considerably increased computational effort required.

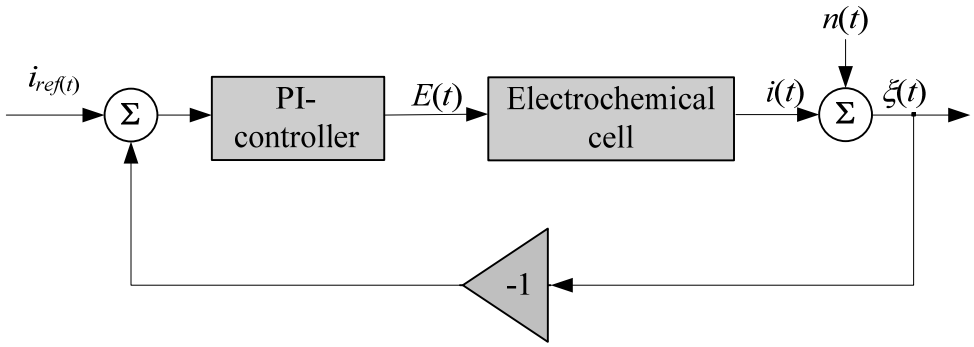

Figure 5.5: General architecture of the PI current control system.

5.4.2 Adaptive boundary concentration control

Maximization of the current density ends up in depletion of the oxidizing species whose concentration control is, therefore, a more relaxed control problem that helps to avoid the depletion while maximizing the current density through a carefully chosen reference concentration.

The functional to be minimized in this problem is

$$v^E(t) = \mathbf{M}\left\{\left(c(0,t) - c_{ref}(t)\right)^2 + \mu E^2(t)\middle| F_{t-h}^{\xi}\right\} \tag{5.38}$$

subject to the partially observed system (5.32)-(5.33).

The crucial difference there is that apart of the unknown kinetic and mass-transfer parameters concentration at the boundary is unobserved. Moreover, concentration at the boundary cannot be found through the measured current, unless the kinetic parameters are known, and, therefore, a conventional PID controller cannot be used to track the desired reference signal. The control problem can be solved only by combining the control algorithm with an estimator for the unknown parameters. The estimator allows finding the hidden concentration at the boundary. Therefore, a model is required to solve tracking concentration at the boundary control problem.

Again after converting the incomplete data control problem (5.38), (5.32)-(5.33) to the complete data control problem the voltage between the electrodes can be found by minimizing the square functional

$$v^E(t) = \int_{R^n} \left(c^E\left(0,t,E(t),\mathbf{x}\right) - c_{ref}(t)\right)^2 p(t,\mathbf{x})\,d\mathbf{x} + \mu E^2(t). \tag{5.39}$$

The general architecture of the adaptive concentration at the boundary tracking control system is depicted in Fig. 5.6. The crucial difference of the presented architecture with that of the current tracking control system is in the controller structure. These controllers minimize the cost functions (5.36) and (5.39) respectively.

Similar to the current tracking control case to save the computational effort, several simplified computational schemes can be introduced:

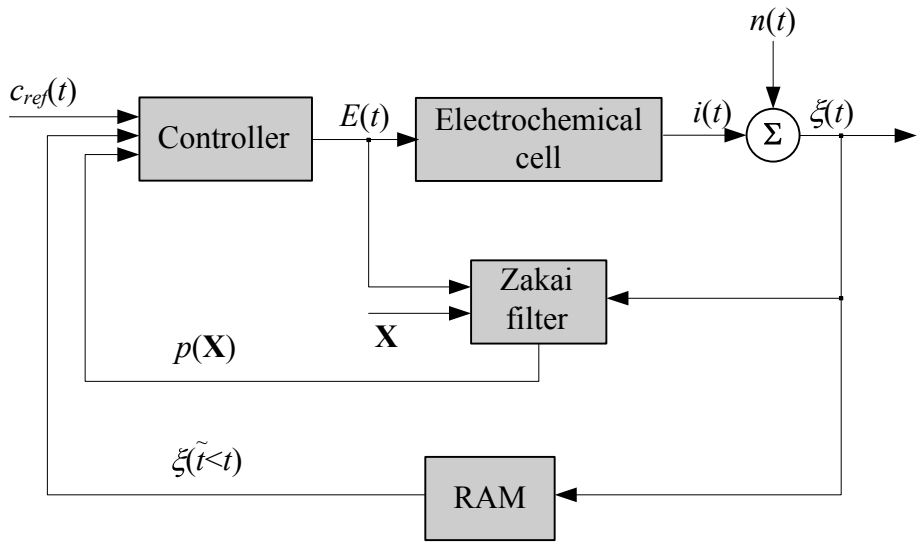

Figure 5.6: General architecture of the adaptive concentration at the boundary tracking control system.

- Tracking control based on instant values of the estimates

  To avoid large number of integrations the estimates of unknown parameters can be computed on every time step and then they can be used as if they were true to find optimal control.

- Tracking control based on assumption that the system is already in steady state

  Assuming that the system is already in perfect tracking mode leads to another simplification. Since the desired concentration trajectory is known in advance, it can be assumed that the system is already in steady state and then concentration dependence on the unknown parameters can be found through computing the desired reference current.

5.4.3 Solving the separated control problem

In theory, the separated control problem can be solved using a Mortensen equation (Beneš, 1983) even in a more general form written for a cost function integrated in time. Unfortunately, this equation has never been employed fully, but partly, in the predicted miss problem (Beneš et al., 2004). Therefore, a Mortensen equation can be started, but its solution is entirely unknown in this problem. Even if solved, the optimal controls cannot be expressed explicitly through the value function in case of a model nonlinear in the unknown parameters.

Approximation of the unnormalized distribution with finite dimensional processes and then formulation of the Bellman equation (Krylov, 1980) does not solve the problem due to a large dimension system needing to be solved. Practical calculations of the Bellman equation are done for systems low in dimensions (1 or 2). Therefore, the numerical direct search method is an option that remains. Alternatively, the control signal can be evaluated using gradient optimization techniques. However these methods

require evaluations of the derivative of the function to be minimized. The controls found with the direct search method

$$E(t) = \arg\inf v^E(t) \tag{5.40}$$

are solved with respect to the systems (5.36), (5.37) and (5.39), (5.37). They gave reasonably good results that are discussed in the next section.

5.5 Simulation results

In this section adaptive current control and adaptive boundary concentration control using Zakai equation are simulated. The computational scheme based on the assumption that the electrochemical system is already in steady state will be utilized in the adaptive control simulation.

5.5.1 Adaptive current control

We consider the deposition model (4.41)

$$i(t) = i_0\left(e^{k(1-\alpha)E(t)} - \frac{c(t,0)}{c_b}e^{-k\alpha E(t)}\right),$$

where concentration of species satisfies the linear diffusion equation (2.7) with a semi-infinite boundary condition (3.1). The control problem is specified as a cheap control $\mu = 0$, and with relatively accurate measurements $B = 10$. The exchange current density $i_0 = 42$, apparent transfer coefficient $\alpha = 0.25$, and diffusivity $D = 4\cdot10^{-10}$ were assumed to be unknown, only their guess estimates specified by the Gaussian a priori distribution (see Table 5.1) are known.

Table 5.1: The parameters of a priori distribution

	i_0	α	D
m_0	100	0.5	$1\cdot10^{-9}$
$\sqrt{\gamma_0}$	89	0.54	$1\cdot10^{-9}$

The desired current density profile has form of sweep with a sweep rate of 280 A/m^2/s. The desired current profile and current profiles obtained by means of adaptive control and PI control and corresponding tracking errors are illustrated in Fig. 5.7. It can be observed that while in general the tracking results obtained by adaptive control are compared to that of PI control, the tracking error is optimal for adaptive control and it increases if the current density is small in the case of PI control. However, the price for this optimality is complexity of the control algorithm. The concentration at the boundary and input voltage corresponding to adaptive control and PI control are shown in Fig. 5.8.

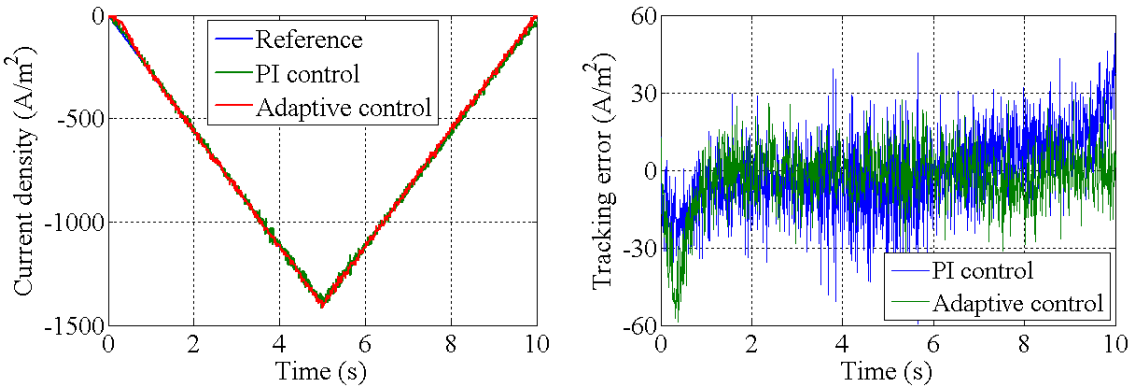

Figure 5.7: Left: The desired and controlled current density with adaptive control and PI control. Right: Tracking error with adaptive control and PI control.

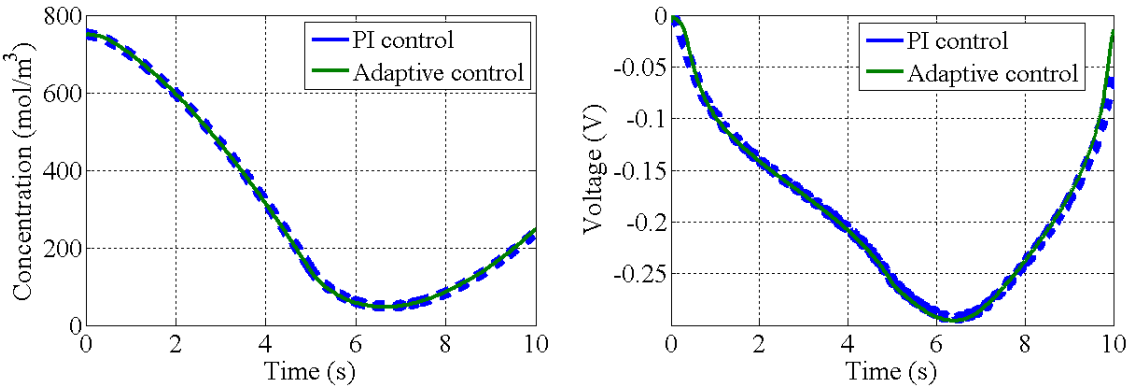

Figure 5.8: Left: Optimal concentration at the boundary with PI and adaptive controls. Right: Input voltage with PI and adaptive controls.

5.5.2 Adaptive boundary concentration control

To make the calculation process quick three simpler problems were solved. The tracking when parameters i_0 and α, D and i_0, and D and α are unknown is considered. These problems will be further in the text referred to as the problems *P1*, *P2* and *P3* respectively.

The reference trajectory was generated similar to that of the semi-infinite diffusion process in Section 5.3. Till t = 5 s the trajectory was taken as the solution of semi-infinite diffusion equation and the electrode kinetic model (4.41) with sweep form of the applied voltage and the following values of parameters: $\alpha = 0.5$, $D = 5{\cdot}10^{-10}$, $i_0 = 100$ and $c_b = 750$. After t = 5 s the trajectory was taken to be constant with the same value as at t = 5 s.

The desired concentration profile of the oxidizing species in close vicinity to the cathode surface along with the controlled profile for the problem *P1* is illustrated in Fig. 5.9. The tracking process is almost perfect in this simulation experiment except for a very small deviation in the initial period where the model uncertainty was set large. This deviation is about 3 times larger for problem *P2* and four times larger for *P3* compared to *P1*.

The applied voltage shown in Fig. 5.10 is the optimal control. Being applied to the electrochemical cell it produces the current density (the right plot in Fig. 5.10) that affects the diffusion process (2.7) through the boundary condition (2.9). Notice that neither of these curves for the applied voltage nor for the current density is constant while they perform transfer of the boundary concentration from the bulk concentration to the low level and then keeps this low level concentration constant.

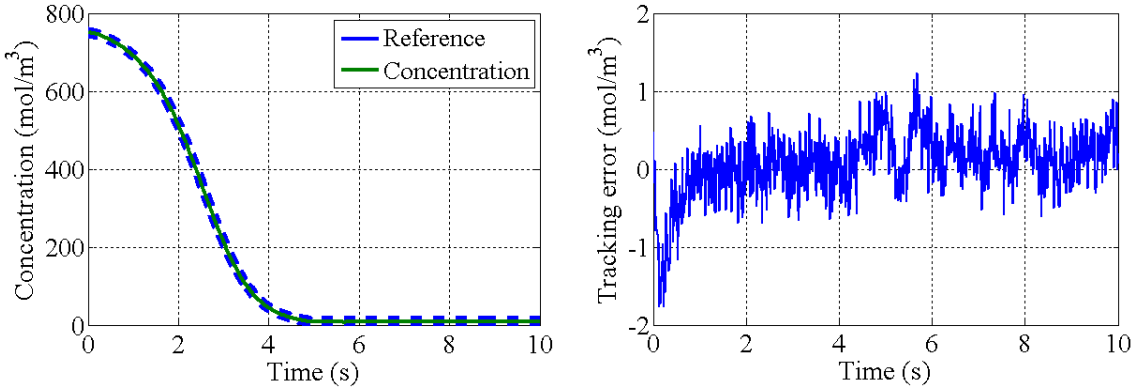

Figure 5.9: Left: The desired and controlled concentration at the cathode boundary for the problem *P1*. Right: The tracking error.

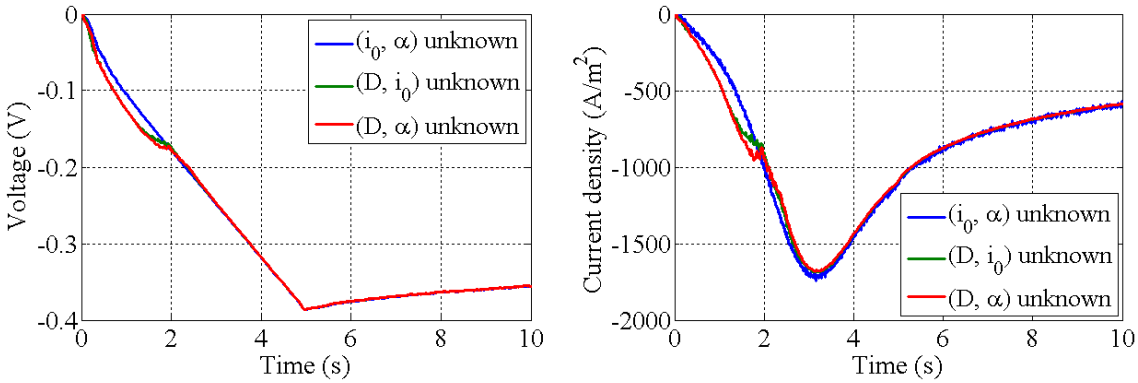

Figure 5.10: Left: The applied cell voltage to track the desired reference concentration as indicated by the problem identifiers. Right: The optimal current density as indicated by the problem identifiers.

In the case of a semi-infinite diffusion process the concentration profile $c(t, x)$ approaches uniformly to the set target concentration $c_{ref}(\infty)$ in infinity

$$c(t,x) = \left(c_{ref}(\infty) - c_{bulk}\right)\operatorname{erfc}\left(\frac{x}{\sqrt{2Dt}}\right) + c_{ref}(\infty) \to c_{ref}(\infty)$$

with less and less power (or current) applied if the time approaches infinity, since the bulk solution boundary moves far away from the cathode. The effect of adaptation is visible in the control signal (the left plot in Fig. 5.10) and the current density (the right plot in Fig. 5.10). The slight differences between the problems *P1*, *P2*, *P3* are also visible in these figures.

The optimal growth of the copper deposit on the cathode surface is shown in Fig 5.11. It is not linear initially as far as one aims for a smooth bounded control that can be set either with nonzero control cost μ or with the proper target profile as chosen in this numerical analysis. Formation of the deposit thickness on the electrode surface obeys Faraday's law

$$\frac{dx_{Cu}}{dt} = \frac{M_{Cu}}{\rho_{Cu}} \frac{i}{2F}$$

where x_{Cu} is the deposit thickness, m, M_{Cu} is the molecular weight, 0.06355 kg/mol, and ρ_{Cu} is the density of copper, 8960 kg/m^3.

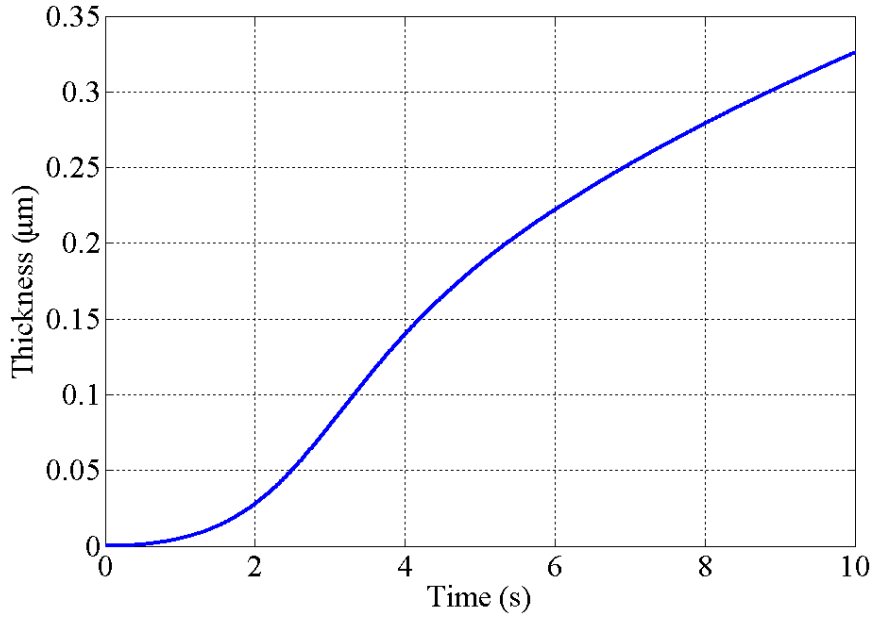

Figure 5.11: The optimal copper deposit thickness on the electrode surface.

The exchange current density and apparent transfer coefficient were assumed to be unknown and estimated simultaneously in the problem *P1*. Their adaptation during the control process is shown in Fig. 5.12 along with standard deviations of the estimates. The convergence of the estimates is rather fast in these figures. The conditional mean has a certain overshoot and the standard deviation (STD) is a non-monotonic process in estimation of the exchange current density (the left plot in Fig. 5.12). The overshoot is also small and the STD is a monotonic process in the estimation of the apparent transfer coefficient (the right plot in Fig. 5.12). In the other problems *P2* and *P3* there is the opposite: a small overshoot of conditional mean and the STD is monotonic and in this way the convergence is slightly faster in problem *P3* while estimating the exchange current density. This latter convergence is similar to that shown in the right plot of Fig. 5.12.

Diffusivity was estimated simultaneously with the exchange current density and then simultaneously with the apparent transfer coefficient as shown in Fig. 5.13. Again there is no movement towards the true diffusivity estimate in low voltage ranges. The reason

for this is that the concentration at the boundary does not differ appreciably from the bulk solution concentration, and hence mass-transfer effects do not contribute to the current density. There is no overshoot in the STD in problem *P2* and a small overshoot in problem *P3* (see the right plot in Fig. 5.13).

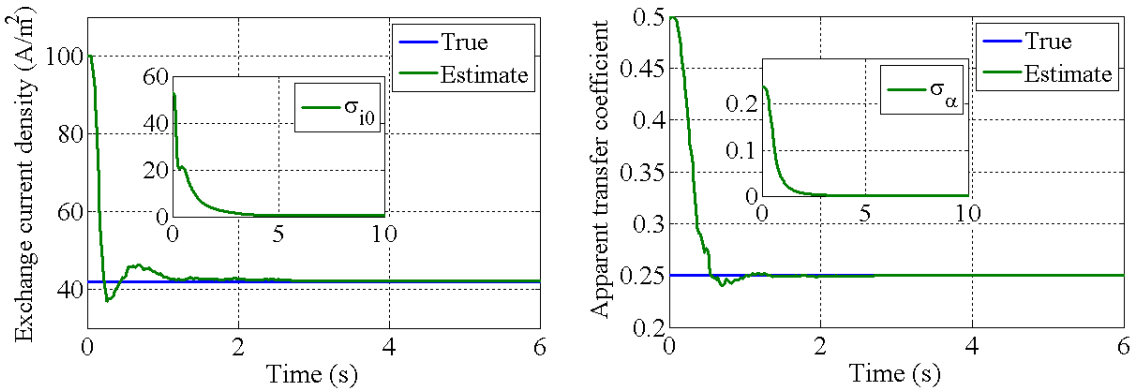

Figure 5.12: Left: The estimated exchange current density: conditional mean and standard deviation. Right: The estimated apparent transfer coefficient: conditional mean and standard deviation.

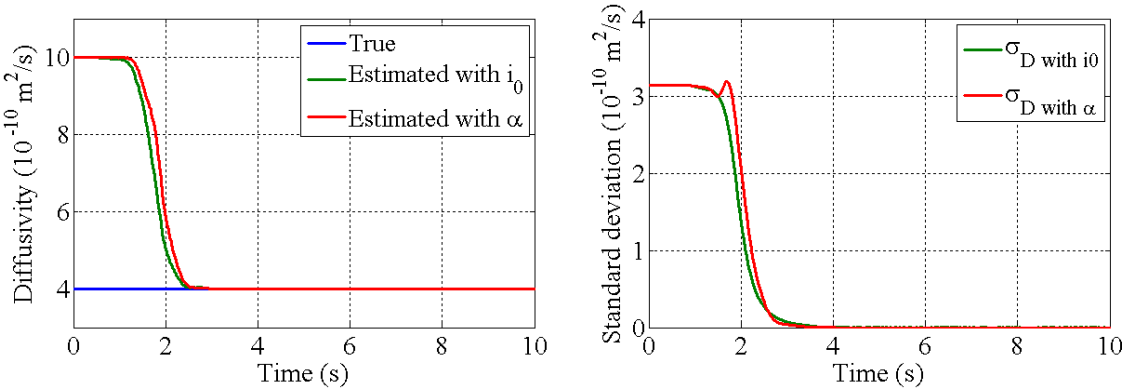

Figure 5.13: Left: The diffusivity estimate. Right: The standard deviation of estimate.

Evolution of the probabilities and correlation between the estimates during control is shown in Figs 5.14-5.15 for the problem *P1*. Since the diffusivity *D* cannot be estimated in the initial period, the evolution of probabilities is slower in the other problems. Also a multi-peaks situation appears at t = 0.5 sec and disappears later in problem *P3*. In this multi-peaks situation the Zakai method is stable which is different in the direct search method of estimation.

There is a strong nonlinear dependence (Fig. 5.15) at t = 0.5 sec and almost linear correlation later (t = 0.5 sec) between the estimates i_0 and α in problem *P1* that makes their independent identification difficult in general. There is no such correlation between the estimates in problem *P3* and a weak correlation in problem *P2* due to mass-transfer effects in the electrochemical cell that are significant if the concentration is considerably lower of the bulk solution concentration. Therefore, the estimation process of the two parameters D and i_0 or D and α is well separated in time.

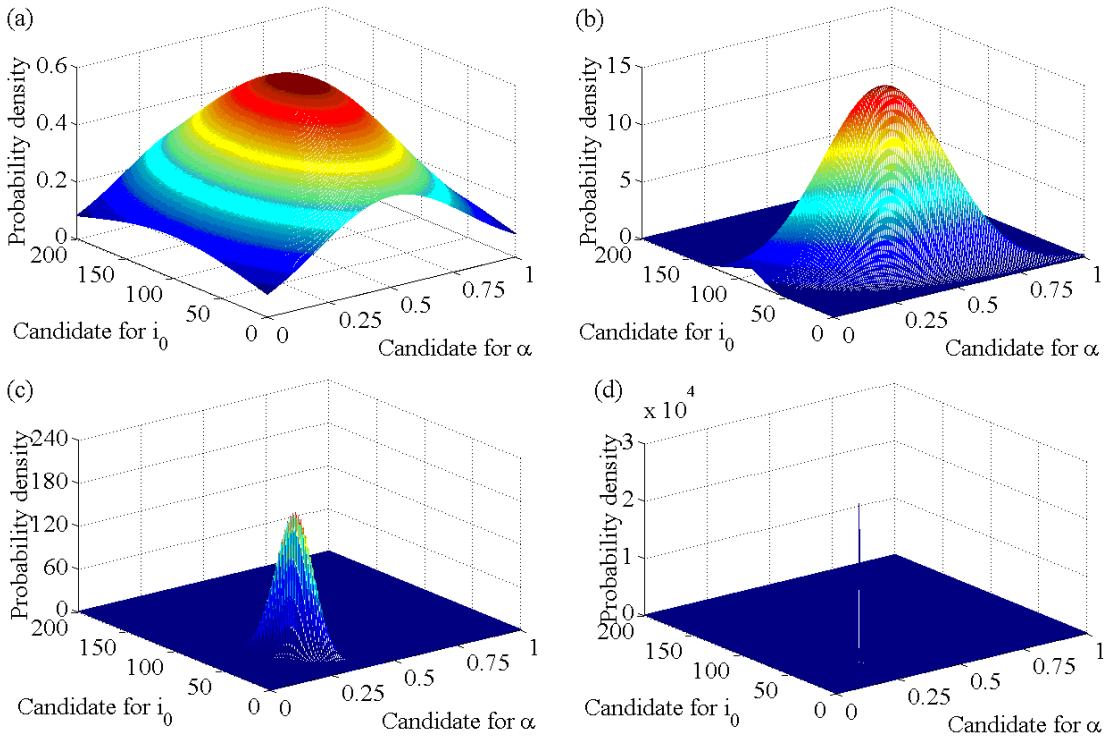

Figure 5.14: Evolution of the probability density distribution during control for the problem *P1* at (a) $t = 0$, (b) $t = 0.5$, (c) $t = 1$ and (d) $t = 10$ seconds.

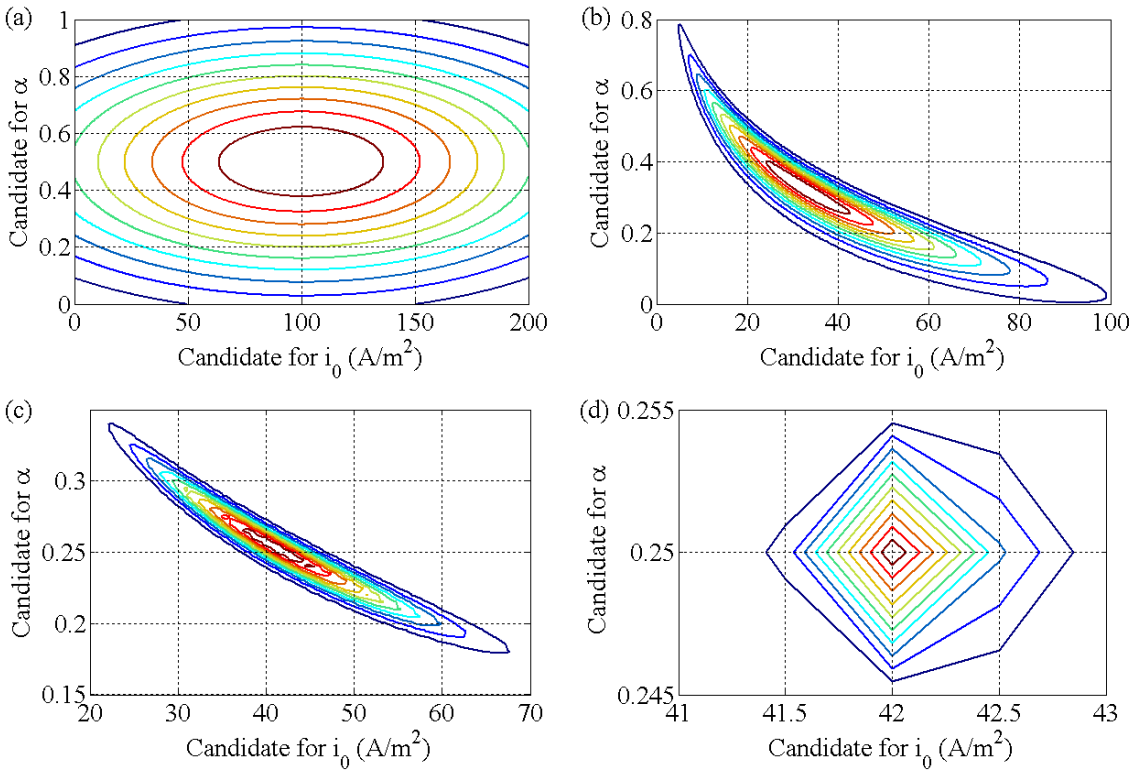

Figure 5.15: Evolution of the contour level lines during control for the problem *P1* at (a) $t = 0$, (b) $t = 0.5$, (c) $t = 1$ and (d) $t = 10$ seconds.

5.6 Conclusion

This chapter has shown that the feedforward controllers for finite-length (2.7)-(2.10) and semi-infinite diffusion processes (2.7)-(2.9), (3.1) can be easily designed in the case of known parameters. Moreover, it has been demonstrated that a relatively complex tracking control problem can be solved in the case of incomplete data. The tracking boundary control (5.39)-(5.40) maximizes the current density through a carefully chosen reference concentration. Therefore, depletion in industrial applications, such as copper deposition baths, can be avoided. Although the applied method leads to the infinite dimensional separated control problem, this problem can be solved with a direct search method using pathwise integration of the Zakai equation. This is sufficient for computing if the number of unknown constant parameters is less than 3, and if the aim of control is minimization of the variance instead of minimization of the integrated cost. However, the control problem solved for a semi-finite diffusion is not as practical as it would be if solved for a finite diffusion process.

Chapter 6

Identification of the mixed potential processes

6.1 Introduction

The electroless nickel plating process is an important process in the metal finishing industry. Its applications include the aerospace industry, oil and gas industry, chemical industry, electronics and computer industry. Electroless nickel deposited components have been used successfully for ABS systems, fuel injection pumps, gears and brake cylinders, pipelines and valves, drilling and support equipment, magnetic memory discs and printed circuit board manufacturing. Electroless nickel plating is defined as the deposition of nickel on a substrate by means of autocatalytic electrochemical reactions (Mallory, 1990). The process is widely used due to good corrosion protection and abrasion resistance of the electroless nickel deposits. Unlike electric nickel plating, it produces a very uniform nickel alloy that can be deposited without an external power source. The other useful properties of the alloy are hardness, lubricity and solderability.

The deposit properties of electroless nickel depend strongly on the nickel alloy thickness and its phosphorous content (Coombs, 2001; Kwok et al., 2002). To stabilize these directly unmeasured parameters at the desired level, a new model based on an electrochemical reaction mechanism, mixed potential theory and the Butler-Volmer equation was developed (Kantola, 2006; Tenno et al., 2006). This model eliminates the drawbacks of the mathematical models proposed by Bindra and White (1990), Chen et al. (2002), Kim and Sohn (1996), Riedel (1991) and Paunovic and Schlesinger (1998). It provides accurate estimates of the crucial deposit properties and process states. It is shown that the nickel alloy thickness and phosphorous content can be controlled effectively by a PI tracking controller with observed pH level and nickel ion concentration of the bath (Kantola, 2006; Kantola et al., 2005) provided that kinetic parameters of the process are known. Therefore, in order to improve the quality of the process and minimize the costs, an identification procedure for unknown parameters is required.

In this chapter the identification problem of a nonlinear model for electroless nickel plating is considered. The studied model is highly nonlinear and involves unknown time-varying mixed potential process. The possibilities of implementing a conventional technique, such as recursive least squares with a forgetting factor, a nonlinear least squares method and the basis function approach, to time-varying identification are

discussed and the identification method is developed for estimation of the kinetic parameters and time-varying mixed potential. The method converts the original nonlinear time-varying identification problem into a time-invariant quadratic optimization problem solvable by the conventional least squares algorithm thanks to the Taylor series expansion procedure. The time-varying mixed potential can then be estimated as a weighted sum of the reaction electrode potentials. The efficiency of the method was tested by simulations.

The results of this chapter have been published in one journal and one conference paper (Mendelson et al., 2006; Mendelson and Tenno, 2007b).

6.2 Contribution

The following contributions are covered in this chapter:

1. A novel identification method for identifying kinetic parameters and the time-varying mixed potential process of the nonlinear electroless nickel plating model is proposed. The method converts the original nonlinear time-varying identification problem into a time-invariant quadratic optimization problem with nonlinear constraints.
2. A method for identifying for identifying kinetic parameters and the time-varying mixed potential process with genetic algorithms is proposed. A method generates candidate solutions in such a way that the nonlinear constraints are always handled and, therefore, candidate solutions are always feasible.

6.3 Process model

The general structure of the process model is depicted in Fig. 6.1 (for details see Tenno et al., 2006). The model is composed of the dynamic linear block in feedback connection with two static nonlinear functions F_1 and F_2 and controller F_3. A set of ordinary linear differential equations is used to describe the concentration dynamics of the process. Concentration of the species affects the equilibrium potentials (function F_1) and equilibrium potentials in turn affect to the current densities of the electrode reactions (function F_2). The process is usually controlled by a proportional (P) or proportional-integral (PI) controller. The reason for a controller to be presented as a nonlinear block is its dead-zone modification that prevents high frequency oscillations of the error signal caused by measurement noise. Thereby, wear of the pumps is minimized.

The state vector $\boldsymbol{c}$ is assumed to be completely observed. According to the Nernst equation (Paunovic and Schlesinger, 1998), the equilibrium potentials $\boldsymbol{u}$ of the electrode reactions can be evaluated from the concentration of substances due to the assumption above. Therefore, the current densities caused by chemical reactions, can be reconstructed from the concentration dynamic equations provided that the vector of

feeding rates $\boldsymbol{Q}_{\mathbf{f}}$ is available, and the nonlinear function F_1 is known from the Nernst equation.

Matrixes $\boldsymbol{A}$ and $\boldsymbol{B}$ of the state-space representation of the concentration dynamics are known from the physical principles included in the process model and given as

$$A = \begin{pmatrix} -\frac{A_r}{2F} & \frac{A_r}{F} & 0 & 0 \\ \frac{A_r}{2F} & 0 & 0 & 0 \\ \frac{A_r}{F} & \frac{2A_r}{F} & \frac{A_r}{F} & 0 \\ 0 & 0 & 0 & \frac{A_r}{2F} \end{pmatrix}, \quad B = \begin{pmatrix} c_{1f} & 0 & 0 \\ 0 & 0 & 0 \\ 0 & -c_{3f} & 0 \\ 0 & 0 & c_{4f} \end{pmatrix},$$

where A_r is the bath loading, cm^2/dm^3, F is the Faraday's constant, 96485 A·s/mol, c_{1f}, c_{2f} and c_{3f} are the feeding solution concentrations of hypophosphite, ammonia and nickel ions equal to 5.2, 6.0 and 1.8 mol/dm^3 respectively (Tenno and Koivo, 2003). The bath loading process is modeled as a Markov jump process with three levels: 33, 66 and 99 cm^2/dm^3.

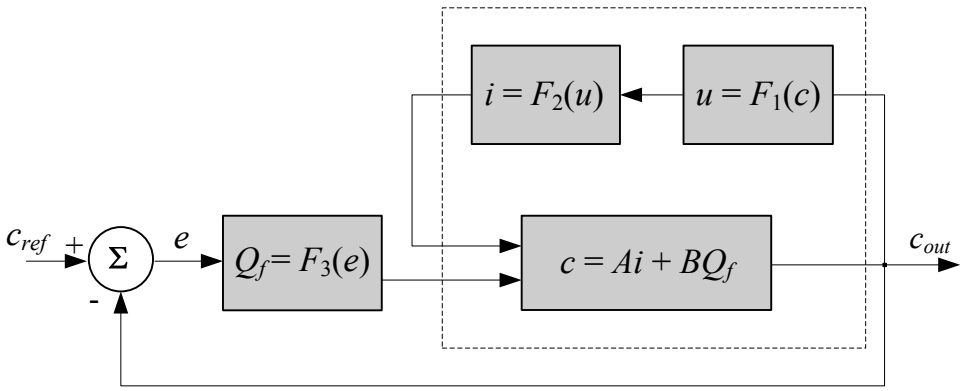

Figure 6.1: The process model

The static nonlinear function F_2, determining current-density-potential relationships, is given by system of four Butler-Volmer equations, which correspond to the four reactions of the process:

$$i_j = i_{0j}\mu_j(\mathbf{c})\left(e^{k_j\alpha_{aj}(\Phi-u_j)} - e^{-k_j(1-\alpha_{aj})(\Phi-u_j)}\right), \; j = \overline{1,4}, \tag{6.1}$$

where i_j is the current density of the jth reaction, A/m^2, i_{0j} is the exchange current density (constant), A/cm^2, α_{aj} is the anodic apparent transfer coefficient (constant), dimensionless, k_j is the temperature voltage, $k_j = \nu n_j F/RT$, V^{-1}, ν is the robustness coefficient, $\nu = 0.1$, dimensionless, n_j is the number of electrons ($n_1 = 2$, $n_2 = 1$, $n_3 = 2$, $n_4 = 2$), dimensionless, F is the Faraday's constant, 96485 A·s/mol, R is the ideal gas constant, 8.314 J/(mol·K), T is the absolute temperature, K, μ_j is the dimensionless

concentration of species, u_j is the reaction equilibrium potential, V and Φ is the mixed potential, V.

The model (6.1) is known as a bi-directional electrode model, being composed of two exponential terms standing for the anodic and cathodic current densities. The dimensionless concentration of species appearing in the model (6.1) is a function of concentration (Tenno et al., 2006; Kantola, 2006). This term results from neglected diffusion phenomena and takes into account the concentration at the boundary. However, because all the concentrations are assumed measured, the dimensionless concentrations of the species are known and can be accounted by forming the ratio with the current density of the corresponding reaction. Therefore, without loss of generality, it is possible to consider the nonlinear electroless nickel plating model to be given as

$$i_j = i_{0j}\left(e^{k_j\alpha_{aj}(\Phi-u_j)} - e^{-k_j(1-\alpha_{aj})(\Phi-u_j)}\right),\ j=\overline{1,4}. \tag{6.2}$$

The equilibrium potential of the reactions are calculated from the Nernst equation using unit activity for solid material and water as well as unit partial pressure for gas (Kantola and Tenno, 2006)

$$\begin{cases} u_1 = U_1 + \kappa\left(\log_{10} c_2 - \log_{10} c_1 - 2pH\right) \\ u_2 = U_2 + 0.2\kappa\left(\log_{10} c_1 - 2pH\right) \\ u_3 = U_3 - 2\kappa pH \\ u_4 = U_4 + \kappa \log_{10} c_4 \end{cases},$$

where $\kappa^{-1} = \dfrac{2F}{RT}\log_{10} e$, U_j is the reaction standard equilibrium potential equal to -0.504 V, -0.391 V, 0 V, and -0.257 V for the four partial reactions respectively, c_j is the concentration of species (hypophosphate, orthophosphate, hydrogen and nickel), mol/m^3, and pH is the acidity level $pH = -\log c_3$.

The mixed potential is an electrode potential resulting from a simultaneous action of the four electrode reactions, while the net electrode current is zero. The mixed potential in (6.2) is an unobserved function in time and, therefore, has to be identified. It is known that the mixed potential satisfies the charge conservation equation:

$$i_1 + i_2 + i_3 + i_4 = 0. \tag{6.3}$$

Equation (6.3) is written in terms of current densities rather than currents. This is possible under the assumption that the reactions occur uniformly on an electrode.

Unfortunately for the nickel plating model depicted in Fig. 6.1 it is not enough to design controls to track the desired reference concentration. The reason for that is because the control objective in electroless nickel plating is stabilization for thickness of the alloy. However, other chemicals utilized in a solution bath, change the value of the mixed potential and the reference concentrations of hydrogen and nickel should be adapted to this new value. Therefore, to relate the reference concentration with the mixed potential process, the known model is required.

The objective of this chapter is to design an estimation technique for the exchange current densities and apparent transfer coefficients of the electrode reactions as well as for the time-varying mixed potential process using the available measurements of concentration $\boldsymbol{c}$ and current densities $\boldsymbol{i}$.

6.4 Parameter identification

Several techniques have been proven to be useful when dealt with time-varying identification. They include recursive least squares with forgetting factor, the basis function approach and the method based on Kalman filtering (Niedzwiecki, 2000). It should be pointed out that in our case nonlinear least squares method is required since the model (6.1) is nonlinear in the unknown parameters.

A simple analysis shows that on every time step in addition to four measurements of reaction current densities one unknown mixed potential value is added. The ratio of number of measurements to number of the unknown parameters approaches to four as time tends to infinity. It is known that the nonlinear least squares method may not converge to the actual parameters. Moreover, the convergence properties get considerably worse as number of the unknown parameters is increased. Kalman filtering assumes differential equation for the unknown state to be given. The most exciting is the basis function approach. In this technique the unknown time-varying coefficient, in this particular case mixed potential process, is expanded onto a set of basis functions $\varphi(t)$ (Zou et al., 2003)

$$\Phi(t) = \sum_{m=1}^{N} a_m \varphi_m(t). \tag{6.4}$$

Then the problem of identifying the time-varying mixed potential is converted to the problem of identifying the unknown constant parameters a_m. As the basis functions, for instance, Fourier sequences, or Legendre and Walsh functions can be utilized (Zou et al., 2003; Niedzwiecki, 2000). The expansion (6.4) also simplifies implementation of the nonlinear least squares. However, the quality of such estimation strongly depends on the number of basis functions used. Moreover, the model remains nonlinear and its optimization is still difficult. To solve the problem we convert the nonlinear model (6.2) into a linear so that its global minimum can be calculated analytically. In addition, we show the relation between the linear model obtained and basis function identification approach.

6.4.1 Converting to a linear optimization problem

The nonlinear model (6.2) can be converted to a linear one using a linearization technique. This linearization is reasonable because the control objective in electroless nickel plating is stabilization for thickness of the alloy. In terms of the model, this means stabilization of the mixed potential and equilibrium potentials of the reactions. Consequently, the variation of the reaction overpotentials is expected to be small enough to justify usage of a linear model equivalent to (6.2). This linear electroless

nickel plating model can be obtained by 1st order Taylor series expansion of the current densities at Φ - u_j

$$i_j\left(\Phi,u_j\right)=i_j\left(\Phi_0,u_{j0}\right)+i_j^{'}\left(\Phi_0,u_{j0}\right)\cdot\left(\eta_j-\eta_{j0}\right)+o\left(\left|\eta_j\right|\right),\ j=\overline{1,4}, \tag{6.5}$$

with the overpotential η_j being defined as

$$\eta_j=\Phi-u_j,\ j=\overline{1,4}. \tag{6.6}$$

Expanding in the model (6.2) every current-potential equation as (6.5) produces the following linear model

$$i_j=a_j+b_j\left(\left(\Phi-\Phi_0\right)-\left(u_j-u_{0j}\right)\right)+o\left(\left|\eta_j\right|\right),\ j=\overline{1,4}, \tag{6.7}$$

where a_j and b_j are the constant and linear terms of the jth equation Taylor series expansion respectively

$$a_j=i_j\left(\Phi_0,u_{0j}\right),\ b_j=i_j'\left(\Phi_0,u_{0j}\right),\ j=\overline{1,4}. \tag{6.8}$$

Combining all the free terms in every equation of (6.7) into one

$$d_j=a_j-b_j\left(\Phi_0-u_{0j}\right),\ j=\overline{1,4} \tag{6.9}$$

and ignoring the approximation error, the next equivalent form of (6.2) is obtained

$$i_j=d_j+b_j\Phi-b_ju_j,\ j=\overline{1,4}. \tag{6.10}$$

By summing the four equations in (6.10) and using charge conservation identity (6.3), we derive the next expression for the mixed potential Φ:

$$\Phi=\frac{-\sum_{i=1}^{4}d_i+\sum_{i=1}^{4}b_iu_i}{\sum_{i=1}^{4}b_i}. \tag{6.11}$$

The equation (6.11) gives a straightforward way to estimate an unknown time-varying mixed potential provided that the estimates of unknown coefficients b_j and d_j are known. Compared with (6.4), the equation (6.11) can be interpreted as an expansion of the mixed potential onto a set of the equilibrium potentials of the partial reactions that act as basis functions.

Substituting (6.11) into (6.10) allows us to eliminate the mixed potential process and to represent the system (6.10) as

$$i_j=\gamma_j+\sum_{m\neq j}\beta_{mj}\Delta u_{mj},\ j=\overline{1,4} \tag{6.12}$$

with $\Delta u_{ij}(t) = u_i(t) - u_j(t)$ and γ_i, β_{ij} being defined as

$$\gamma_i = \frac{d_i \sum_{j \neq i} b_j - b_i \sum_{j \neq i} d_j}{\sum_{j=1}^{4} b_j}, \tag{6.13}$$

and

$$\beta_{ij} = \frac{b_i b_j}{\sum_{k=1}^{4} b_k} \tag{6.14}$$

respectively. The model (6.12) is linear in the unknown parameters and, unlike (6.10) it does not involve an unknown time-varying function. With respect to the linear model (6.12) the objective is to minimize the cost functions

$$J_k = \sum_{l=1}^{N} \left(\xi_k(t_l) - i_k(t_l) \right)^2, k = \overline{1,4} \tag{6.15}$$

subject to linear constraints (6.16) and (6.17)

$$\sum_{i=1}^{4} \gamma_i = 0, \tag{6.16}$$

$$\beta_{ij} = \beta_{ji}, \tag{6.17}$$

and nonlinear constraints (6.18)

$$\beta_{ij} = \frac{\beta_{ik} \beta_{jl}}{\beta_{kl}}. \tag{6.18}$$

In the equation (6.15) $\xi_k(t_l)$ are the measured current densities of the four reactions of the process at time t_l and $i_k(t_l)$ are the modeled current densities (6.12). The constraints (6.16)-(6.18) arise naturally from the definitions (6.13)-(6.14).

At this point we notice that the optimization problem under consideration is a multi-objective optimization problem, because four different cost functions should be minimized. Several methods have been proposed to solve multi-objective optimization problems. They include the simple weighting method, p-norm methods, such as the goal attainment method, goal programming, the minimax reference point method and interactive methods, such as Geoffrion's method, the STEM and ISTM methods and the gradient projection method (Liu et al., 2003). Consider the simple weighting method. According to it the multiply cost functions (6.15) are converted into a scalar cost function by summing the four cost functions with weights ω_k

$$J = \frac{1}{2} \sum_{k=1}^{4} \omega_k \sum_{l=1}^{N} \left(\xi_k(t_l) - i_k(t_l) \right)^2, k = \overline{1,4}. \tag{6.19}$$

Now the optimization problem is to find the regression vector

$$\theta = \left[\gamma_1\ \gamma_2\ \gamma_3\ \gamma_4\ \beta_{12}\ \beta_{13}\ \beta_{14}\ \beta_{23}\ \beta_{24}\ \beta_{34}\right]^T \tag{6.20}$$

that minimizes the cost function (6.19) subject to the constraints (6.16)-(6.18). While the cost function (6.19) is linear in the parameters the constraints (6.18) are nonlinear. The optimality conditions require the first derivatives of (6.19) with respect to the regression vector (6.20) to be zero in optimum point. In a well-posed case the nonlinear constraints (6.18) can be omitted and the performance function (6.19) can be minimized only under the linear constraints (6.16) and (6.17). Consequently, the problem can be solved by the linear least squares method.

Setting the first derivatives of (6.19) to zero produces a linear system of nine equations in nine variables. Such a system is solvable and its solution is unique if the matrix of coefficients has full rank. Though due to the charge conservation identity (6.3) and a small approximation error this problem is ill-posed, for identification purposes small input noise can be injected into the system to improve the posedness of the problem.

The constrained optimization problem (6.19) can be solved iteratively by the Zoutendijk method of feasible directions (Himmelblau, 1972). Alternatively, by using penalty functions the problem (6.19) can be replaced by a series of unconstrained problems that can be solved by unconstrained optimization methods. While these numerical methods may converge to a local extremum, genetic algorithms considered in the next subsection can be utilized to find the global extremum.

6.4.2 Solving the constrained optimization problem with genetic algorithms

Genetic algorithms (GAs) are adaptive search algorithms that employ evolutionary biology techniques for solving the optimization problem (Reeves and Rowe, 2003). Genetic algorithms have found numerous applications in control engineering due to their possibility to cope with ill-posed problems (Fleming and Purshouse, 2002). These applications include controller design, system identification and fault diagnosis. The typical scheme of GA is the following. The algorithm starts from an initial population of randomly generated solution candidates (*chromosomes*). While usually candidates are presented by binary strings, other forms such as integer or real-valued representations are of great interest. A certain measure of the potential candidate quality known as the fitness function is chosen to range the chromosomes. Then solution candidates are naturally selected according to their fitness function and transformed to form a new population. For transformation recombination of the selected candidates and, possibly, mutation are used. Typically, the individuals are selected using the roulette wheel selection method with or without replacement. According to this method the probability of selection is proportional to the relative fitness of individuals (Reeves and Rowe, 2003). Alternatively, the candidates can be selected using stochastic universal sampling (Baker, 1987). In the case of binary representation, the new candidates are generated using the single-point, multi-point or uniform crossover. The multi-point crossover operator exchanges the bits at randomly chosen positions between the selected parents. The uniform crossover does the same by using the crossover mask. For real-valued individuals intermediate recombination is used to generate the new population. Often, in

addition to offspring produced by the crossover, the best chromosome is copied to the next generation to increase performance of GA. Consequently, one population is replaced with another and useful properties of parents are inherited in offspring. Typically, GAs terminate if a sufficiently good value of fitness function has been reached, or, due to a lack of improvement, after a maximum number of generation has been passed (Liu et al., 2003). Usually, a candidate with the best fitness function is reported as the approximate solution.

Genetic algorithms have been applied to solve multi-objective optimization problems (see Liu et al., 2003 and references therein). Unlike conventional methods, GAs evaluate the fitness function of several candidates simultaneously, and because of that they are suitable for solving multi-objective problems. A traditional approach to calculate the fitness function, when the multiply cost functions are converted into a scalar cost function, also can be used. GAs can be easily modified to handle constrained optimization problems. The simplest approach to assign an arbitrary low fitness functions to inferior candidates was proposed by Goldberg (1989). In our particular case, the problem is subject only to equality constraints. Therefore, a population of potential candidates can be generated in such a way that these nonlinear constraints are always handled. Initially, a population is formed be generating the potential solutions composed of any four of the parameters subject to nonlinear constraints, for instance, β_{12}, β_{13}, β_{14} and β_{23}. Then the potential candidates are supplemented by other two β-parameters calculated from the nonlinear constraints (6.17). The γ-parameters of the regression vector (6.19) can be found by the linear least squares method from (6.11). Assume θ_{unc} is an unconstrained least squares solution for the γ-parameters. Then to solve the constrained optimization problem (6.15), this solution θ_{unc} is corrected in the following way (Söderström and Stoica, 1989)

$$\theta_{constr} = \theta_{unc} - \left(X^T X\right)^{-1} A\left(A \cdot \left(X^T X\right)^{-1} \cdot A^T\right)^{-1} \left(A\theta_{unc} - b\right),$$

where matrix X is the regression matrix and matrix A and vector b are chosen according to the constraint (6.15). Therefore, operations of recombination and mutation are always applied to the four selected β-parameters, while the other six parameters are calculated to satisfy to the constraints (6.15) and (6.17). In such a scheme all the potential solutions that form an initial population and consequent generations are always feasible. A flowchart of the proposed genetic algorithm is illustrated in Fig. 6.2.

6.4.3 Converting the solution to primary regression vector

The solution of (6.19) with the constraints (6.16) and (6.18) is the least squares solution of the optimization problem given in terms of the regression vector (6.20). According to the initial objective exchange current densities and apparent transfer coefficients as well as the mixed potential process have to be identified. Therefore, certain transformation from (6.20) into the mentioned parameters is needed. We refer to this transformation as inverse transformation.

According to the definitions (6.13) and (6.14), the γ-parameters depend on both the free and linear parts of the Taylor series expansion, while the β-parameters depend only on

the linear parts of the Taylor series expansion. Therefore, first we have to calculate b_i. Due to the constraints (6.17), any four of the β-parameters are independent. Selecting, for instance, β_{12}, β_{13}, β_{14} and β_{23}, the system to find the linear part of the Taylor series expansion b_i takes the following form

$$\begin{cases} \beta_{12} = b_1 b_2 \Big/ \sum_{j=1}^{4} b_j \\ \beta_{13} = b_1 b_3 \Big/ \sum_{j=1}^{4} b_j \\ \beta_{14} = b_1 b_4 \Big/ \sum_{j=1}^{4} b_j \\ \beta_{23} = b_2 b_3 \Big/ \sum_{j=1}^{4} b_j \end{cases} . \tag{6.21}$$

The straightforward way to solve the system (6.21) is to find partial ratios between, for instance, b_1 and b_2, b_3, b_4. They are given as

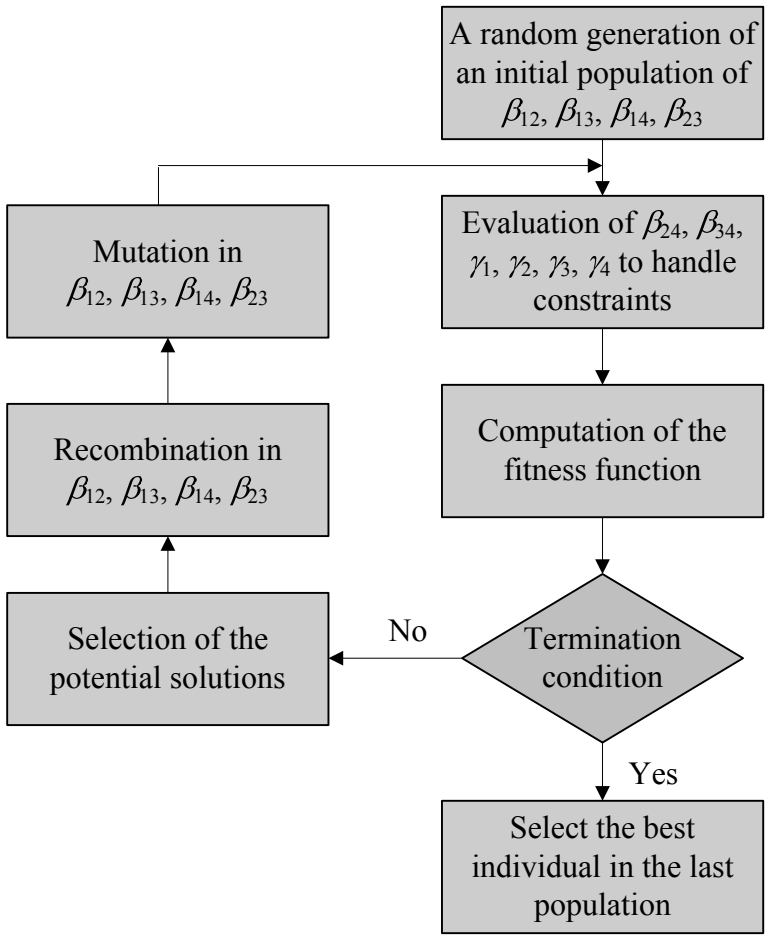

Figure 6.2: Flowchart of the proposed genetic algorithm.

$$b_2 = b_1 \frac{\beta_{23}}{\beta_{13}},\ b_3 = b_1 \frac{\beta_{23}}{\beta_{12}},\ b_4 = b_1 \frac{\beta_{14}\beta_{23}}{\beta_{12}\beta_{13}}. \tag{6.22}$$

Substituting (6.22) into (6.21) the following solution is obtained

$$\begin{cases} b_1 = \beta_{12} + \beta_{13} + \beta_{14} + \dfrac{\beta_{12}\beta_{13}}{\beta_{23}} \\ b_2 = \beta_{12} + \beta_{23} + \dfrac{\beta_{12}\beta_{23}}{\beta_{13}} + \dfrac{\beta_{14}\beta_{23}}{\beta_{13}} \\ b_3 = \beta_{13} + \beta_{23} + \dfrac{\beta_{13}\beta_{23}}{\beta_{12}} + \dfrac{\beta_{14}\beta_{23}}{\beta_{12}} \\ b_4 = \beta_{14} + \beta_{14} \dfrac{\beta_{14}\beta_{23}}{\beta_{12}\beta_{13}} + \dfrac{\beta_{14}\beta_{23}}{\beta_{13}} + \dfrac{\beta_{14}\beta_{23}}{\beta_{12}} \end{cases}. \tag{6.23}$$

Now the free terms d_i given by (6.9) can be calculated provided that γ_i and b_i are given. One can observe that the four unknown coefficients have to be estimated while only three of them are linearly independent due to the linear constraint (6.16). In other words, the problem of estimating d_j is ill-posed and additional information is required. To overcome this problem and perform the inverse transformation, we propose to utilize the mean value of the mixed potential process.

Utilizing the mean value of the mixed potential is reasonable, because to start the algorithm the linearization point for the mixed potential process must be specified. Therefore, it is natural to use as the mean value the value of the mixed potential at the point where the Taylor series expansion was performed.

Assume that we know one of d_i, for instance d_4. Then the system to identify others d_i is given by

$$\begin{bmatrix} \gamma_1 \sum_{i=1}^{4} b_i + d_4 b_1 \\ \gamma_2 \sum_{i=1}^{4} b_i + d_4 b_2 \\ \gamma_3 \sum_{i=1}^{4} b_i + d_4 b_3 \end{bmatrix} = \begin{bmatrix} b_2 + b_3 + b_4 & -b_1 & -b_1 \\ -b_2 & b_1 + b_3 + b_4 & -b_2 \\ -b_3 & -b_3 & b_1 + b_2 + b_4 \end{bmatrix} \begin{bmatrix} d_1 \\ d_2 \\ d_3 \end{bmatrix}. \tag{6.24}$$

The system (6.24) is linear in the unknown parameters and can be solved by the classical Gaussian elimination method (Golub and Van Loan, 1996). Let us specify the following constants

$$d_{i,0} = \frac{b_i(\gamma_1 + \gamma_2 + \gamma_3) + b_4\gamma_i}{b_4},\ d_{i,1} = \frac{b_i}{b_4},\ i = \overline{1,4}. \tag{6.25}$$

Then the solution of (6.24) can be written as a linear function of the constant d_4

$$d_j = d_{j,0} + d_4 d_{j,1},\ j = \overline{1,3}. \tag{6.26}$$

Substituting (6.26) into (6.11) gives

$$\Phi = \frac{-\sum_{i=1}^{3} d_{i,0} - d_4\left(1 + \sum_{i=1}^{3} d_{i,1}\right) + \sum_{i=1}^{4} b_i u_i}{\sum_{i=1}^{4} b_i}. \tag{6.27}$$

Equation (6.27) contains only one unknown constant d_4 that can be found due to our assumption about the known mean value of the mixed potential. Indeed, ask for the mean value of the estimated mixed potential process to be equal to its value in the chosen linearization point

$$\frac{1}{N}\sum_{i=1}^{N} \Phi_i = \Phi_0, \tag{6.28}$$

where N is the number of available concentration measurements. Substituting (6.27) into (6.28) leads to

$$\frac{1}{N}\sum_{i=1}^{N}\left[\frac{-\sum_{j=1}^{3} d_{j,0} - d_4\left(1 + \sum_{j=1}^{3} d_{j,1}\right) + \sum_{j=1}^{4} b_j u_i}{\sum_{j=1}^{4} b_j}\right] = \Phi_0. \tag{6.29}$$

The equation (6.29) solved for d_4 gives

$$d_4 = \frac{-N\sum_{j=1}^{3} d_{j,0} - N\Phi_0 \sum_{j=1}^{4} b_j + \sum_{i=1}^{N}\sum_{j=1}^{4} b_j u_i}{N\left(1 + \sum_{j=1}^{3} d_{j,1}\right)}. \tag{6.30}$$

Substituting (6.30) into (6.26) makes it possible to find the unknown d_1, d_2, and d_3. Then starting from the identity $d_j = a_j - b_j(\Phi_0 - u_{0j})$, the coefficients of the Taylor series expansion for all four reactions can be evaluated. Then the separate nonlinear systems to identify parameters of the two-directional model (6.2) are given by

$$\begin{cases} i_{0j}\left[e^{k_j \alpha_{aj} \eta_{0j}} - e^{-k_j(1-\alpha_{aj})\eta_{0j}}\right] = a_j \\ i_{0j} k_j \left[\alpha_{aj} e^{k_j \alpha_{aj} \eta_{0j}} + \left(1-\alpha_{aj}\right) e^{-k_j(1-\alpha_{aj})\eta_{0j}}\right] = b_j \end{cases},\ j = \overline{1,4}. \tag{6.31}$$

Finally, expressing the exchange current densities from the first equation of (6.31) and substituting these to the second equation the solution of (6.31) is obtained

$$\begin{cases} \alpha_{aj} = \dfrac{b_j}{a_j k_j} - \dfrac{e^{-k_j \eta_{0j}}}{1 - e^{-k_j \eta_{0j}}} \\ i_{0j} = \dfrac{a_j}{e^{k_j \left(\frac{b_j}{a_j k_j} - \frac{e^{-k_j \eta_{0j}}}{1 - e^{-k_j \eta_{0j}}} \right) \eta_{0j}} \left(1 - e^{-k_j \eta_{0j}} \right)} \end{cases}, \; j = \overline{1,4}. \tag{6.32}$$

The equations (6.20)-(6.32) give a way to perform an inverse transformation moving from the parameters of the linear approximation (6.11) to the parameters of the bi-directional electrode kinetics model (6.2). The overall identification procedure is briefly outlined in Table 6.1.

It should be mentioned that the true values of the estimated parameters cannot be reached due to unaccounted approximation errors. The best estimate we can reach without knowledge of the noise structure is bounded by the approximation error. When the overpotential (6.6) varies a lot, a possible way to reduce an approximation error is data clustering.

Table 6.1: The overall identification procedure of the mixed potential process

1. Specify the mixed potential linearization point and calculate equilibrium potential linearization points based on the available measurements.
2. Find the least-squares solution of the problem (6.15)-(6.18) by linear least squares, the Zoutendijk method of feasible directions, penalty functions method, genetic algorithms, etc.
3. Estimate the Taylor series expansion coefficients as in (6.23), (6.26) and (6.30).
4. Calculate the estimates of the unknown parameters of the bi-directional model (6.2) according to the equation (6.32).
5. Estimate the mixed potential curve as given in (6.11).

6.5 Simulation results

Approximately four hours work of the electroless nickel plating process was modeled with discretization time Δt = 5 s. In this period the desired pH reference level has been changed from 4.75 to 5.0 to stabilize the mixed potential process. The true values of the exchange current densities and apparent transfer coefficients utilized in the simulation are listed in Table 6.2. Ranges of the electrode equilibrium potentials were [-895 -865], [-483 -477], [-365 -333] and [-288.74 -288.73] mV for the first, second, third and forth reactions respectively. The range of the mixed potential was [-752 -728] mV. In accordance with the electrode potentials and mixed potential process ranges the Taylor series expansion was performed at the following point: u_{01} = -880 mV, u_{02} = -480 mV, u_{03} = -349 mV, u_{04} = -288.74 mV, Φ_0 = -740 mV.

Table 6.2: The true values of the unknown parameters

Reaction	i_0^{true}, mA/cm^2	α_a^{true}
1	17.68	0.53
2	0.498	0.38
3	2.509	0.413
4	1.611	0.535

The best possible estimates of the unknown parameters that can be reached in such a simulation are listed in Table 6.3. They have been calculated in the following way. First, the free and linear terms of the Taylor series expansion were calculated. Then, the best possible estimates were found using inverse transformation based on the free and linear terms. In other words, no identification procedure was employed.

Table 6.3: The best possible estimates

Reaction	i_0^{est}, mA/cm^2	α_a^{est}
1	17.65	0.532
2	0.494	0.370
3	2.526	0.412
4	1.561	0.525

One can observe that the true parameters and the best estimates are slightly different. However, the maximum error is about 3% and it seems that this accuracy is quite enough for identification purposes.

The same parameters were used to identify the parameters from the current density and electrode equilibrium potential measurements. Then the problem (6.14)-(6.17) was solved by the linear least squares method and genetic algorithms. The genetic algorithm utilized in the simulation used binary coded 16-bit word candidate solutions. The individuals have been chosen for reproduction using the basic roulette wheel selection method. A single-point crossover was used for generating new potential candidates. In addition, two the best individuals were also copied to the next generation. The number of generations was taken to be 100, and after producing 100 generations the algorithm terminated. The generation was consisted of 1000 potential solutions, and the mutation probability was 0.05.

The mixed potential evolution in time and its estimate obtained by the linear least squares method are illustrated in Fig. 6.3. The genetic algorithms estimate of the mixed potential process is similar to that of the least squares algorithm and is not reported here. The parameter estimates obtained using the linear least squares method and genetic algorithms are listed in Table 6.4.

It should be pointed out that the linear least squares method does not take into account the nonlinear constraints (6.17), and, therefore, the estimates strongly depend on the β-parameters chosen to find the linear terms of the Taylor series expansion. The results presented in Table 6.4 used β_{12}, β_{13}, β_{14} and β_{23} to find the linear part of Taylor series expansion. However, in practice several different subsets of the β-parameters can be utilized. In such a case, it is natural to choose the solution with minimum residual of the nonlinear constraints.

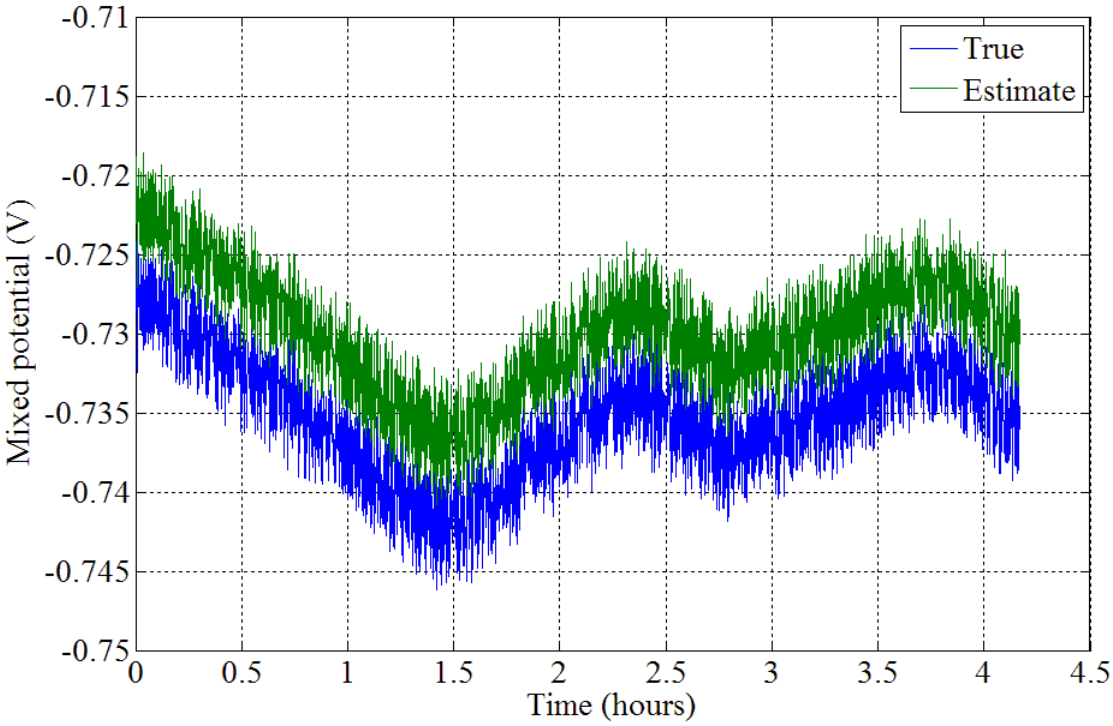

Figure 6.3: Mixed potential evolution in time and its estimate obtained by the linear least squares method.

Table 6.4: Estimates of the electrochemical parameters

Reaction	The linear least squares		Genetic algorithms	
	i_0^{est}, mA/cm^2	α_a^{est}	i_0^{est}, mA/cm^2	α_a^{est}
1	16.19	0.561	17.1	0.61
2	0.52	0.404	0.48	0.36
3	2.56	0.417	2.11	0.36
4	1.64	0.533	1.56	0.53

Knowledge of the good average values of mixed potential is significant in the proposed identification algorithm. Otherwise though the estimate of the mixed potential will still track its true dynamics, the estimates of the exchange current density and anodic apparent transfer coefficients will be biased.

6.6 Conclusion

In this chapter a novel identification method for identifying the kinetic parameters and time-varying mixed potential process of the nonlinear electroless nickel plating model (6.2) was proposed. The method converts nonlinear a time-varying identification problem to a linear identification problem by means of the Taylor series expansion procedure. Next an optimization technique such as the traditional linear least squares method or a genetic algorithm is applied to estimate the parameters.

The proposed method can be used for synthesis of the model-based control law, thickness alloy and phosphorous content estimation. For example, the tracking PI control proposed by Kantola (2006) can be applied provided that the kinetic parameters of the process are identified.

The process and identification method were simulated and it was shown that the estimates of kinetic parameters are practically insensitive relative to small deviations of the mean value of mixed potential against its real value.

Bibliography

Ahmed, N.U. and Radaideh, S.M. (1997). A powerful numerical technique solving Zakai equation for nonlinear filtering. *Dynamics and Control*, **7**(3), pp. 293-308.

Aihara, S. and Bagchi, A. (2006). Filtering and identification of stochastic volatility for parabolic type factor models. *International Journal of Innovative Computing, Information and Control*, **2**(5), 917-925.

Aström, K.J. and Hägglund, T. (2005). *Advanced PID Control*. ISA, 461 p.

Aström, K.J. and Wittenmark, B. (1994). *Adaptive Control*. Prentice Hall, 580 p.

Bain, A. and Crisan, D. (2009). *Fundamentals of Stochastic Filtering*. Springer, New-York, 390 p.

Baker, J. E. (1987). Reducing bias and inefficiency in the selection algorithm. *Proceedings of the 2nd international conference on genetic algorithms*, Cambridge, USA, pp. 14–21.

Balakrishnan, A.V. and Lions, J.L. (1967). State estimation for infinite dimensional systems. *Journal of Computer and System Sciences*, **1**(4), pp. 391-403.

Bamford, C.H. and Compton, R.G. (1986). *Electrode Kinetics: Principles and Methodology*, Elsevier, 450 p.

Bard, A.J. and Faulkner, L.R. (2001). *Electrochemical Methods: Fundamentals and Applications.* John Wiley & Sons, New-York, 856 p.

Barbarisi, O., Vasca, F., and Glielmo, L. (2006). State of charge Kalman filter estimator for automotive batteries. *Control Engineering Practice*, **14**(3), pp. 267-275.

Beck, J.V. (1970). Nonlinear estimation applied to the nonlinear inverse heat conduction problem. *International Journal of Heat and Mass-Transfer*, **13**(4), pp. 703-716.

Bellman, R. and Aström, K. (1970). On structural identifiability. *Mathematical Biosciences*, **7**, pp. 329-339.

Beneš, V.E. (1981). Exact finite dimensional filter for certain diffusions with nonlinear drift. *Stochastics*, **5**, pp. 65-92.

Beneš, V.E., (1983). On the relation of Zakai's and Mortensen's equations, *SIAM Journal on Control and Optimization*, **21**(3), pp. 472-489.

Beneš, V.E., Kratzas, I., Ocone, D., and Wang, H. (2004). Control with partial observations and an explicit solution of Mortensen's equation. *Applied Mathematics and Optimization*, **49**, pp. 218-239.

Bensoussan, A., Glowinski, R., and Rascanu, A. (1990). Approximation of the Zakai equation by the splitting up method. *SIAM Journal on Control and Optimization*, **28**(6), pp. 1420–1431.

Berthier, F., Diard, J.-P., Pronzato, L., and Walter, E. (1996). Identifiability and distinguishability concepts in electrochemistry. *Automatica*, **32**(7), pp. 973-984.

Berzins, T. and Delahay, P. (1953). Oscillographic polarographic waves for the reversible deposition of metals on solid electrodes. *Journal of the American Chemical Society*, **75**(3), pp. 555-559.

Bhikkaji B. and Söderström, T. (2001). Reduced order models for diffusion systems. *International Journal of Control*, **74**(15), pp. 1543-1557.

Bindra, P. and White, J.R. (1990). *Fundamental Aspects of Electroless Copper Plating*. In Electroless Plating: Fundamentals and Applications, ed. G.O. Mallory G.O, J. B. Haidu, American Society of Civil Engineers, Orlando, pp. 290-329.

Bockris, J., Reddy, A.K.N., and Gamboa-Aldeco, M. (2000). *Modern Electrochemistry 2A. Fundamentals of Electrodics* (*2nd Edition*), Kluwer, 817 p.

Borkar, V.S. (2005). Controlled diffusion processes. *Probability Surveys*, **2**, pp. 213-244.

Boyd, J. (2001). *Chebyshev and Fourier Spectral Methods*. Dover Publications, 688 p.

Bresch-Pietri D. and Krstic, M. (2009). Adaptive trajectory tracking despite unknown input delay and plant parameters. *Automatica*, **45**(9), pp. 2074-2081.

Brett, C. and Brett A.M. (1993). *Electrochemistry. Principles, Methods and Applications*. Oxford University press, 427 p.

Briechle, K. and Hanebeck, U.D. (2004). Localization of a mobile robot using relative bearing measurements. *IEEE Transactions on Robotics and Automation*, **20**(1), pp. 36-44.

Britz, D. (1978). *iR* elimination in electrochemical cells. *Journal of Electroanalytical Chemistry*, **88**(3), pp. 309-352.

Chen, C. and Wan, C. (1989). A study of the current efficiency decrease accompanying short pulse time for pulse plating. *Journal of Electrochemical Society,* **136**(10), pp. 2850-2855.

Chen, L., Crnic, M., Lai, Z., and Liu, J. (2002). Process development and adhesion behavior of electroless copper on liquid crystal polymer (LCP) for electroless packaging application. *IEEE Transactions on Electronic Manufacturing*, **25**(4), pp. 273-278.

Chen, Z. (2003). *Bayesian Filtering: From Kalman Filters to Particle Filters, and Beyond.* Technical report, Adaptive Syst. Lab., McMaster Univ.

Christensenand, P.A. and Hamnett, A. (1994). *Techniques and Mechanisms in Electrochemistry*, Kluwer, 379 p.

Coca, D. and Billings, S.A. (2000). Direct parameter identification of distributed parameter systems. *International Journal of Systems Science*, **31**(1), pp. 11-17.

Coombs, C. (2001). *Printed Circuit Handbook*. McGraw-Hill, New York, United States, 1200 p.

Corless, R., Gonnet, G., Hare, D., Jeffrey, D., and Knuth, D. (1996). On the Lambert W function. *Advances in Computational Mathematics,* **5**(1), pp. 329-359.

Courdesses, M., Polis, M., and Amouroux, M. (1981). On identifiability of parameters in a class of parabolic distributed systems. *IEEE Transactions on Automatic Control*, **26**(2), pp. 474-477.

Crank, J. (1975). *The Mathematics of Diffusion*. Clarendon Press, Oxford, 414 p.

Crisan, D., Gaines, J., and Lyons, T. (1998). Convergence of a branching particle method to the solution of the Zakai equation. *SIAM Journal on Applied Mathematics,* **58**(5), pp. 1568-1590.

Cvetanovic, R.J. and Singleton, D.L. (2004). Comment on the evaluation of the arrhenius parameters by the least squares method. *International Journal of Chemical Kinetics*, **9**(3), pp. 481-488.

Davis, M.H.A. (1981). Pathwise non-linear filtering. *Stochastic Systems: The Mathematics of Filtering and Identification and Applications*. Reidel Publishing Company, pp. 505-528.

Delahay, P. (1953). Theory of irreversible waves in oscillographic polarography. *Journal of the American Chemical Society*, **75**(5), pp. 1190-1196.

Deligianni, H. (2006). Electrodeposition and microelectronics. *The Electrochemical Society Interface*, **15**(1), 33-35.

Demetriou, M.A. and Rosen, I.G. (1994). Adaptive identification of second order distributed parameter systems. *Inverse Problems*, **10**(2), pp. 261–294.

Dmitriyev, S.P., Stepanov, O.A., Shepel, S.V. (1997). Nonlinear filtering methods application in INS alignment. *IEEE Transaction on Aerospace and Electronics Systems*, **33**(1), 260–272.

Dondo, R. and Marquers, D. (2003). Simulation results for on-line optimization of a batch bioreactor using nonlinear filtering and optimal control. *ISA Transactions*, **42**, pp. 289–303.

Dunbar, W.B., Petit, N., Rouchon, P., and Martin, Ph. (2003a). Boundary control for a nonlinear Stefan Problem. *Proceedings of the 42nd IEEE Conference on Decision and Control*, pp. 1309-1314.

Dunbar, W., Petit, N., Rouchon, P., and Martin, P. (2003b). Motion planning for a nonlinear Stefan problem. *ESAIM Control, Optimisation and Calculus of Variations,* **9**, pp. 275-296.

Farina A., Benvenuti D., and Ristic B. (2002). A comparative study of the Benes filtering problem. *Signal Processing*, **82**(2), pp. 133-147.

Fleming, W.H. and Pardoux, E. (1982). Optimal control of partially observed diffusion. *SIAM Journal on Control and Optimization*, **20**(2), pp. 261-285.

Fleming, P. and Purshouse, R. (2002). Evolutionary algorithms in control systems engineering: a survey. *Control Engineering Practice*, **10**(11), pp. 1223–1241.

Gabrielli, C., Mocoteguy, P., Perrot, H., Nieto-Sanz, D., and Zdunek, A. (2006). A model for copper deposition in the damascene process. *Electrochimica Acta*, **51**, pp. 1462-1472.

Giudici, M. (1991). Identifiability of distributed physical parameters in diffusive-like systems. *Inverse Problems*, **7**(2), pp. 231-245.

Goldberg, D. (1989). *Genetic Algorithms in Search, Optimization and Machine Learning*. Addison Wesley Publishing Company, 432 p.

Golub, G. and Van Loan, C. (1996). *Matrix Computations* (*3rd Edition*). The Johns Hopkins University Press, 694 p.

Gorskii, V., Katsman, E., Klebanova, F., and Grigor'ev, A. (1987). Numerical study of parameter identifiability for nonlinear models, *Theoretical and Experimental Chemistry*, **23**(2), pp. 181-186.

Gozzi, F. and Swiech A. (2000). Hamilton-Jacobi-Bellman equation for the optimal control of the Duncan-Mortensen-Zakai equation. *Journal of Functional Analysis*, **172**(2), pp. 466-510.

Gradshteyn, I. and Ryzhik. I. (1963). *Table of Integrals, Series, and Products.* Nauka, 1108 p. (in Russian).

Haussmann, U.G. (1986). The maximum principle for optimal control with partial information. *Lecture Notes in Control and Optimization*, **81**, pp. 50-58.

Himmelblau, D. (1972). *Applied Nonlinear Programming*. McGraw-Hill, 498 p.

Hinatsu, J.T. and Foulkes, F.R. (1991). Electrochemical kinetic parameters for the cathodic deposition of copper from dilute aqueous acid sulfate solutions. *The Canadian Journal of Chemical Engineering*, **69**(2), pp. 571-577.

Hong, K.S. and Bentsman, J. (1994). Direct adaptive control of parabolic systems: algorithm synthesis and convergence and stability analysis. *IEEE Transactions on Automatic Control*, **39**(10), pp. 2018-2033.

Hooke, R., and Jeeves, T. (1961). Direct search solution of numerical and statistical problems. *Journal of the Association for Computing Machinery*, **8**(2), pp. 212-229.

Hurlen, T., Ottesen, G., and Staurset, A. (1978). Kinetics of copper dissolution and deposition in aqueous sulphate solution. *Electrochimica Acta*, **23**(1), pp. 39-44.

Hwang, M., Seinfeld, J.H., and Gavalas, G.R. (1972). Optimal least square filtering and interpolation in distributed parameter systems", *Journal of Mathematical Analysis and Applications*, **39**(1), 49-74.

Ito, K. and Rozovskii, B. (2000). Approximation of the Kushner equation for nonlinear filtering. *SIAM Journal on Control and Optimization*, **38**(3), pp. 893-915.

Jetto, L., Longhi, S., and Venturini, G. (1999). Development and experimental validation of an adaptive extended Kalman filter for the localization of mobile robots. *IEEE Transactions on Robotics and Automation*, **15**(2), pp. 219-229.

Kaminer, I., Wei Kang, Yakimenko, O., and Pascoal, A. (2001). Application of nonlinear filtering to navigation system design using passive sensors. *IEEE Transaction on Aerospace and Electronics Systems*, **37**(1), pp. 158-172.

Kantola, K. (2006). *Modelling, Estimation and Control of Electroless Nickel Plating Processes of Printed Circuit Board Manufacturing*. PhD thesis, Helsinki University of Technology.

Kantola, K., Tenno, R., and Koivo, H. (2005). Electroless nickel plating: bath control. *Proceedings of the 16th IFAC World Congress*, Prague, Czech Republic, 6 pp.

Katzur R., Bobrovsky B.Z., and Schuss Z. (1984). Asymptotic analysis of the optimal filtering problem for one-dimensional diffusions measured in a low noise channel. *SIAM Journal on Applied Mathematics*, **44**(3), 591-604.

Khalil, H. (2002). *Nonlinear Systems* (*3rd Edition*). Prentice-Hall, 750 p.

Kim, Y.-S. and Sohn, H.-J. (1996). Mathematical modeling of electroless nickel deposition at steady state using rotating disk electrode. *Journal of the Electrochemical Society,* **143**(2), pp. 505-509.

Kitamura, S. and Nakagiri, S. (1977). Identifiability of spatially-varying and constant parameters in distributed systems of parabolic type. *SIAM Journal on Control and Optimization*, **15**(5), pp. 785-802.

Klibanov, M., Spivak, S., Timoshenko, V., and Slinko, M. (1973). The number of independent parameters in a stationary kinetic model. Dokl. An SSSR, **208**(5), pp. 1387-1390.

Krstic, M. (2006). Systematization of approaches to adaptive boundary stabilization of PDEs. *International Journal of Robust and Nonlinear Control*, **16**(16), pp. 812-818.

Krstic, M., and Smyshlyaev, A. (2008). *Boundary Control of PDEs.* SIAM, Philadelphia, 192 p.

Krylov, N.V. (1980). *Controlled Diffusion Processes.* Springer-Verlag. New York, 324 p.

Kushner, H.J. (1967). Nonlinear filtering: The exact dynamical equations satisfied by the conditional models. *IEEE Transactions on Automatic Control,* **12**(3), pp. 262-267.

Kushner, H.J. (1970). Filtering for linear distributed parameter systems. *SIAM Journal on Control and Optimization,* **8**(3), pp. 346-359.

Kushner, H.J. (1977). *Probability Methods for Approximation in Stochastic Control and for Elliptic Equations. Academic Press*, New-York – San-Francisco – London, 222 p.

Kwok, R., Chan, K., and Bayes, M. (2004). Development of an electroless nickel immersion gold process for PCB final finishes. *Circuit World*, **30**(3), pp. 37-42.

Lagarias, J., Reeds, J., Wright, M., and Wright, P. (1989). Convergence properties of the Nelder-Mead simplex method in low dimensions. *SIAM Journal on Control and Optimization*, **9**(1), pp.112-147.

Lahouaoula, A., and Courdesses, M. (1989). Identifiability and identification of a class of parabolic distributed systems under approximation. *International Journal of Systems Science*, **20**(4), pp. 683-697.

Lebedev, N. (1965). *Special Functions and Their Applications*. Prentice-Hall, 308 p.

Li, R., Corripio A., Henson M., and Kurtz, M. (2004). On-line state and parameter estimation of EPDM polymerization reactors using a hierarchical extended Kalman filter. *Journal of Process Control*, **14**(8), pp. 837-852.

Lide, D.R. (2006). *CRC Handbook of Physics and Chemistry,* 86th ed. CRC Press, Boca Raton, FL.

Liptser, R.S. and Shiryayev A.N. (2004). *Statistics of Random Processes* (*2nd Edition*). I. Springer. New York, 400 p.

Liptser, R.S. and Shiryayev A.N. (2000). *Statistics of Random Processes* (*2nd Edition*). II. Springer. New York, 417 p.

Liu, G., Yang, J., and Whidborne, G. (2003). *Multiobjective Optimisation and Control*. Research Studies Press Ltd, 300 p.

Ljung, L. (1999). *System Identification: Theory for the User (2nd Edition)*. Prentice Hall, 672 p.

Ljung, L. and Glad, T. (1994). On global identifiability for arbitrary model parametrizations. *Automatica*, **30**(2), pp. 265-276.

Lototsky, S. and Rozovskii, B. (1998). Recursive nonlinear filter for a continuous discrete-time model: separation of parameters and observations. *IEEE Transactions on Automatic Control*, **43**(8), pp. 1154-1158.

Lukashenok, V. (1979). Determining kinetic constants for the compound reaction from incomplete information. *Chemical Kinetics and Catalysis*, Nauka, Moscow, pp. 9-13 (in Russian).

Mallory G.O. (1990). *The fundamental Aspects of Electroless Nickel Plating.* In Electroless plating: fundamentals and applications, ed. G.O. Mallory G.O, J. B. Haidu, pages 1-56. American Society of Civil Engineers, Orlando.

Marino, R., Tomei, P., and Verrelli, C. (2008). An adaptive tracking control from current measurements for induction motors with uncertain load torque and rotor resistance. *Automatica*, **44**(10), pp. 2593-2599.

Matsuda, H. and Ayabe, Y. (1955). Zur Theorie der Randles-Sevcikschen Kathodenstrahl-Polarographie. *Zeitschrift für Elektrochemie*, **59**, pp. 494-503.

Mattson, E. and Bockris, O'M.J. (1959). Galvanostatic studies of the kinetics of deposition and dissolution in the copper + copper sulphate system. *Transactions of the Faraday Society*, **55**(5), pp.1586-1601.

Maybank, S. (1996). Finite-dimensional filters. *Philosophical Transactions: Mathematical, Physical and Engineering Sciences*, **354**(1710), pp. 1099-1123.

Mendelson, A. and Tenno, R. (2009a). Identification of uncertainties of electrode kinetics using factorized Zakai equation. *Proceedings of the International Automatic Control Conference CACS 2009*, Taipei, Taiwan, 2009, 6 pp.

Mendelson, A. and Tenno, R. (2009b). Electrode kinetics parameters estimation using Zakai equation. *Journal of Process Control*, **19**(10), pp. 1698-1706.

Mendelson, A. and Tenno, R. (2009c). Application of Zakai equation in parameter identification of electrode kinetics. *Preprints of the 15th IFAC Symposium on System Identification, SYSID2009*, Saint-Malo, France, pp. 1423-1428.

Mendelson, A. and Tenno, R. (2008a). Modelling and parameter identification of electrochemical Cu-Cu cell. *Proceedings of the UKACC International Conference on Control 2008*, Manchester, UK, 6 pp.

Mendelson, A. and Tenno, R. (2008b). Model for electrode kinetics of copper-copper system. *Proceedings of the 17th IASTED International Conference on Applied Simulation and Modelling*, Corfu, Greece, IASTED, pp. 271-276.

Mendelson, A. and Tenno, R. (2007a). Identification of the mass-transfer and kinetic parameters from voltammograms. *IEEE International Symposium on Industrial Electronics*, Vigo, Spain, 2007, pp. 142-146.

Mendelson, A. and Tenno, R. (2007b). Identification of time-varying mixed potential processes. *Proceedings of the 9th WSEAS International Conference on Automatic Control, Modeling and Simulation*, *ACMOS '07,* Istanbul, Turkey, 2007, pp. 278-283.

Mendelson, A.M., Benderskaya, E.N., and Tenno, R.A. (2006). Genetic based identification of electrochemical processes. *Information and Control Systems*, №2, pp. 53-56 (in Russian).

Mitter, S.K. (1982). Existence and non-existence of finite dimensional filters. *Rendiconti del Seminario Matematico, Fascicolo Speciale*, pp. 173-188.

Myland, J. and Oldham, K.B. (2000). Which of three voltammetric methods, when applied to a reversible electrode reaction, can best cope with double-layer capacitance and severe uncompensated resistance? *Analytical Chemistry*, **72**(14), pp. 3210-3217.

Nelder, J. and Mead, R. (1965). A simplex method for function minimization. *The Computer Journal*, **7**(4), pp. 308-313.

Newman, J. and Thomas-Alyea, K. (2004). *Electrochemical Systems*. John Wiley & Sons, New Jersey, 672 p.

Nguyen, V. and Wood, E. (1982). Review and unification of linear identifiability concepts. *SIAM Review*, **24**(1), pp. 34-51.

Nicholson, R.S. and Shain, I., (1964). Theory of stationary electrode polarography: single scan and cyclic methods applied to reversible, irreversible, and kinetic systems. *Analytical Chemistry*, **36**(4), pp. 706-723.

Nicholson, R.S. (1965a). Some examples of the numerical solution of nonlinear integral equations. *Analytical Chemistry*, **37**(6), pp. 667-671.

Nicholson, R.S. (1965b). Theory and application of cyclic voltammetry for measurement of electrode reaction kinetics. *Analytical Chemistry*, **37**(11), pp. 1351-1355.

Niedzwiecki, M. (2000). *Identification of Time-Varying Processes*. John Wiley & Sons, 340 p.

Noulty, R.A., and Leaist, D.G. (1987). Diffusion in aqueous copper sulphate and copper sulphate-sulphuric acid solutions. *Journal of Solution Chemistry,* **16**(10), pp. 813-825.

Orlov, Y. and Bentsman, J. (1995). Model reference adaptive control (MRAC) of heat processes with simultaneous plant identification. *Proceedings of the 34th Conference on Decision & Control, New-Orleans*, pp. 1165-1170.

Orlov, Y. and Bentsman, J. (2000). Adaptive distributed parameter systems identification with enforceable identifiability conditions and reduced-order spatial differentiation. *IEEE Transactions on Automatic Control*, **45**(2), pp. 203-216.

Pardoux, E. (1981). Equations of non-linear filtering and application to stochastic control with partial observation. *Lecture Notes in Mathematics,* **972**, pp. 208-248.

Paunovic, M. and Schlesinger, M. (1998). *Fundamentals of Electrochemical Deposition*. John Wiley & Sons, 312 p.

Pham, H. (2005). On some recent aspects of stochastic control and their applications, *Probability Surveys*, **2**, pp. 506-649.

Pierce, A. (1979). Unique identification of eigenvalues and coefficients in a parabolic problem. *SIAM Journal on Control and Optimization*, **17**(4), pp. 494-499.

Pinchover, Y. and Rubinstein, J. (2005). *An Introduction to Partial Differential Equations*. Cambridge University Press, 384 p.

Pirogov, B.Ya. and Zelinsky, A.G. (2004). Numerical simulation of electrode process in $Cu/CuSO_4 + H_2SO_4$ system. *Electrochimica Acta*, **49**(20), pp. 3283-3292.

Pohjoranta, A., Mendelson, A., and Tenno, R. (2010). A copper electrolysis cell model including effects of the ohmic potential loss in the cell. *Electrochimica Acta,* **55**(3), pp. 1001-1012.

Pohjoranta, A. and Tenno, R. (2007). A method for microvia-fill process modeling in a Cu plating system with additives. *Journal of the Electrochemical Society,* **154(**10), pp. D502-D509.

Polis, M.P., Goodson, R.E., and Wozny, M. J. (1973). On parameter identification for distributed systems using Galerkin's criterion. *Automatica*, **9**(1), pp. 53-64.

Polsyn, D.S. and Shain, I. (1966). Multistep charge transfers in stationary electrode polarography. *Analytical Chemistry*, **38**(3), pp. 370-375.

Polyanin, A. (2005). Inverse Laplace transforms: expressions with square roots. http://eqworld.ipmnet.ru/en/auxiliary/inttrans/LapInv3.pdf.

Pragarauskas, H. (1981). Bellman's equation in a lattice of measures for general controlled stochastic processes. Part I. *Lithuanian Mathematical Journal.* **21**(4), pp. 353-363.

Pragarauskas, H. (1982). Bellman's equation in a lattice of measures for general controlled stochastic processes. Part II. *Lithuanian Mathematical Journal,* **22**(11), pp. 68-73.

Rakitskii, Y., Ustinov, S., and Khokhlov, V. (1982). Problems in model construction and stiff-system theory. *Abstracts for the 4-th All-Union Conference on Mathematical Models in Chemistry*, Erevan, pp. 232-233 (in Russian).

Reeves, C. and Rowe, J. (2003). *Genetic Algorithms - Principles and Perspectives: A Guide to GA Theory*. Springer, 344 p.

Reid J. (2001). Copper electrodeposition: principles and recent progress. *Japanese Journal of Applied Physics*, **40**, pp. 2650-2657.

Riedel, W. (1991). *Electroless Nickel Plating*. Finishing Publications Ltd, 328 p.

Riley, K., Hobson, M., and Bence, S. (2006). *Mathematical Methods for Physics and Engineering.* Cambridge University Press, 1362 p.

Rozovskii, B.L. (1983). *Stochastic Evolution Systems. Linear Theory and Applications to the Statistics of Random Processes (in Russian)*. Nauka, Moscow, 208 p.

Rozovskii, B.L. (1990). *Stochastic Evolution Systems.* Kluwer Academic Publishers, Dordrecht, 340 p.

Rugh, W. (1991). Analytical framework for gain scheduling. *IEEE Control Systems Magazine*, **11**(1), pp. 79 – 84.

Seinfeld, J.H. (1969). Nonlinear estimation for partial differential equations. *Chemical Engineering Science*, **24**, pp. 75-83.

Seinfeld, J.H. and Chen, W.H. (1971). Estimation of parameters in partial differential equations from noisy experimental data. *Chemical Engineering Science*, **26**(6), pp. 753-766.

Seinfeld, J.H., Gavalas, G.R., and Hwang, M. (1971). Nonlinear filtering in distributed parameter systems. *Journal of Dynamic Systems, Measurement and Control*, **93**, pp. 157-163.

Simon, D. (2006). *Optimal State Estimation: Kalman, H∞ and Nonlinear Approaches*. Wiley, New Jersey, 552 p.

Smyth, M.R. and Vos, J.G. (1992). *Analytical Voltammetry*. Elsevier, 578 p.

Strauss, W. (1992). *Partial Differential Equations: An Introduction*. John Wiley & Sons, 464 p.

Subramanian K., Periasamy, V., Pushpavanam, M., and Ramasamy, K. (2009). Predictive modeling of deposition rate in electro-deposition of copper–tin using regression and artificial neural network. *Journal of Electroanalytical Chemistry*, **636**, pp. 30-35.

Söderström, T. and Stoica, P. (1989). *System Identification*. Prentice Hall, New York, 612 p.

Tenno, R., Kantola, K., and Tenno, A. (2006). Electroless nickel plating process model for plated-through-hole board manufacturing. *Journal of Electronic Materials,* **35**, pp. 1825-1836.

Tenno, R. and Koivo, H. (2003). State estimation and bath control for the electroless nickel-plating process. *Proceedings of the European Control Conference, ECC'03, Cambridge, UK: EUCA, IEE*, 6 pp.

Tenno, R. and Mendelson, A. (In press). Adaptive boundary concentration control using Zakai equation. *International Journal of Control*.

Tsai, W.C., Wan, C.C., and Wand, Y.Y. (2002). Mechanism of copper electrodeposition by pulse current and its relation to current efficiency. *Journal of Applied Electrochemistry*, 32, pp. 1371–1378.

Tzafestas, S.G. and Nightingale, J.M. (1968). Optimal filtering, smoothing, and prediction in linear distributed parameter systems. *Proc. IEE*, **115**, pp. 1207-1212.

Walter, E. and Pronzato, L. (1990). Qualitative and quantitative experiment design for phenomenological models – A survey. *Automatica*, **26**(2), pp. 195-213.

Wang, J. (2000). *Analytical Electrochemistry*. Wiley-VCH, 209 p.

Weisstein, E. (2009). Lambert W-Function. http://mathworld.wolfram.com/LambertW-Function.html.

White, N. and Lawson, F. (1970). Potential sweep voltammetry of metal deposition dissolution. Part I. Theoretical analysis. *Journal of Electroanalytical Chemistry*, **25**(3), pp. 409-419.

Wipf, D. (1996). Ohmic Drop Compensation in Voltammetry: Iterative Correction of the Applied Potential. *Analytical Chemistry*, **68**(11), pp. 1871-1876.

Wong, E. and Zakai, M. (1965). On the convergence of ordinary integral to stochastic integral. *Annals of Mathematical Statistics*, **36**(5), pp. 1560-1564.

Wu, H. (2009). Decentralised adaptive controllers for robust tracking and model following of uncertain large scale systems. *International Journal of Control*, **82**(2), pp. 268-278.

Yoke Lin Tan (1996). Nonlinear filtering for the estimation of glycated hemoglobin in the presence of fetal hemoglobin using microcolumn ion-exchange chromatography. *IEEE Transactions on Biomedical Engineering*, **43**(5), pp. 545-547.

Zakai, M. (1969). On the optimal filtering of diffusion processes. *Z. Wahrsch. Verw. Geb.* **11**, pp. 230-243.

Zhao, W.-X. and Chen, H.-F. (2009). Adaptive tracking and recursive identification for Hammerstein systems. *Automatica*, **45**(12), pp. 2773-2783.

Zou, R., Wang, H., and Chon, K. (2003). A robust time-varying identification algorithm using basis functions. *Annals of Biomedical Engineering,* **31**(7), pp. 840–853.

HELSINKI UNIVERSITY OF TECHNOLOGY CONTROL ENGINEERING

Editor: H. Koivo

Report 154 Mohamed, F. A.
Microgrid Modelling and Online Management. January 2008.

Report 155 Eriksson, L., Elmusrati, M., Pohjola, M. (eds.)
Introduction to Wireless Automation - Collected papers of the spring 2007 postgraduate seminar. April 2008.

Report 156 Korkiakoski, V.
Improving the Performance of Adaptive Optics Systems with Optimized Control Methods. April 2008.

Report 157 Al.Towati, A.
Dynamic Analysis and QFT-Based Robust Control Design of Switched-Mode Power Converters. September 2008.

Report 158 Eriksson, L.
PID Controller Design and Tuning in Networked Control Systems. October 2008.

Report 159 Pohjoranta, A.
Modelling Surfactant Mass Balance with the ALE Method on Deforming 2D Surfaces. May 2009.

Report 160 Kaartinen, J.
Machine Vision in Measurement and Control of Mineral Concentration Process. June 2009.

Report 161 Hölttä, V.
Plant Performance Evaluation in Complex Industrial Applications. September 2009.

Report 162 Halmevaara, K.
Simulation Assisted Performance Optimization of Large-Scale Multiparameter Technical Systems. September 2009.

Report 163 Haavisto, O.
Reflectance Spectrum Analysis of Mineral Flotation Froths and Slurries. November 2009.

Report 164 Cosar, E. I.
A Wireless Toolkit for Monitoring Applications. October 2009.

Report 165 Pohjoranta, A.
Computational Models for Microvia Fill Process Control. February 2010.

Report 166 Mendelson, A.
Identification and Control of Deposition Processes. March 2010.

ISBN 978-952-60-3126-2 (printed)

ISBN 978-952-60-3127-9 (pdf)

ISSN 0356-0872

Yliopistopaino, Helsinki 2010